Norwegian University
of Life Sciences

Master's Thesis 2016
60 ECTS
Department of Chemistry, Biotechnology and Food Science

Studies on proteins from *Methylococcus capsulatus* Bath: Expression in *Lactobacillus plantarum* WCFS1, purification and large-scale fermentation

Arild Sveen
Food Science – Food and Health

Acknowledgements

The work presented in this thesis was performed at the Department of Chemistry, Biotechnology and Food Science at the Norwegian University of Life Sciences. The supervisors for the thesis were Professor Tor Lea and Researcher Geir Mathiesen.

First of all, I would like to thank both of my eminent advisors. Tor, you are an endless fountain of knowledge of everything related to immunology and cell biology. Additionally, it is clear that you care deeply about everything and everyone in your lab. I am grateful for being allowed to be part of that environment. Geir, first of all I have to thank you for lending me the use of your lab bench for such an exceedingly long time. Second, thank you so much for all the practical and theoretical help throughout the year.

My heartfelt thanks especially go out to Lise Øverland at the PEP lab, and Lars Fredrik Moen and Stine Indrelid at the Laboratory for Molecular Cell Biology. Lise, you've been a great friend and an invaluable authority on everything methodological I've done. Lars, first of all, the 12-liter fermentations never would have happened without you. Thanks for putting in the work. Second, you make good coffee. Stine, you have been a great source of support. Thank you for believing in me.

I would also like to thank my fellow master students Ine Myrbråten and Silje Harvei, who both also required extensions on their respective theses, but who delivered with quite a bit more time to spare than myself.
Kamilla, I wish you luck in your future endeavors, wherever they may lead.

Finally, I have to thank the entirety of the PEP and Molecular Cell Biology labs for your respective, awesome social environments. It's been a pleasure working with all of you.

Abstract

The work described in this thesis is part of a larger project investigating the non-commensal methanotroph *Methylococcus capsulatus* Bath. This species has shown anti-inflammatory and obesity-reducing effects in animal models when given as an extract in the diet. *In silico* studies of the *M. capsulatus* Bath genome revealed four genes (*mam, tir, mif* and *sim*) that encode proteins which are homologous to proteins with known immunomodulatory functions. They might therefore contribute to the observed effects. These proteins (Mam, Tir, Mif and Sim) were the focus of this thesis.

The genetic sequences from *M. capsulatus* Bath were cloned into the pSIP401 vector of the pSIP inducible gene expression system. They were successfully transformed into the lactic acid bacteria *Lactobacillus plantarum* WCFS1. Inducible protein expression was successfully accomplished as verified with Western blot. The genetic sequences were also cloned into the pNIC-CH vector for purification of protein. The proteins were successfully produced in *Escherichia coli* BL21 and purified with immobilized metal ion affinity chromatography.
.

After successfully producing purified protein and lysate from *L. plantarum* harbouring the pSIP401-derivatives, *in vitro* assays were performed. In the first assay, effects of these bacterial stimuli on interleukin (IL)-1β-induced production of IL-8 was investigated. In the second assay, effects on transepithelial electrical resistance when co-incubated with tumour necrosis factor (TNF)α. Neither of these assays were successful, however.

Finally, *L. plantarum* harbouring pSIP401_MAM or empty vector were cultured in 12-liter batch fermentations by using a 15-liter bioreactor. The resulting broth was lysed via French pressing and lyophilized before being shipped away to Copenhagen, to be used in a murine study.

Sammendrag

Arbeidet som ble gjennomført i denne masteroppgave er en del av et større prosjekt som undersøker den metanotrofe bakterien *Methylococcus capsulatus* Bath. Denne bakterien, som ikke finnes i tarmfloraen, har fått påvist betennelsesdempende og fedmereduserende effekter i dyreforsøk når den blir gitt som et ekstrakt i fôret. *In silico*-studier av genomet til *M. capsulatus* Bath viste at fire gener (*mam, tir, mif* og *sim*) koder for proteiner som har homologi til proteiner med kjente immunomodulerende effecter. Disse proteinene (Mam, Tir, Mif og Sim) var fokuset I denne oppgaven.

Gensekvensene fra *M. capsulatus* Bath ble klonet inn i pSIP401-vektoren som er en del av det induserbare genuttrykkssystemet pSIP. De ble deretter transformert inn i melkesyrebakterien *Lactobacillus plantarum* WCFS1. Induserbar produksjon av protein ble deretter verifisert ved bruk av Western blot. Gensekvensene ble også klonet inn i pNIC-CH-vektoren for rensing av protein. Proteinene ble produsert i *Escherichia coli* BL21 og renset ved bruk av kolonnekromatografi.

Etter at renset protein og lysat fra *L. plantarum* med pSIP401-derivatene var gjennomført ble to *in vitro*-forsøk utført. I det første forsøket ble effekter av de bakterielle stimuliene på interleukin (IL)-1β-indusert produksjon av IL-8 undersøkt. I det andre forsøket ble effekter av stimuliene sammen med tumour necrosis factor (TNF)-α på elektrisk motstand over et epitelcellelag undersøkt. Ingen av disse to assayene var vellykket.

Til slutt ble *L. plantarum* med pSIP401_MAM eller tom vektor dyrket i 12-liters batch-fermenteringer i en 15-liters bioreaktor. Bakteriemassen ble deretter lysert med French press, før den ble frysetørket og sendt til København for å brukes i et museforsøk.

Abbreviations

aa Amino acid(s)
APC Antigen presenting cell
bp Base pair(s)
c-di-GMP Cyclic-di-guanosine monophosphate
BSA Bovine serum albumin
CBS Cystathionine β-synthase
CD Crohn's disease
DC Dendritic cell
DNA Deoxyribonucleic acid
dsDNA Double-stranded DNA
DSS Dextran sodium sulfate
dNTP Deoxyribose nucleoside triphosphate
DTT 1,4-dithiothreitol
EDTA Ethylenediaminetetraacetic acid
GALT Gut-associated lymphoid tissue
HK Histidine-protein kinase
HRP Horseradish peroxidase
IBD Inflammatory bowel disease
IFN Interferon
IMAC Immobilized metal ion affinity chromatography
IP Inducer peptide
IPTG Isopropyl β -D-1-thiogalactopyranoside
LAB Lactic acid bacteria
LIC Ligase independent cloning
LPS Lipopolysaccharide
MALT Mucosa-associated lymphoid tissue
MAM Microbial Anti-inflammatory Molecule
MAMP Microbial Associated Molecular Pattern
MHC Major histocompatibility complex
MIF Macrophage migration inhibitory factor
NF-κB Nuclear factor κ-light-chain-enhancer of activated B cells
NICE Nisin-controlled expression
NK Natural killer
OD Optical density
ORF Open reading frame
PAGE Polyacrylamide gel electrophoresis
PBS Phosphate-buffered saline
PCR Polymerase chain reaction
PRR Pattern recognition receptor
RR Response regulator
SDS Sodium dodecyl sulphate
SIMPL signaling molecule that associates with the mouse pelle-like kinase
TBS Tris-buffered phosphate
Tcp TIR-domain containing proteins
TEER Transepithelial electrical resistance
TIR Toll/interleukin-1 receptor
TLR Toll-like receptor
TNF Tumor necrosis factor

Contents

1. INTRODUCTION

Two billion years before the first signs of eukaryotic life, bacteria inhabited the earth. Throughout time, they have played an active role in the evolution of higher-order organisms. Mitochondria and chloroplasts are descendants of bacteria which at some point were absorbed by the larger eukaryotic cells. In addition, every external surface of our bodies, including the contents of the intestinal lumen, are populated by a rich ecosystem of bacteria and other microbes called the microbiota. This commensal microbiota exists in a symbiotic relationship with its host, where the various species of bacteria inhabit different anatomical niches on the host and metabolize otherwise indigestible substances into nutrients usable by the host (Lee & Mazmanian 2010). The immune system in the intestinal mucosa exists in a state of homeostasis with the microbiota, selectively sampling microbial antigens from the lumen. Disruption of this homeostasis can lead to disease states such as colitis (Manichanh et al. 2012).

The non-commensal bacterium *Methylococcus capsulatus*, strain Bath, has been shown to exert anti-inflammatory effects in animal models with enteritis or colitis when included in diet as a lyophilized meal (Kleiveland et al. 2013; Romarheim et al. 2011). In searching for possible causes of the anti-inflammatory effect, four genes from *M. capsulatus* Bath which encode potentially immunomodulatory proteins were identified. This thesis describes studies on these genes, involving the construction and use of plasmids for expression of the genes in *Lactobacillus plantarum* WCFS1 and *Escherichia coli* BL21, as well as the exposure of the human colonic adenocarcinoma cell line Caco-2 to these proteins.

1.1 *Methylococcus capsulatus* Bath

M. capsulatus is a Gram-negative methanotrophic bacterium, which grows under aerobic conditions using methane as the sole source of carbon and energy. It uses a methane monooxygenase to catalyze the oxidation of methane to methanol, a reaction which is dependent on NADH and oxygen (Colby et al. 1977). The methanol is then converted by methanol dehydrogenases to formaldehyde, which is further oxidized via several pathways to formate and CO_2 for energy production or used as an enzyme substrate (Ward et al. 2004). Due to its utilization of the ribulose monophosphate pathway for formaldehyde assimilation,

M. capsulatus is classified as a type I methanotroph (Kleiveland et al. 2012). The genome sequence of *M. capsulatus* Bath also shows high potential for metabolic flexibility, with a possible ability to oxidize chemolithotrophic hydrogen and sulfur, as well as the ability to live under conditions with reduced oxygen tension (Ward et al. 2004). In nature, it has been found in freshwater-, marine- and terrestrial habitats (Whittenbury et al. 1970).

When Atlantic salmon were fed a bacterial meal (BioProtein) containing 88 % *M. capsulatus* Bath and smaller fractions of *Aneurinibacillus* sp., *Brevibacillus* sp. and *Ralstonia* sp., Romarheim et al. (2011) showed that soybean meal-induced enteritis could be prevented in a dose-dependent manner. In a dextran sodium sulfate (DSS)-induced model of colitis in mice, Kleiveland et al. (2013) showed similar results when using BioProtein as a replacement for casein and corn starch in the feed. This murine model has many similarities to ulcerative colitis in humans, e.g. reduced body weight, shortening of the colon and damage to the intestinal epithelial cell layer. These factors were significantly improved in this trial. The authors also used a single-strain bacterial meal to show that these effects were due to *M. capsulatus* Bath and not the other species contained in BioProtein.

Compared to *E. coli* Nissle 1917, the *M. capsulatus* strains Bath and Texas have been shown to be relatively poor inducers of inflammation via nuclear factor κ-light-chain-enhancer of activated B cells (NF-κB), a protein complex which controls transcription of genes involved in production of cytokines, cell proliferation and survival. However, when monocyte-derived dendritic cells (moDCs) were exposed to the three strains, *M. capsulatus* Bath caused the moDCs to produce a less inflammatory cytokine profile than *E. coli* Nissle 1917 and *M. capsulatus* Texas. (Christoffersen et al. 2015). Kleiveland et al. (2012) performed a shotgun genome sequencing of *M. capsulatus* Texas, which showed a 93.9 % shared genomic alignment and 340 open reading frames (ORFs) without homologs in *M. capsulatus* Bath.

Additional, unpublished research in murine models of diet-induced obesity has shown that feeding with *M. capsulatus* Bath leads to reduced fat mass and increased insulin sensitivity (Tor Lea, 12.08-2016, personal communication). Following on from this research, *in silico* computational analyses and proteomics of the *M. capsulatus* Bath secretome were performed by Indrelid et al. (2014), with the purpose of identifying its secretion systems and predicting secreted proteins. In addition, the genome was searched for genes which might contribute to the anti-inflammatory effects of *M. capsulatus* Bath (Indrelid 2015, manuscript under

preparation). Four genes coding for proteins homologous to proteins with possible immunoregulatory activity were identified. These proteins were the focus of this thesis.

1.2 Proteins of interest from *Methylococcus capsulatus* Bath

The genes (*mam, tir, mif* and *sim*) and proteins (Mam, Tir, Mif and Sim), have been given temporary names in this thesis based on their designations in the annotated *M. capsulatus* Bath genome (Ward et al. 2004) or, as is the case with Mam, based on other known anti-inflammatory proteins (Quevrain et al. 2016a).

1.2.1 Putative diguanylate phosphodiesterase, Mam

The first gene, with locus MCA_RS01660, encodes a 588 amino acid (aa) long GGDEF/EAL domain protein, classified as a putative diguanylate phosphodiesterase (Ward et al. 2004). A search for conserved domains showed that the protein contains one region with a cystathionine β-synthase (CBS) pair at aa 44-115, one GGDEF domain at aa 157-315 and one EAL domain at aa 333-573 (Marchler-Bauer et al. 2015). It was selected for this thesis based on its structural homology to a protein with known anti-inflammatory properties; Microbial Anti-inflammatory Molecule (MAM) from *Faecalibacterium prausnitzii*, discovered by Quevrain et al. (2016a). The *M. capsulatus* Bath homolog is here referred to as Mam.

F. prausnitzii is a commensal bacterium with known anti-inflammatory properties. It is one of the most prevalent species in the gut microbiota of healthy humans and is significantly reduced in patients with Crohn's disease (CD), one of the forms of inflammatory bowel disease (IBD) where dysbiosis is believed to play a role in the onset of the disease (Sokol et al. 2008). The anti-inflammatory properties of *F. prausnitzii* are associated with secreted molecules that block interleukin-8 (IL-8) production and NF-κB activation. These metabolites were identified by Quevrain et al. (2016a) to be peptides from a single protein, which was named MAM. When mice were fed *Lactococcus lactis* overexpressing MAM, they had fewer intestinal macroscopic lesions and a less inflammatory cytokine profile produced by lymphocytes. The protein has also been identified in human feces (Quevrain et al. 2016b). The authors performed a BLAST search against the PDB database and found a homolog in

the *M. capsulatus* Bath putative diguanylate phosphodiesterase, with 15 % sequence identity and a similar tertiary structure (Quevrain et al. 2016a).

Mam from *M. capsulatus* Bath is a GGDEF/EAL-tandem containing protein. GGDEF and EAL domain-containing proteins are found in all major bacterial phyla. They modulate cellular contents of cyclic-di-guanosine monophosphate (c-di-GMP), a universal bacterial second messenger which is implicated in various cellular functions, e.g. motility, biofilm formation and dispersion, regulation of the cell cycle and virulence (Romling et al. 2013). c-di-GMP is also a Microbial Associated Molecular Pattern (MAMP), recognized by the innate immune system (Karaolis et al. 2007). In mammals, several intracellular receptors for c-di-GMP have been identified. Their activation stimulates production of type I interferons (IFN). Type I IFNs are pleiotropic cytokines that (1) activate macrophages and Natural Killer (NK) cells, (2) upregulate the major histocompatibility complex (MHC) class I molecules found on all cell types and (3) are integral to activation and survival of $CD4^+$ and $CD8^+$ T cells (Romling et al. 2013; Siegal et al. 1999).

The GGDEF domain forms a homodimer that has diguanylate cyclase activity, catalyzing c-di-GMP formation from two GTP molecules via 5'-pppGpG. The EAL domain also forms di- or oligomers *in vitro*, and has phosphodiesterase activity (Romling et al. 2013). However, in proteins with GGDEF and EAL domains in tandem, more than half have one or more inactive binding sites (Seshasayee et al. 2010). In these proteins, the domains may have other biological activities such as contributing to protein-protein interactions or binding GTP. Similarly, the CBS pair in Mam likely contributes to binding of GTP, as the domain pair has been shown to bind adenosyl compounds *in vitro* (Kemp 2004). However, what metabolic functionality Mam has, if any, has not been investigated.

1.2.2 Molecular chaperone Tir

The second of the selected genes, with locus tag MCA_RS14775, encodes the molecular chaperone Tir, a 314 aa long protein (Ward et al. 2004). Wu et al. (2012) identified this protein as containing a SEF/IL-17 receptor (SEFIR) domain, which is structurally similar to domains in the Toll/interleukin-1 receptor (TIR) family. In this thesis, the protein is referred to as Tir.

The innate immune system found in vertebrates responds rapidly to potentially pathogenic stimuli via pattern recognition receptors (PRRs). These receptors, located either on the immune cell's surface or intracellularly, bind MAMPs, unique and conserved components of bacteria or viruses, such as lipopolysaccharides (LPS), double-stranded RNA or bacterial flagellins (Latz et al. 2007).

The largest and best characterized class of PRRs is the Toll-like receptors (TLRs), which all share a conserved leucine-rich repeat domain forming a solenoid structure, a transmembrane segment and a cytoplasmic TIR domain, the latter of which mediates downstream TLR signaling. This signaling involves six different adaptor proteins, the myeloid differentiation factor 88 (MyD88); the MyD88-adaptor-like (Mal); the TIR domain containing IR domain containing adaptor protein inducing interferon- α/ β (TRIF); the TRIF-related adaptor molecule (TRAM), the sterile α and armadillo-motif containing protein (SARM) and B-cell adaptor for PI3K (BCAP). All TLRs except TLR3 use these adapter proteins in a MyD88 dependent pathway, while TLR3 and TLR4 can use a TRIF-dependent pathway. The MyD88 dependent pathway uses TIR-TIR interactions to recruit MyD88 to the TIR domain. MyD88 can activate TNF receptor-associated factor 6 (TRAF6) which leads to induction of genetic transcription factors such as NF-κB, resulting in production of pro-inflammatory cytokines; it can activate TRAF3, leading to induction of interferon regulatory factors; or it can bind to Fas-associated death domain, leading to apoptosis (O'Neill et al. 2013). The TRIF-dependent pathway recruits TRIF to the TLR, leading to production of interferons (IFN) (Guven-Maiorov et al. 2015). See Fig. 1.1 for an overview.

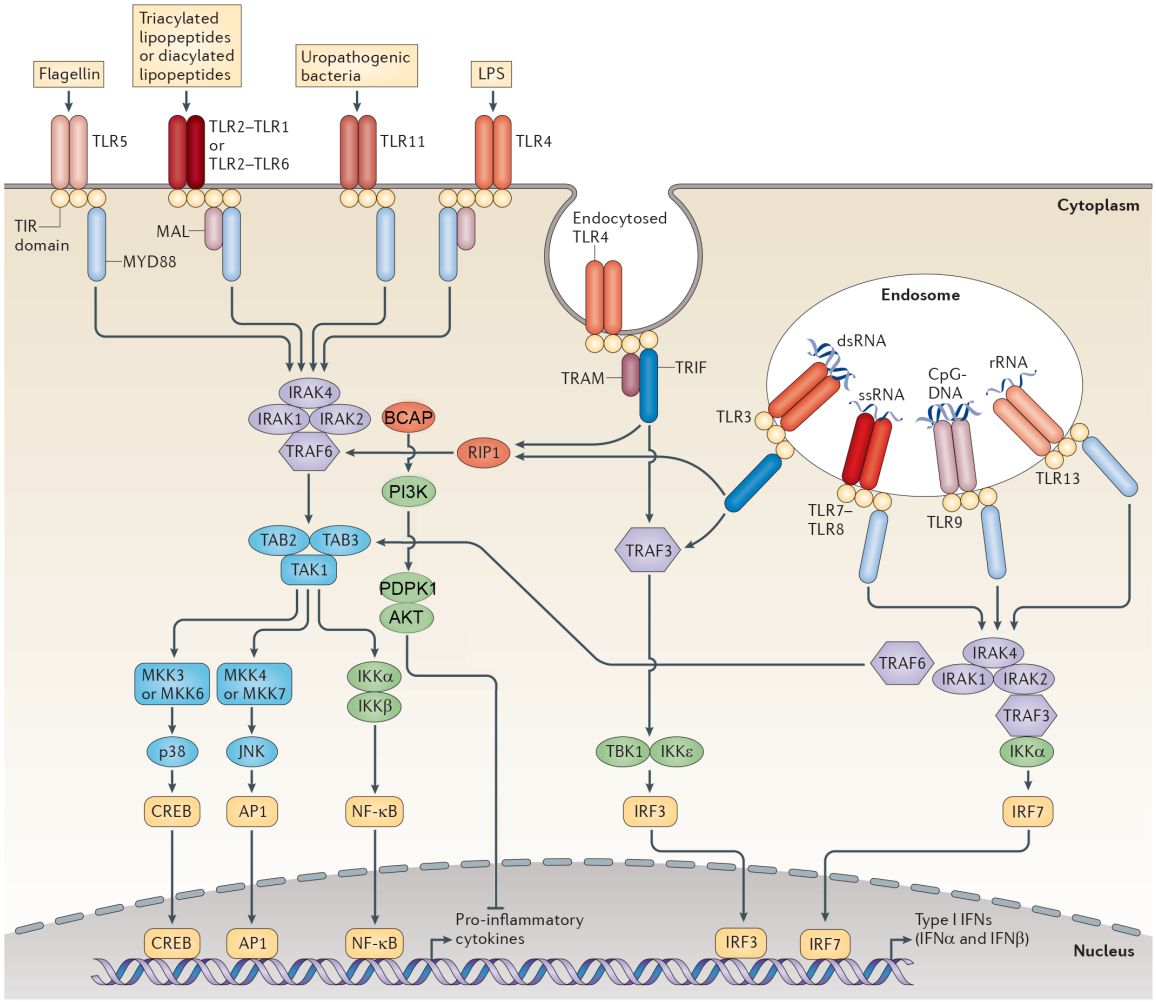

Figure 1.1. Mammalian TLR signaling pathways. The figure shows membrane-bound and endosomal TLRs with their respective adaptor proteins, as well as the metabolic pathways they induce. The figure is adapted from (O'Neill et al. 2013), with the addition of the pathway initiated by BCAP, proposed as the sixth TIR-domain containing adaptor molecule. This protein may interact with the MyD88-TRAF6 pathway, inhibiting NF-kB-dependent pro-inflammatory cytokines.

The SEFIR domain is found in IL-17 receptors (IL17R) as well as their adaptor protein, Connection to IKK and SAPK/JNK (CIKS). The IL17R-CIKS signaling system is important in the innate immune system's response to pathogenic infections (Wu et al. 2012). SEFIR is also found in the NF-κB activator 1 (Act1), which is recruited to IL17R-complexes in a SEFIR-dependent manner and leads to downstream production of IL-17 cytokines (Zhang et al. 2014). SEFIR is similar to TIR domains in primary and secondary structure. The TIR domains contain three highly conserved sequence motifs and form heterotypic TIR-TIR complexes, both characteristics which are shared by the SEFIR domain (Wu et al. 2012).

Unlike TIR domains, the structural elements of SEFIR domains seem to be specific for IL17R (Zhang et al. 2014).

TIR-domain containing proteins (Tcps), which have structural homology with the TIR domains, are found in bacteria, archaea and viruses in addition to eukaryotes. Tcps are likely integral to host immune evasion by pathogens, by interfering with host TIR-dependent signaling. The role of TIR–TIR protein–domain interactions in non-pathogenic bacteria remains poorly understood and the role of SEFIR-SEFIR interaction is yet to be investigated (Patterson & Werling 2013). However, many of the currently identified SEFIR-containing bacterial proteins, including Tir, have only a single copy of the domain, indicating that these may form complexes with similar proteins from the host. The bacterial SEFIR domains are also electrostatically and structurally similar to the CIKS of the host. Both of these similarities indicate that bacterial SEFIR proteins may interfere with the IL17R-mediated signaling pathway (Wu et al. 2012).

1.2.3 MIF domain-containing protein, Mif

The third of the selected genes, with locus tag MCA_RS13685, encodes a 114 aa long hypothetical protein containing one putative phenylpyruvate tautomerase, or macrophage migration inhibitory factor (MIF) domain. The entire sequence codes for this domain (Ward et al. 2004).

MIF is a pro-inflammatory and immunomodulatory cytokine. It was one of the first cytokines to be discovered and had its activity being described 50 years ago. It also has enzyme activity as a phenylpyruvate tautomerase (Rosengren et al. 1997). It has a N-terminal proline residue which is essential to its catalytic activity, but it is unknown whether the enzymatic activity is relevant to its function as a cytokine. MIF is found in humans and mice as a homotrimer with structural homology to the microbial enzymes oxalocrotonate tautomerase, 5-carboxymethyl-2-hydroxymuconate isomerase and chorismate mutase (Calandra & Roger 2003).

MIF is expressed in a large number of tissues, including those in direct contact with the external environment, such as the skin, gastrointestinal- and genitourinary epithelial cells. It is also highly expressed by some endocrine tissues, such as the hypothalamus, anterior pituitary

gland and adrenal glands (Larson & Horak 2006). T cells are one of the main immune sources of MIF, but it is also expressed by B cells and many innate immune cells. MIF is constitutively expressed and stored in intracellular pools, in contrast to most other cytokines which must be produced *de novo* in a response to external stimuli. Because of this, MIF can be more rapidly secreted when the cells are exposed to other pro-inflammatory cytokines or microbial products (Calandra & Roger 2003). In the human genome, there is only one gene with marked homology to MIF, namely D-dopachrome tautomerase (D-DT). *In vitro* studies in macrophages and cancer cell lines have shown that the two proteins have overlapping functions, although macrophages produce 20 times more MIF than D-DT does. D-DT also has the same enzymatic tautomerase activity as MIF (Merk et al. 2012).

Secreted MIF has a receptor, CD74, which is expressed by antigen presenting cells like DCs, macrophages and lymphocytes. By binding to CD74 or being endocytosed by the cell, MIF induces rapid and sustained cell proliferation via phosphorylation and activation of the extracellular signal-regulated kinase 1 (ERK1) and ERK2 proteins. ERK1 and ERK2 are involved in the mitogen-activated protein kinase (MAPK) pathway. The activation is associated with higher intracellular levels of cytoplasmic phospholipase 2 (PLA2), which is part of a cascade leading to production of pro-inflammatory arachidonic acid, prostaglandins and leukotrienes (Calandra & Roger 2003; Roger et al. 2003). MIF also upregulates TLR4, which is the receptor for LPS, facilitating the detection of endotoxin-containing bacteria (Doyle & O'Neill 2006). Finally, it suppresses p53-mediated growth arrest and apoptosis, which are involved in tumorigenesis, implicating a potential role of MIF in this process (Larson & Horak 2006).

Expression of MIF is upregulated in inflamed tissues in rheumatoid arthritis, where it is implicated in the disease's pathology via recruitment, proliferation and survival of leukocytes as well as in bone and cartilage injury (Leech et al. 1999). MIF is also implicated in atherogenesis (Burger-Kentischer et al. 2006) as well as in accelerated atherosclerosis during hormone therapy with anti-inflammatory glucocorticoid hormones: Immune cell secretion of MIF is induced by these hormones, in contrast to other pro-inflammatory cytokines. In addition, MIF reverses glucocorticoid inhibition of IL-1β, IL-8, IL-10 and TNF-α (Calandra et al. 1995).There is also evidence that p53 deficiency leads to increased severity in both atherosclerosis and rheumatoid arthritis, adding to the potential role of MIF as a cause of accelerated development of atherosclerosis (Morand et al. 2006).

Homologs of MIF also occur in infective nematodes and malaria parasites, which seem to express MIF in order to modulate the host's immune response. These homologs have the same enzymatic activities as human MIF (Augustijn et al. 2007).

1.2.4 SIMPL domain-containing protein, Sim

The fourth selected gene encodes a 232 aa long protein, with the entire sequence coding for a signaling molecule that associates with the mouse pelle-like kinase (SIMPL) domain. It has the locus MCA_RS01535 (Ward et al. 2004).

In mammals, SIMPL is a signaling component required for tumor necrosis factor (TNF)-α dependent activation of NF-κB. TNF-α is a cytokine involved in regulation of hematopoietic cells. It activates mature cells, regulates proliferation, differentiation and survival and prevents uncontrolled expansion of hematopoietic stem cells (Benson et al. 2010). TNF-α binds to TNF receptor type I (TNF-RI) on the surface of the cell. This leads to activation of cytosolic SIMPL and the dissociation of the NF-κB-IkBα complex. NF-κB and SIMPL are separately localized to the cell's nucleus, where SIMPL functions as a coactivator of the NF-κB p65 subunit (Kwon et al. 2004). SIMPL has also been shown to be necessary for TNF-RI-dependent expression of NF-κB-controlled cytokines in endothelial cells (Benson et al. 2010). Functions in bacteria have not been studied. *sim* is the only one of the four genes studied here where a Signal-BLAST search reveals a signal sequence (Frank & Sippl 2008). This may imply it is located to the membrane or secreted into the surrounding environment by *M. capsulatus* Bath.

1.3 Lactic acid bacteria

Lactic acid bacteria (LAB) are a heterogeneous group of microaerophilic, Gram-positive bacteria, characterized by their ability to metabolize hexose sugars into lactic acid. Some species of LAB utilize a homofermentative pathway with lactic acid as the main product. Others use a heterofermentative pathway with lactic acid, CO_2, acetic acid and/or ethanol as the products (Makarova et al. 2006). LAB have been used by humans for food production and

preservation for thousands of years, and are designated Generally Recognized As Safe (GRAS) according to the US Food and Drug Administration and European Food Safety Authority (Bermudez-Humaran et al. 2013). Some species are naturally found in foodstuffs, while others inhabit the human gastrointestinal tract as commensal bacteria. Some species of LAB are classified as probiotics, which according to the World Health Organization are "live organisms that provide a benefit to the host when provided in adequate quantities" (Gareau et al. 2010).

Recombinant LAB have also been extensively investigated for their potential benefits to health, e.g. recombinant *Lactococcus* spp. and *Lactobacillus* spp. secreting anti-proteases to combat IBD, producing antioxidant enzymes or secreting anti-inflammatory cytokines. They are also good candidates for live vaccine delivery, as they interact with the intestinal mucosa and can deliver antigen to the intestinal immune cells (Bermudez-Humaran et al. 2013).

1.3.1 *Lactobacillus plantarum* WCFS1

L. plantarum is a versatile and flexible facultative heterofermentative LAB species which is found in dairy, meat, fish and plant-based food products as well as in the human gastrointestinal tract (Siezen et al. 2012). Kleerebezem et al. (2003) isolated a single colony, *L. plantarum* WCFS1, from the human saliva isolate *L. plantarum* NCIMB8826 and published its 3.3 Mb complete genome. This was the first *Lactobacillus* species to have its entire genome sequence published and it is now one of 26 strains with their genomes available in the NCBI database (van den Nieuwboer et al. 2016). The genome has subsequently been resequenced and reannotated on a more accurate Illumina platform (Siezen et al. 2012). *L. plantarum* WCFS1 is able to survive the passage of the human stomach and remain active, and can persist for up to 7 days in the gastrointestinal tract (Kleerebezem et al. 2003).

L. plantarum WCFS1 has one of the largest known genomes of *Lactobacillus* spp., which helps explain its environmental versatility. It has at least 293 genes involved in the degradation of sugars, it produces a large variety of surface-anchored proteins and has a high number of regulatory functions (van den Nieuwboer et al. 2016). It has a high transformation efficiency and a variety of systems used to express or knock out genes, including inducible

gene expression systems (Sørvig et al. 2003; Sørvig et al. 2005) and prophage-mediated genome engineering (Yang et al. 2015). Combined with the species' status as GRAS, this makes it valuable for use in research. It is also used in commercial probiotic blends such as VSL#3, which have beneficial effects on the intestinal epithelial barrier function. (Chapman et al. 2007; Madsen et al. 2001)

1.4 Inducible gene expression in lactic acid bacteria

Gene expression systems in LAB have been in development for several decades, and allow for overproduction of desired proteins (Kuipers et al. 1997). The gene expression systems may be constitutive or inducible. Constitutive systems allow for a high, constant production of proteins under control by strong promoters (Brurberg et al. 1994). Inducible systems are more flexible with regard to the desired protein, as they allow for production of toxic proteins or proteins which otherwise interfere with normal cellular processes. These systems should optimally have a low basal production of the protein, and a high production when induced.

Quorum sensing is a process where induction of gene expression by a molecule only happens when a certain concentration of the molecule is reached. Several species of LAB use quorum sensing to produce antimicrobial peptides (Kuipers et al. 1998). Nisin, a lanbiotic produced by *Lacotococcus lactis*, is used in the nisin-controlled expression (NICE) system developed by de Ruyter et al. (1996). It is a two-component regulatory system where nisin is used to activate a histidine-protein kinase (HK). The HK is autophosphorylated and subsequently phosphorylates a response regulator (RR) which activates the *nisA* or *nisF* promoters, initiating transcription. By inserting a sequence coding for a desired protein downstream of *nisA* or *nisF*, the gene can be expressed in high amounts (Kuipers et al. 1998). A two-plasmid NICE system was developed for expression in other LAB by Kleerebezem et al. (1997), then a single-plasmid system was developed by Pavan et al. (2000). However, the NICE system shows considerable basal activity in *L. plantarum*, and Sørvig et al. (2003) therefore developed the pSIP vector expression system.

The pSIP vectors are circular plasmids which consist of cassettes; subunits which are easily exchangeable using restriction enzyme digestion and ligation. This enables a great deal of flexibility in what genes the vector contains. Although the mechanism differs from nisin

regulation, the pSIP system is also based on quorum sensing. It utilizes three genes in the regulatory operon for production of the class II bacteriocins sakacin A (*sap* genes) and sakacin P (*spp* genes), with the pSIP300-series being *sap*-based and the pSIP400 series being *spp*-based. The first gene encodes a peptide pheromone precursor, also known as an inducible peptide (IP). In pSIP300 and pSIP400, the native pheromone gene has been deleted to minimize basal activity, whereas in pSIP301 and pSIP401 they are replaced with a mutated, non-functional version with its cognate promoter (P_{SapIP} or P_{SppIP}, respectively) intact. See Fig. 1.2 for a schematic overview of pSIP401.The second gene encodes a pheromone-sensing HK, and the third a cognate RR. When activated by the IP, the HK activates the RR via a series of phosphorylations. The RR then activates the inducible promoters P_{SppA} and P_{SppIP}. The gene of interest, which is cloned into the vector downstream of P_{SppA}, is expressed, as are the HK- and RR-encoding genes, amplifying the induction signal and leading to overproduction of protein (Sørvig et al. 2003; Sørvig et al. 2005). In addition, an antibiotic resistance gene is generally included to avoid vector instability. This ensures that only bacteria carrying the exogenous plasmid will survive in a medium with appropriate antibiotics added (Fakruddin et al. 2013). The amount of protein produced in a batch fermentation can also be increased by controlling external factors, such as temperature, pH and glucose concentration in the growth medium, leading to a higher biomass of bacteria per volume of medium used (Nguyen, T. T. et al. 2015).

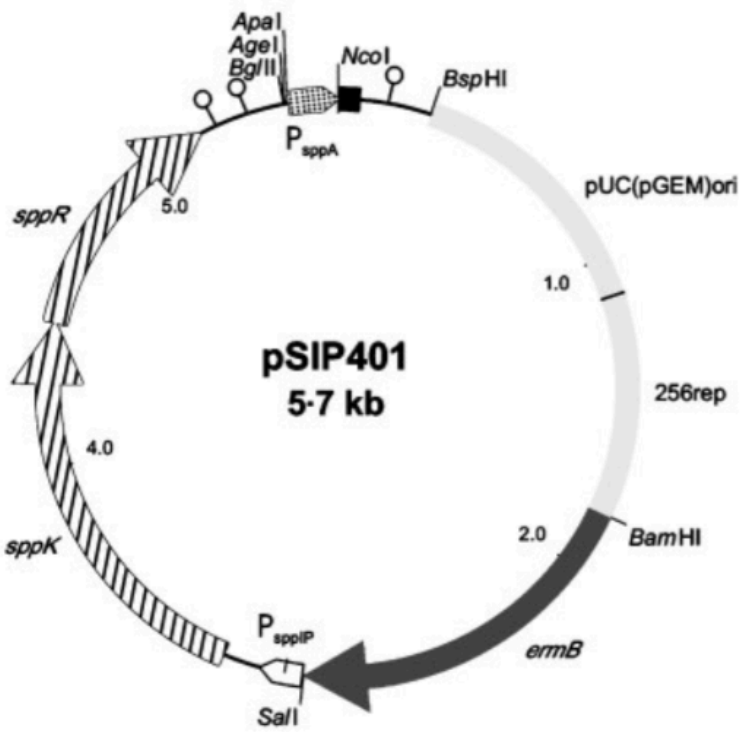

Figure 1.2. pSIP401, a vector in the pSIP400 series. Light grey regions, replication determinants pUC(pGEM)ori from *E. coli* and 256rep from *L.* plantarum; dark gray region, erythromycin resistance gene *ermB*; white region, inducible promoter P_{sppIP}; vertically hatched regions, HK and RR genes *sppK* and *sppR*; dotted region, inducible promoter P_{sppA}; black region, multicloning site where target genes are cloned. Figure modified from Sørvig et al. (2005).

1.5 The human mucosal immune system

The human mucosal immune system is associated with the various mucous membranes in the body, such as the oral, nasal, gastrointestinal or vagal mucosae. These mucous membranes vary in morphology and anatomy based on location, but all are made up of an epithelial cell layer and a deeper layer of connective tissue called the lamina propria. In the intestinal mucosa, a thin layer of muscle called the muscularis mucosae lies below the lamina propria. Deeper structures include a layer of connective tissue called the submucosa as well as more layers of muscle. See Fig. 1.3 for an overview.

The epithelial cell layer is a heterogeneous, single-cell layer that contains specialized cells which are held together by tight junctions. It is selectively permeable to both digested nutrients and bacterial metabolites (Lea 2015b). In the small intestine, the epithelium is

shaped into myriad finger-like protrusions called villi. Between the villi are invaginations called crypts of Lieberkühn, which, unlike the villi, also are found in the large intestine. The epithelial layer is under constant renewal from multipotent stem cells found in the crypts. They give rise to specialized epithelial cells, which migrate toward the tips of the villi, where they eventually become apoptotic and are sloughed off after 4-5 days (Mowat & Agace 2014).

The cell types which make up the epithelium have a variety of functions, related to the absorption of nutrients or secrettion of various molecules into the lumen: The nutrient-absorbing enterocytes in the small intestine are characterized by numerous microvilli, called the brush border, on the apical side. The combination of villi and brush border lead to a large intestinal surface area (historically approximated to be 250-300 m^2, although more recent data suggest it is around 30-40 m^2 (Helander & Fandriks 2014)) in an adult human. Enterocytes in the colon lack microvilli and absorb water and ions via passive diffusion (Hooper et al. 2012). Goblet cells produce mucins, the main component in the viscous layer of mucus covering the membrane. In addition to being a physical barrier between the epithelial layer and microbiota, the mucus traps secreted antimicrobial peptides (AMPs) and secretory immunoglobulin A (SIgA). The small intestine contains a single layer of mucus, while the colon contains a two-layered system with the inner layer mostly impermeable to the larger amount of bacteria in the colon (Lea 2015b). Paneth cells, found in the small intestine, migrate to the bottom of the crypt where they produce AMPs such as lysozyme and defensins. Additionally, microfold cells (M cells) are localized over mucosal lymphoid structures, such as Peyer's patches, and mediate sampling of luminal antigens and microorganisms to the mucosal immune system (Peterson & Artis 2014). Intraepithelial lymphocytes and hormone-producing enteroendocrine cells are also found in the epithelial layer (Mowat & Agace 2014).

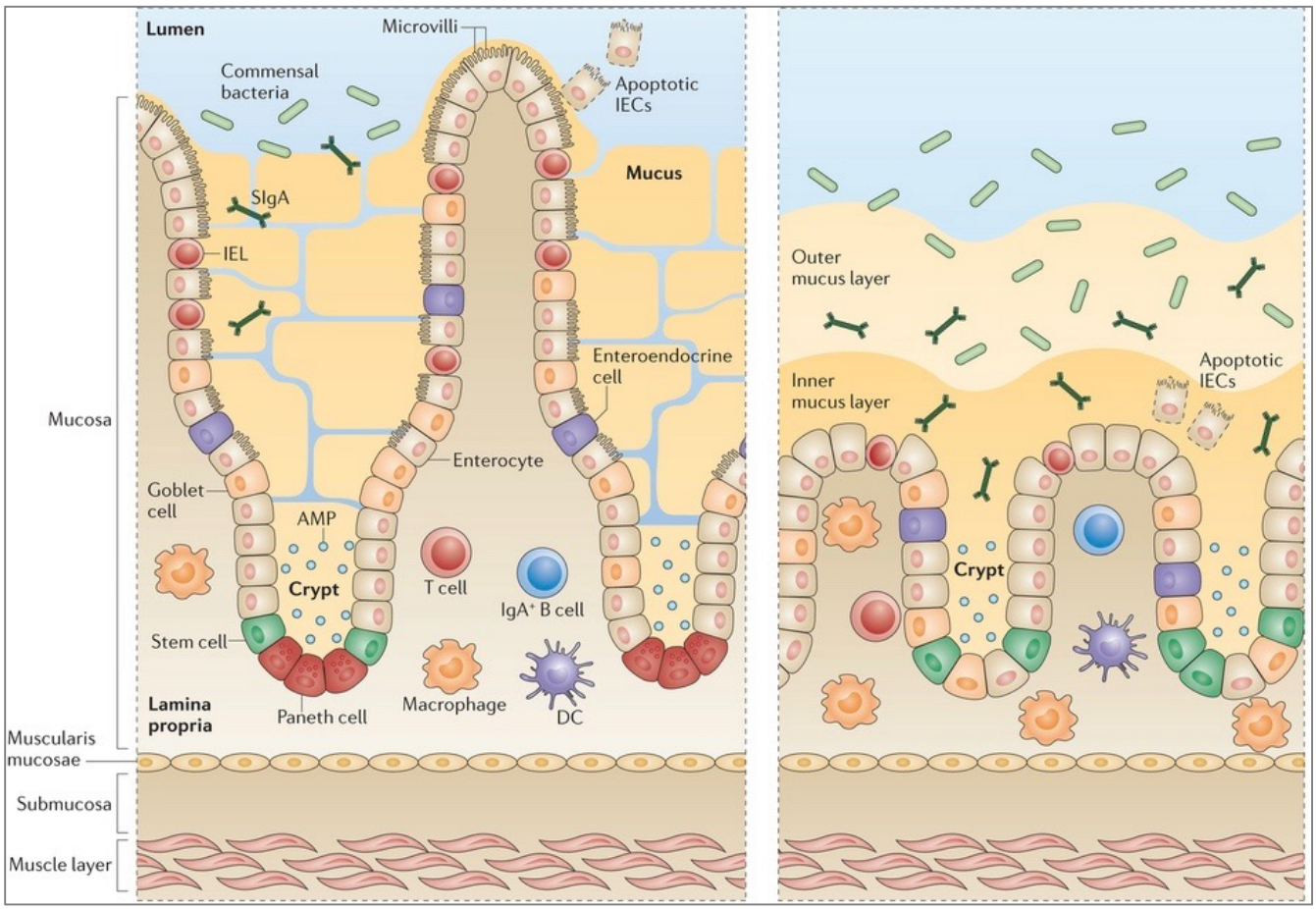

Figure 1.3. Schematic depiction of the mucosa of the jejunum (left) and colon (right). The various cell types found in the epithelial layer and lamina propria are indicated, as are commensal bacteria (green rods), shown in the gut lumen. AMP, antimicrobial peptide; DC, dendritic cell; IEC, intestinal epithelial cell; IEL, intraepithelial lymphocytes; SIgA, secreted IgA. Figure adapted from Mowat and Agace (2014).

Beneath the epithelial layer, the lamina propria hosts immune cells like B cells, T cells and antigen presenting cells (APCs) such as DCs. APCs sample foreign material such as bacteria or viruses directly from the gut lumen, process them and present them on MHC class II molecules to T cells in the mesenteric lymph nodes (Iwasaki & Medzhitov 2010).

The vertebrate immune system consists of two branches; innate and adaptive immunity. The innate system includes macrophages, neutrophils, dendritic cells (DCs) and innate lymphoid cells (ILCs), among others. It is programmed to detect MAMPs, invariant molecular patterns, via PRRs on the innate immune cells and to respond quickly. There are three broad classes of PRRs: secreted, transmembrane and cytosolic. Binding of a MAMP to a PRR initiates a signal transduction pathway leading to gene transcription and the expression of downstream effector molecules (Iwasaki & Medzhitov 2010).

The adaptive immune system differs from the innate immune system in that it is represented by B and T lymphocytes; cells with antigen specificity. Naïve T cells have two subtypes, $CD4^+$ and $CD8^+$, which become mature T cells when stimulated by antigens presented on MHC class I or II molecules. Class I is found on all cell types, while class II is found on APCs (Cella et al. 1997). When an antigen is presented to a naïve $CD8^+$ T cell by an MHC class I molecule, the T cell may become stimulated to differentiate into an active cytotoxic T cell (T_C) that can kill infected host cells. Antigens presented by MHC class II molecules stimulate activation of naïve $CD4^+$ T cells, also known as T helper (T_H) cells. Depending on a variety of factors, e.g. the cytokines in the environment, the type of APC and the antigen presented, the T_H cell will differentiate into specific subtypes with unique effector cytokine profiles and functions. These subtypes can then promote different inflammatory responses (Akdis et al. 2011). Additionally, $CD4^+$ T cells can differentiate into regulatory T cells (Treg) (Bettelli et al. 2006). Tregs are anti-inflammatory, they hinder autoimmunity and dampen inflammation after pathogens have been eradicated (Lee & Mazmanian 2010).

Naïve B cells may be activated and stimulated to differentiate by a variety of factors such as binding of TLR ligands, presence of bacterial DNA or interactions with T_{FH} cells (Hua & Hou 2013; Krieg et al. 1995; Vinuesa et al. 2005). The main effector B cell is the plasma cell. Plasma cells produce and secrete antigen-specific antibodies, immunoglobulins (Ig), of different classes depending on input from T_H cells. Naïve B cells may also express MHC class II molecules and thus act as APCs for T cells (Lee & Mazmanian 2010).

The adaptive immune system is closely linked to the microbiota, with recent evidence showing that commensal bacteria may help "program" aspects of T cell differentiation: In mice, segmented filamentous bacteria, which adhere tightly to the mucosa, drive production of T_H17-inducing cytokines in the lamina propria, inducing a non-pathological inflammatory response which is protective against pathogenic infections (Lee & Mazmanian 2010)

1.5.1 The intestinal microbiota

On the external or internal body surfaces of most vertebrates, a large community of microorganisms exists, called the microbiota. Humans are colonized with this microbiota naturally at birth, and the complex interplay between the host and microbiota can be referred

to as a symbiotic ecosystem. (Gareau et al. 2010). The microbiota is mostly made up of bacteria, with a core set of species found in all humans, as well as a highly variable set of species for each individual, associated with factors such as diet, levels of body fat and disease (Lankelma et al. 2015; Le Chatelier et al. 2013; Manichanh et al. 2012; Tremaroli & Backhed 2012). The amount of bacterial cells in the gut is traditionally estimated to be 10 times larger than the amount of cells in the human host (newer estimates are around 1:1 (Sender et al. 2016)), and the microbiome is approximately 150 times larger than the human genome (Lankelma et al. 2015). The intestinal microbiota is essential for correct development of the host's immune system, as shown in germ-free or gnotobiotic animal models which develop abnormal intestinal anatomy: gnotobiotic mice, pigs and dogs all have a reduced amount of lamina propria and mucosal surface area, smaller Peyer's patches and shallower crypts (Thompson & Trexler 1971). Although the relationship is symbiotic, the interactions are normally strictly controlled by the host, as an invasion by bacteria can lead to serious consequences including inflammation or sepsis (Hooper et al. 2012).
The commensal bacteria degrade nutrients ingested by the host, many of which are non-digestible, and convert them into digestible substances. One such example is resistant starches, which are degraded mainly by bacteria from the phylum *Bacteroidetes* into short-chain fatty acids (SCFA). SCFAs are absorbed by epithelial cells for energy use. Some kinds, especially C2:0 (acetic acid), C3:0 (propionic acid) and C4:0 (butyric acid) also have anti-inflammatory and immune-signaling effects (Lankelma et al. 2015). In addition, the types of nutrients ingested by the host or produced by endogenous bacterial species directly shape the structure of the microbiota (Hooper et al. 2012). There is also evidence that the gut microbiota influences biological markers internal to the host, e.g. with fecal transplants from healthy individuals increasing insulin sensitivity in individuals with metabolic syndrome (van Nood et al. 2013; Vrieze et al. 2012).

While some species of bacteria are pathogenic and directly linked to diseases, others are linked to a healthy intestine. *Akkermansia muciniphila* is a Gram-negative bacterium which normally constitutes 3-5 % of the gut microbial population and which may play a key role in the pathophysiology of metabolic syndrome, obesity and type II diabetes (Everard et al. 2013). *Faecalibacterium prausnitzii* is another species with proven anti-inflammatory effects, some of which are related to its secretion of MAM (See section 1.2.1). It constitutes between 5 and 15 % of the total fecal microbiota in healthy adults (Miquel et al. 2013). *A. muciniphila* and *F. prausnitzii* also produce the anti-inflammatory SCFA propionate and butyrate,

respectively (Lankelma et al. 2015). However, unlike these species, *M. capsulatus* Bath is peculiar in that it has anti-inflammatory effects despite being a non-commensal bacterium.

Anti-inflammatory species such as *F. prausnitzii* and *A. muciniphila* are more prevalent in individuals who have a microbiota with high genetic diversity, while potentially pro-inflammatory *Bacteroides* and *Ruminococcus gnavus* are found with higher frequency in lower genetic diversity individuals, and are associated with inflammatory bowel disease (IBD) (Le Chatelier et al. 2013). IBD involves chronic inflammation of the intestinal mucosa in either parts of or the whole digestive tract. The primary constituents of IBD are ulcerative colitis and Crohn's disease. It is believed to be the result of a complex interaction of environmental, genetic and immunological factors. One of these factors is a dysfunctional host immune response to normal luminal components, or vice versa. The mucus layer covering the epithelial layer also becomes more permeable to bacteria in both experimental models of IBD and *in vivo* (Bischoff et al. 2014). IBD patients also have lower genetic diversity in their microbiota compared to healthy subjects (Lankelma et al. 2015).

Diet may also play a role in the onset of IBD. A high fat diet in mice leads to increased absorption of LPS, which is a component of the outer membrane of Gram-negative bacteria. LPS in the plasma triggers the release of cytokines that are key inducers of insulin resistance, which is associated with metabolic syndrome (Cani et al. 2007). IFNγ-producing ILCs, if chronically activated, can induce inflammation at the mucosal barriers and may also be a contributing factor to IBD (Artis & Spits 2015). Helminths may also play a role in the prevalence of IBD. Some research shows a much lower incidence of IBD in populations with endemic helminth colonization, compared to populations without (Ramanan et al. 2016).

Many experimental studies are performed in murine models. The similarities between mouse and human are numerous, involving anatomy, physiology and genetics, with only around 300 genes unique to each species (Mestas & Hughes 2004). Further, years of research in murine models have led to extensive knowledge about immunology, gastroenterology and genetics. In addition, it is relatively easy to control the genetic background of mice, creating inbred animals with a variety of knockout genes to illuminate specific mechanisms in host-microbiota interactions. They also have a relatively short life cycle and low maintenance cost (Mestas & Hughes 2004; Nguyen, T. L. A. et al. 2015). However, there are differences to keep in mind between the two species. Both the innate and adaptive immune systems differ,

e.g. with regard to defensin secretion in the gut, balance between lymphocytes and neutrophils in blood and types of antibodies generated by B-cells (Mestas & Hughes 2004). The microbiota is also species-specific, as is cross-talk between the host's immune system and its microbiota (Nguyen, T. L. A. et al. 2015). Another important point to consider when using murine models is that animals with the same genotype will have variable microbiota compositions. This varies depending on the conditions in the laboratory where the mice are maintained as well as the supplier of the animals. This could lead to conflicting results in otherwise similar murine trials concerning intestinal immunity (Hooper et al. 2012).

1.6 The Caco-2 cell line

The Caco-2 (Cancer coli-2) cell line was one of several epithelial cell lines established from gastrointestinal tumors in the 1970s (Fogh et al. 1977). Because of difficulties in obtaining differentiated intestinal cell lines from normal tissue, these tumor cell lines were re-examined a decade later. As opposed to the other lines, the Caco-2 line spontaneously differentiated in long-term cultures into cells with morphological and biochemical characteristics similar to small intestinal enterocytes. They grow in monolayers which develop microvilli on the apical side, tight junctions between cells and small intestine hydrolase enzyme activity. For this reason, they are commonly used as approximations of small intestine enterocytes *in vitro* (Sambuy et al. 2005).

Caco-2 cells can be grown on permeable filters in order to provide a closer approximation to the epithelial cell layer *in vivo*. The permeability of a polarized Caco-2 monolayer has a high correlation to absorption data from studies performed on humans, where drugs or other compounds are absorbed orally (Lea 2015a). However, as a Caco-2 monolayer is relatively homogenous, they only give an indication of the situation in the small intestine, which also involves the interplay between several types of epithelial cells as well as immune cells in the lamina propria. Their enzyme profile also suggests a closer resemblance to fetal than adult enterocytes (Sambuy et al. 2005).

1.7 Goals of the study

There were three main goals of the present study. First, selected genes from *M. capsulatus* Bath had to be cloned prior to overexpression in *L. plantarum* WCFS1, using an inducible vector expression system. The genes were also to be overexpressed in *E. coli* BL21 for production of purified protein. Second, one of the proteins, Mam, was to be produced in a large-scale system using a bioreactor. The bacterial biomass was then to be lyophilized and used as a bacterial meal in the diet in a future murine trial. Finally, functional effects of the overexpressed proteins in *L. plantarum* and *E. coli* were to be studied in a simplified model of the human epithelial layer, using the Caco-2 cell line. The vector used for overexpression in *L. plantarum* was modified from a plasmid constructed by Øverland (2013), while the vector used for expression in *E. coli* BL21 was constructed by Gileadi (2006) and provided by the PEP group at NMBU.

2. MATERIALS

2.1 Laboratory equipment

Laboratory equipment	Supplier
Amicon® Ultra 15 ml Centrifugal Filters Ultracel® 3K, 10K MWCO	Millipore
CL-Xposure™ Film	Thermo Scientific
Cuvettes	
Disposable cuvettes, 1,5 ml semi-micro	Brand
Gene Pulser® Cuvette, 0.2 cm	Bio-Rad Laboratories
Falcon® Tissue Culture Plates, Multiwell 6, 24 and 96 well	Corning
Falcon® Cell Culture Inserts 0.4 micron PET	Corning
Falcon® Tissue Culture Flasks with vented cap, 250 ml	Corning
Filtropur S 0.2 syringe filters	Sarstedt
Glassware	Schott, VWR
Glass beads, acid-washed ≤106 μm (−140 U.S. sieve)	Sigma
GP Millipore Express® PLUS Membrane 250ml Funnel (0.22 μM)	Millipore
Macrosep® Advance Centrifugal Device 10K MWCO	Pall Corporation
Pipettes	
Finnpipette® F2 (0,2-2, 1-10, 5-50, 40-200, 100-1000 μL)	Thermo Scientific VWR
Pipet tips (0.1-10, 1-200, 100-1250 μL)	
Ovation® BioNatural Pipette (100-1000 μL)	VistaLab Technologies
Pipet tips with filtered tips (100-1250 μL)	
Serological Pipette, 5, 10 and 25 ml	Sarstedt
SnakeSkin® Dialysis Tubing (MWCO 10 000)	Thermo Scientific
Spectra/Por® Membrane (MWCO 3500)	Spectrum
Spectra/Por® Closures	
Syringes, with Luer-lock, 1-50 ml	BD Plastipak™
Tubes	

Cellstar® Tubes 15 ml and 50 ml	greiner bio one
Corex tubes	Corning Inc.
FastPrep® Tubes and Blue Caps	MP Biomedicals
Microtubes 1,5 ml and 2,0 ml, clear	Axygen
Micro tube 2ml, PP	Sarstedt
QuBit Assay tubes	Thermo Fisher
PCR tubes 0.2 ml	Axygen
Tube 13 ml, PP	Sarstedt

2.2 Instruments

Laboratory Instruments	**Supplier**
827 pH lab pH-meter	Metrohm
Primatrode with NTC	
Azure c400	Azure biosystems
Benchtop UV Transilluminator	UVP
BioLogic LP	Bio-Rad
Econo-Column Chromatography columns (1.0 x 10 cm)	
BioPhotometer	Eppendorf Bio Tools
Carver Laboratory Press, Model C	Fred S. Carver, Inc.
40 ml French pressure cell	
Centrifuges	
Allegra X-30R Centrifuge	Beckman Coulter
Avanti™ J-25 Centrifuge	
Avanti J-26S XP Centrifuge	
Eppendorf Centrifuge 5418 R	Eppendorf Bio Tools
Heraeus Multifuge X1R centrifuge	Thermo Scientific™
Heraeus MegaFuge 1.0	
Mini Star silverline tabletop centrifuge	VWR
CertoClav CV-EL	OneMed
Countess® II Automated Cell Counter	life technologies
Countess™ cell counting chamber slides	Invitrogen

E-POD® Elix	Millipore
EVOM^2 Epithelial Voltohmmeter	World Precision
ENDOHM-6 Probe for EVOM^2	Instruments
FastPrep® FP120	MP Biomedicals LLC.
Gel Doc™ EZ Imager	Bio-Rad
Stain-Free Tray	
UV Tray	
Gene Pulser® II	Bio-Rad
Pulse Controller Plus	
Glass Autoclavable Lab Scale Bioreactor, 3 liter, jacketed	Applikon
Glass Autoclavable Lab Scale Bioreactor, 15 liter, jacketed	Biotechnology
ADI 1030 Bio Controller	
ADI 1000 Stirrer Controller P100	
ADI 1032 Stirrer Controller P140, i=2	
ADI 1018 Thermo Circulator	
Masterflex® L/S® easy-load peristaltic pump	
	Cole-Parmer
Heto Drywinner Freeze Drier	Thermo Fisher
iBlot™ Gel Transfer Device	Invitrogen™
LEX-48 Bioreactor	Harbinger Biotech
MD142 microwave oven	Whirlpool
MS 3 basic shaker	IKA®
Mini-PROTEAN® Tetra Cell	Bio-Rad
Mini-PROTEAN Tetra Electrode Assembly	
Mini Cell Buffer Dams	
Buffer Tank and Lid	
PowerPac 300	
Mini-Sub® Cell GT Cell	Bio-Rad
Mini-Gel Caster	
Sub-Cell GT UV-Transparent Mini-Gel Tray	
8-Well and 15-Well Comb	
PowerPac™ Basic	
Qubit™ fluorometer	Invitrogen

RCT classic safety control magnetic stirrer	IKA®
SimpliAmp Thermal Cycler	life technologies
SNAP i.d.® 2.0	Millipore
Steri-Cycle CO2 Incubator	Thermo
TECAN Sunrise™ Microplate reader	TECAN
Ultrospec 10 Cell density meter	Amersham Biosciences
VACUSAFE comfort	Integra Biosciences
VACUBOY	
VCP 80 pump, vacuum/press	VWR
Vibra-Cell VCX 500	Sonics & Materials, Inc.
Water baths	
Julabo® heating immersion circulator (MP, MB and ED)	Julabo
SBB Aqua 5 Plus water bath	Grant
Weights	
PJ3600 DeltaRange®	METTLER TOLEDO
LC621P	Sartorius

2.3 Software

Software	**Supplier**
Image Lab 4.1	Bio-Rad
CLC Main Workbench	CLC bio
LP Data View 1.03	Bio-Rad
cSeries Capture Software	Azure biosystems
Magellan™	TECAN
pDraw32	AcaClone software

2.4 Chemicals

Chemical	**Supplier**

1,4-Dithiothreitol (DTT), $C_4H_{10}O_2S_2$	Sigma-Aldrich
Ampicillin, $C_{16}H_{19}N_3O_4S$	Sigma-Aldrich
Antifoam 204	Sigma-Aldrich
D-(+)-glucose, $C_6H_{12}O_6$	Sigma
Dipotassium hydrogen phosphate, K_2HPO_4	Merck
Disodium hydrogen phosphate, Na_2HPO_4	Merck
EDTA, $C_{10}H_{16}N_2O_8$	Merck
Erythromycin, $C_{37}H_{67}NO_{13}$	Sigma-Aldrich
Ethanol, C_2H_5OH	Arcus
Gentamicin, $C_{21}H_{43}N_5O_7$	Sigma
Glycerol, $C_3H_8O_3$	Merck
Glycine, $C_2H_5NO_2$	Merck
IPTG, $C_9H_{18}O_5S$	Sigma-Aldrich
Kanamycin sulfate, $C_{18}H_{36}N_4O_{11}$	Sigma-Aldrich
Magnesium chloride, $MgCl_2$	Sigma
Magnesium sulfate, MgSO4	Sigma
peqGreen DNA/RNA Dye	VWR peqlab
Phenylmethane sulfonyl fluoride (PMSF), $C_7H_7FO_2S$	Sigma
Polyethylene glycol (PEG1450), $H(OCH_2CH_2)_nOH$	Sigma-Aldrich
Potassium chloride, KCl	Merck
Potassium dihydrogen phosphate, KH_2PO_4	Merck
Protein Assay Dye Reagent Concentrate	Bio-Rad
Protino® Ni-NTA Agarose	Macherey-Nagel
SeaKem® LE Agarose	Lonza
Sodium chloride, NaCl	VWR
Sodium hydroxide, NaOH	Sigma-Aldrich
Sucrose, $C_{12}H_{22}O_{11}$	Sigma
Technical Buffer Solution pH 4.01	METTLER TOLEDO
Technical Buffer Solution pH 7.00	METTLER TOLEDO
Tris base, $C_4H_{11}NO_3$	Sigma
Tris HCl, $C_4H_{11}NO_3$ HCl	Sigma
Trypan Blue Solution, 0.4%	Amresco®
Tween-20	Sigma-Aldrich

Urea, CH_4N_2O	Sigma-Aldrich

2.5 Proteins and enzymes

Protein/enzyme	**Supplier**
Antibodies	
Anti-*myc* (Monoclonal anti-mouse IgG1, c-Myc)	Invitrogen
Polyclonal Rabbit Anti-Mouse Immunglobulin HRP	Dako
Bovine Serum Albumin (BSA)	Sigma-Aldrich
Fetal Calf Serum (FCS)	PAA
Inducer peptide (SppIP)	Sigma
5X In-Fusion HD Enzyme Premix	Invitrogen
Protein standards	
MagicMark™ XP Western Standard	
Q5® High-Fidelity DNA Polymerase	New England BioLabs
2X Quick Ligation Buffer	New England BioLabs
Quick T4 DNA Ligase	New England BioLabs
Recombinant human interleukin-1β (IL-1β)	Immunotools
Recombinant human tumor necrosis factor α (TNF-α)	Immunotools
Red Taq DNA Polymerase Master Mix	VWR
Restriction enzymes and buffers	
BglI	New England Biolabs
BsmI	
10x CutSmart® Buffer	
10x FastDigest® Green Buffer	Thermo Fisher
FastDigest® HindIII	
FastDigest® NdeI	
NEBuffer 2	New England Biolabs
NEBuffer 3.1	
T4 DNA Polymerase	New England Biolabs
Trypsin-EDTA Solution 1X	Sigma
Tryptone	Sigma

2.6 DNA

DNA	Supplier
dGTP-mix, 10 mM	New England Biolabs
DNA standards	
BenchMark™ 1 kb DNA ladder	Invitrogen
dNTP-mix, 10 mM	New England Biolabs

2.7 Primers

The primers used in this thesis are listed in Table 2.1, while their purposes are listed in Table 2.2.

Table 2.1. Primer sequences

Name	Sequence (5'-3')	Restriction site in sequence
Mam_F	TTAAGAAGGAGATATACTATGCCATTAGCTGTTTTAGA	
Mam_R	AATGGTGGTGATGATGGTGCGCTGCAACAAACAAATCAACT	
Mif_F	TTAAGAAGGAGATATACTATGCCATACTTGAAGATTCA	
Mif_R	AATGGTGGTGATGATGGTGCGCAAACGTTGAACCGTTCC	
Simpl_Myc_F	TTAAGAAGGAGATATACTATGGATGAACAAACTCCT	
Simpl_Myc_R	AATGGTGGTGATGATGGTGCGCATCCGCTTGTAATTCAATC	
SimplF	GGAGTATGATTcatatgGATGAACAAACTCCTTTAACCT	NdeI
SimplR1	TTCACTAATTAACTTTTGTTCATCCTGCTTGTAATTCAATC	
SimplR2	CTGTAATTTGaagcttTCATAAATCTTCTTCACTAATTAACTTTTGTTCATCC	HindIII
Sek_NicF	GGGGAATTGTGAGCGGAT	

Sek_NicR	GGGGTTATGCTAGTTATTGCT	
SekF	GGCTTTTATAATATGAGATAATGCCGAC	
SekR	GCCTTGACGAACTAaagcttC	HindIII
SeqRR	AGTAATTGCTTTATCAACTGCTGC	
Tir2_F	TTAAGAAGGAGATATACTATGACTGCACCAAAAGTTTT TGTTA	
Tir2_R	AATGGTGGTGATGATGGTGCGCAGCTGATTGCAATGCC	

Restriction sites are indicated with lowercase letters.

Table 2.2. Primer descriptions

Name	**Description**
Mam_F	Forward primer for addition of His-tag to Mam
Mam_R	Reverse primer for addition of His-tag to Mam
Mif_F	Forward primer for addition of His-tag to Mif
Mif_R	Reverse primer for addition of His-tag to Mif
Simpl_Myc_F	Forward primer for addition of His-tag to Simpl
Simpl_Myc_R	Reverse primer for addition of His-tag to Simpl
SimplF	Forward primer for addition of Myc-tag to Simpl
SimplR1	Reverse primer for addition of Myc-tag to Simpl
SimplR2	Reverse primer for addition of Myc-tag to Simpl
Sek_NicF	Forward primer for sequencing of inserts in pNIC-CH-vector
Sek_NicR	Reverse primer for sequencing of inserts in pNIC-CH-vector
SekR	Reverse primer for sequencing of inserts in pSIP401-vector
SekF	Forward primer for sequencing of inserts in pSIP401-vector
SeqRR	Reverse primer for sequencing of Simpl without Myc in pSIP401-vector
Tir2_F	Forward primer for addition of His-tag to Tir2
Tir2_R	Reverse primer for addition of His-tag to Tir2

2.8 Bacterial strains and plasmids, cell lines

Bacterial strains, plasmids and human cell lines used in this thesis are listed in Table 2.3, Table 2.4 and Table 2.5.

Table 2.3. Bacterial strains

Strain	**Source**
Escherichia coli GeneHogs®	Thermo Fisher
Escherichia coli TOP10	Invitrogen
Escherichia coli BL21	Thermo Fisher
Lactobacillus plantarum WCFS1	Kleerebezem et al. (2003)

Table 2.4. Plasmids

Plasmid	**Description**	**Source**
pEV	Empty vector, pSIP401-derivative without insert.	(Øverland 2013)
pNIC-CH	Expression vector with C-terminal His_6 tag, for protein production in *E. coli*. Gene of interest under control of IPTG-inducible promoter. Contains Kan^R. Contains the SacB gene, allowing negative selection on 5 % sucrose.	(Gileadi 2006)
pNIC-CH_MAM	pNIC-CH-derivative with *mam* as target gene. Contains Kan^R	This study
pNIC-CH_MIF	pNIC-CH-derivative with *mif* as target gene. Contains Kan^R	This study
pNIC-CH_SIMPL	pNIC-CH-derivative with *sim* as target gene. Contains Kan^R	This study
pNIC-CH_TIR2	pNIC-CH-derivative with *tir* as target gene. Contains Kan^R	This study
pSIP401	*spp*-based expression vector for heterologous protein production in	Sørvig et al. (2003)

	Lactobacillus, expression induced with SppIP. Contains Em^R.	
pSIP401_MAM	pSIP401 derivative with *mam* as target gene. Contains Em^R	This study
pSIP401_MIF	pSIP401 derivative with *mif* as target gene. Contains Em^R	This study
pSIP401_SIMPL	pSIP401 derivative with *sim* as target gene. Contains Em^R	This study
pSIP401_TIR2	pSIP401 derivative with *tir* as target gene. Contains Em^R	This study
pUC57	pUC57 derivatives with target genes were used as templates for PCR amplification. Contains Amp^R	GenScript

Table 2.5. Cell lines

Cell line	**Source**
Caco-2	Sigma

2.9 Kits

Kit	**Supplier**
Human IL-8 ELISA Development Kit	PeproTech®
Capture Antibody	
Detection Antibody	
Human IL-8 Standard	
Avidin-HRP Conjugate	
iBlot™ Gel Transfer Stack Nitrocellulose, Mini	novex® by life
iBlot™ Transfer Stack, Mini	technologies
iBlot™ Cathode Stack, Top	
iBlot™ Anode Stack, Bottom	

iBlot™ Disposable Sponge	
iBlot™ Filter Paper	
Blotting roller	
SNAP i.d.® 2.0 Mini Blot Holders	Millipore
Spacers	
Blot roller	
SuperSignal® West Pico Chemiluminescent Substrate	Thermo Scientific
Luminol/Enhancer Solution	
Stable Peroxide Buffer	
NucleoSpin® Plasmid	Macherey-Nagel
NucleoSpin® Plasmid Column and Collection Tube (2 ml)	
Resuspension Buffer A1	
Lysis Buffer A2	
Neutralization Buffer A3	
Wash Buffer AW	
Wash Buffer A4	
Elution Buffer AE	
NucleoSpin® Gel and PCR Clean-up	Macherey-Nagel
NucleoSpin® Extract II Column and Collection Tube (2 ml)	
Binding Buffer NTI	
Wash Buffer NT3	
Elution Buffer NE	
Qubit® dsDNA BR Kit	invitrogen
Qubit® dsDNA BR Standard #1	
Qubit® dsDNA BR Standard #2	
Qubit® dsDNA BR Buffer	
Qubit® dsDNA BR Reagent	
Qubit® Protein Assay Kit	invitrogen
Qubit® Protein Standard #1	
Qubit® Protein Standard #2	
Qubit® Protein Standard #3	

Qubit® Protein Reagent

Qubit® Protein Buffer

SDS-PAGE

Mini-PROTEAN® TGX Stain-Free™ Precast Gels	Bio-Rad
NuPAGE® LDS Sample Buffer (4x)	Invitrogen
NuPAGE® Sample Reducing Agent (10x)	Invitrogen

2.10 Agar and media

Medium	**Supplier**
BHI (Brain-Heart-Infusion)	Oxoid

Medium:

37 g BHI

dH_2O to 1 L

Mixed on a magnet stirrer and sterilized for 15 minutes at 115° C.

Stored at room temperature without light.

Addition of appropriate antibiotics when using: See table 3.1.

Agar:

37 g BHI

16 g agar (1.5 % w/v)

dH_2O to 1 L

Mixed on a magnet stirrer and sterilized for 15 minutes at 115° C.

Addition of antibiotics after cooling to approx. 60° C: See table 3.1.

Approx. 20 ml per dish poured into petri dishes.

Stored at 4° C without light.

BHI + sucrose	Oxoid

Agar:

BHI medium

1.5 % (w/v) agar

2 % (w/v) sucrose

Procedure as with BHI agar.

Sucrose sterile filtered (0.2 micron filter) and added after autoclaving.

MRS (de Man, Rogosa, Sharpe) Oxoid

Medium:

52 g MRS

dH_2O to 1 L

Mixed on a magnet stirrer and sterilized for 15 minutes at 115° C.

Stored at room temperature, no light.

Addition of appropriate antibiotics when using: See table 3.1

Agar:

52 g MRS

16 g agar

dH_2O to 1 L

Mixed on a magnet stirrer and sterilized for 15 minutes at 115° C.

Addition of antibiotics after cooling to approx. 60° C: See table 3.1.

Approx. 20 ml per dish poured into petri dishes.

Stored at 4° C, no light.

MRSSM

MRS medium Oxoid

0.5 M sucrose Sigma

0.1 M $MgCl_2$

Sterile filtered with a 0.2 micron filter.

Stored at room temperature without light.

MRS + glycine

MRS medium Oxoid

1% (w/v) glycine Merck

Sterile filtered (0.2 micron filter).

Stored at room temperature without light.

RPMI-1640 medium	Sigma
Pre-mixed from supplier.	
Complete RPMI-1640 (cRPMI)	
500 ml RPMI-1640 Medium	Sigma
10% (v/v) Fecal Calf Serum	PAA
5 ml ME Nonessential Amino Acids 100 x	Laboratories
5 ml 100 mM Sodium pyruvate	Sigma Aldrich
25 µL 1 M Monothioglycerol	
250 µL 50 mg/ml Gentamicin	Lonza BioWhittaker
Mixed under sterile conditions.	
Stored at 4° C.	
S.O.C. medium	Thermo Fisher
Pre-mixed from supplier.	
TB (Terrific Broth)	
12 g tryptone	Sigma
24 g yeast extract	Oxoid
4 ml glycerol	Merck
dH_2O to 900 ml	
Mixed on a magnet stirrer and sterilized for 15 minutes at 115° C.	
Stored at room temperature without light.	

2.11 Buffers and solutions

Buffer or solution	**Content**	**Supplier (if applicable)**
Phosphate-buffered saline (PBS) pH 7.4	8 g/L NaCl	
	0.2 g/L KCl	
	1.44 g/L Na_2HPO_4	
	0.24 g/L KH_2PO_4	
	NaOH to pH 7.4	
	dH_2O to 1L	

Dulbecco's PBS (DPBS)	Pre-mixed by supplier.	Sigma
Tris-acetate EDTA (TAE) buffer, 50 x	242 g Tris base 57.1 ml acetic acid 100 ml 500 mM EDTA, pH 8.0 dH_2O to 1 L	
Tris-buffered saline (TBS) pH 7.4	150 mM NaCl 10 mM Tris HCl, pH 8.0	
TBS with Tween-20 (TTBS)	TBS pH 7.4 0.1% Tween-20 (v/v)	
Harbinger phosphate buffer	0.17 M H_2KPO_4 0.72 M K_2HPO_4	
Tris-glycine-SDS (TGS) buffer, 50 x	Pre-mixed by supplier.	Bio-Rad

3. METHODS

3.1 Culturing and growing of bacteria

The bacterial strains used in this thesis were either cultured in a liquid medium or grown on agar plates appropriate to the species. Antibiotics were added to the media in order to select for bacteria containing the chosen plasmids.

E. coli cultures were grown in liquid BHI medium and incubated overnight at 37° C with shaking. Agar plates with BHI were incubated overnight at 37° C. *L. plantarum* cultures were incubated overnight in liquid MRS medium or for two days on MRS plates at 37° C without shaking. Antibiotics were added when using liquid culture or when pouring agar dishes as shown in Table 3.1. The specific plasmid constructs used are listed in Table 2.4.

Table 3.1. Addition of antibiotics to media.

Species	**Plasmid**	**Antibiotic**	**Concentration liquid medium (**µg/ml**)**	**Concentration agar (**µg/ml**)**
E. coli	pUC57-derivatives	Ampicillin	200	100
E. coli	pSIP401-derivatives	Erythromycin	200	200
E. coli	pNIC-CH-derivatives	Kanamycin	50	50
L. plantarum	pSIP401-derivatives	Erythromycin	10	10

3.2 Long-term storage of bacteria in glycerol stocks

Materials:

Antibiotics

Bacteria

85% (v/v) glycerol

Liquid medium

Methods:

1. The bacteria were cultured overnight in a glass tube containing appropriate liquid medium with antibiotics added in accordance with section 3.1. 10 ml medium was generally used.
2. 1 ml of the culture was added to a 1.5 ml cryotube. 300 µL sterile 85% (v/v) glycerol was added to the tube, which was gently inverted a few times to mix.
3. The tube was labeled and placed in a -80° C freezer for long-term storage.
4. When using bacteria from glycerol stocks, a sterile toothpick was dabbed into the glycerol stock to retrieve a small amount. The toothpick was placed in a glass tube containing appropriate medium and antibiotics (see table 3.1) for overnight incubation under appropriate conditions.

3.3 Plasmid isolation from *Escherichia coli*

Materials:

Overnight culture with *E. coli* containing selected plasmids

NucleoSpin® Plasmid kit (see section 2.9)

Methods:

The procedure was carried out in accordance with the "Isolation of high-copy plasmids from *E. coli*" protocol and can be found in the "Plasmid DNA purification User Manual" from Macherey-Nagel (MACHEREY-NAGEL 2015).

3.4 Measurement of DNA concentration with Qubit®

Materials:

Qubit® assay tubes

Qubit® dsDNA BR Assay Kit (See section 2.9)

Qubit® fluorometer

Methods:

The assay was carried out in accordance with the protocol in "QuBit dsDNA BR Assay Kits" from the manufacturer, life technologies.

1. Qubit® Working Solution was prepared by mixing Qubit® dsDNA BR Reagent and Qubit® dsDNA BR Buffer at a ratio of 1:200 in an Eppendorf tube.
2. 190 µL Qubit® Working Solution was mixed with 10 µL of Qubit® dsDNA BR Standard #1 or #2 in 2 Qubit® assay tubes.
3. 1 µL sample was mixed with 199 µL Qubit® Working Solution in Qubit® assay tubes.
4. Standards and samples were vortexed and briefly centrifuged before incubating for 2 minutes at room temperature.
5. After incubation, the Qubit® fluorometer was calibrated using Standard #1 and #2 in that order. Samples were then immediately analysed and the DNA concentration calculated by inputting the amount of sample used in the Qubit® fluorometer.
6. If the results returned were out of range (concentration too low), new samples were prepared from step 3 with up to 20 µL sample, to a total volume of 200 µL when mixed with Qubit® Working Solution.

3.5 Restriction enzyme digestion of DNA

Materials:

DNA to be cut

Restriction buffers (See section 2.5)

Restriction enzymes (See section 2.5)

Methods:

1. The components were gently mixed in an Eppendorf tube at room temperature, as shown in Table 3.2, with appropriate restriction buffer and enzyme chosen for the DNA used.

Table 3.2. Setup for digestion of DNA.

Component	**Amount (μL)**
DNA	Up to 1 μg
Restriction buffer	5
Restriction enzyme	5
dH_2O	Adjust to 50

2. The reaction mixture was centrifuged briefly and incubated in a water bath at appropriate temperatures for the restriction enzymes, generally 37° C, for 30 minutes to 1 hour.
3. After digestion, the reaction mixture was loaded onto an agarose gel as detailed in Method 3.6.

3.6 Agarose gel electrophoresis

Materials:
DNA ladder
Mini-Sub® Cell GT Cell
peqGreen DNA dye
SeaKem® LE Agarose
1x TAE buffer

Methods:
1. SeaKem® LE Agarose and 1x TAE buffer were mixed at a ratio of 1.02 g agarose per 60 ml TAE buffer (8.5 g agarose in 500 ml buffer) and dissolved by stirring on a magnet stirrer for a final concentration of 1.7% (w/v) agarose. The solution was sterilized in a certoclav at 115° C for 15 minutes and stored at 50° C.
2. When making a gel, 60 ml of solution was mixed with 2,5 μL peqGreen DNA dye and poured into a Mini-Sub® Cell casting tray with well combs.
3. After 20 to 30 minutes, the gel had solidified and the well combs were removed. The gel was then transferred in the casting tray to an electrophoresis chamber and submerged in 1x TAE buffer.

4. If the samples had not been treated with a buffer containing loading dye, they were mixed with 10% v/v loading dye. An appropriate DNA ladder and the samples were then pipetted into the wells.
5. The gel was run at 90V for 15 minutes or longer, depending on how far the dye had migrated when the running time had ended.

3.7 Purification of DNA from agarose gels

Materials:
NucleoSpin® Gel and PCR Clean-up Kit (See section 2.9)

Methods:
The procedure was carried out in accordance with the "DNA extraction from agarose gels" protocol and can be found in the "NucleoSpin® Gel and PCR Clean-up
User manual" from Macherey-Nagel (MACHEREY-NAGEL 2014).

3.8 Cloning of DNA

3.8.1 Quick T4 DNA ligation

Materials:
DNA fragments containing insert
Plasmid vector
2X Quick Ligation Buffer
Quick T4 DNA Ligase

Methods:
The "Quick Ligation Protocol (M2200)" protocol from New England BioLabs® Inc (New England Biolabs) was followed for this procedure, with the following changes:

1. 50 ng vector was combined with a 3-fold molar excess of insert in an Eppendorf tube. The total volume was then adjusted to 10 µL. Where a ratio of 1:3 gave poor results, 1:1 was also tried.

3.8.2 In-Fusion cloning

In-Fusion is a method for fast and directional cloning of DNA fragments into a linearized vector. It requires a 15 base-pair overhang at the 5' and 3' ends of the vector and insert DNA, and uses a proprietary enzyme to fuse the ends. Although restriction enzymes are required to linearize the vector, the cloning takes place without the need for restriction digestion or ligation. The overhangs on the insert are engineered by running PCR with primers designed to add 15 bp extensions upstream and downstream of the gene. The In-Fusion enzyme mix then generates 15 nucleotide long overhangs on the vector, and it spontaneously fuses with the insert at the sites of complementarity.

Materials:

In-Fusion HD Cloning kit (See section 2.9)

Linearized vector

PCR-amplified template DNA

Primers (See section 2.7)

Methods:

The "In-Fusion Cloning Procedure for Spin-Column Purified PCR Fragments" protocol from Clontech Laboratories Inc. was followed for this procedure.

1. The vector was linearized by restriction enzyme digestion in accordance with section 3.5.
2. The reaction components were mixed in an Eppendorf tube as shown in table 3.3.

Table 3.3. Setup for In-Fusion cloning.

Component	**Volume/reaction (μL)**	**Final concentration**
Purified PCR fragment	Varies	33 ng
Linearized vector	Varies	150 ng
5x InFusion HD Enzyme Premix	2	1x
dH_2O	To 10	-

3. The reaction mixture was then incubated in a water bath at 50° C for 15 minutes.

4. After incubation, the mixture was chilled on ice. It was then stored at -20° C or immediately transformed into *E. coli* GeneHogs® in accordance with section 3.12.3.

3.8.3 Ligation Independent Cloning

Ligation independent cloning (LIC) is an alternative to cloning with restriction enzymes and ligases. The vector and insert are linearized by PCR or restriction enzyme digestion. T4 DNA Polymerase, which has 3'→5' exonuclease activity, creates overhangs with complementarity between the vector and insert. The digestion of the vector is done in the presence of dCTP, and the insert with dGTP. By using only one type of dNTP, the exonuclease activity is stopped at the first "C" or "G" in the sequence. Mixing the digested vector and insert leads to spontaneous annealing at the regions of complementarity. The plasmid is then transformed into *E. coli* which repairs the 4 nicks in the sequence.

Materials:

BHI agar with 2 % sucrose
BSA
dGTP
DTT
25 mM EDTA
IPTG
NEBuffer 2
T4 DNA Polymerase
PCR-amplified insert
Pre-digested linearized pNIC-CH vector

Methods:

1. Components were mixed in descending order as shown in Table 3.4.

Table 3.4. Setup for LIC

Component	**Amount (μL)**
NEB Buffer 2	2
BSA	1

dGTP	2
DTT	1
T4 DNA Polymerase	1
Insert	0.2 pmol
dH_2O	Total 20

2. The reaction mixture was incubated in a thermocycler at 22° C for 1 hour to make the T4 DNA Polymerase digest the insert, then 75° C for 21 minutes to inactivate the polymerase.
3. 2 µL of digested insert was mixed with 1 µL of pre-digested pNIC-CH plasmid and incubated at room temperature for 5 minutes.
4. 2 µL EDTA at 25 mM was added and the mixture was incubated at room temperature for 10 minutes.

The mixture was immediately transformed into *E. coli* TOP10 in accordance with section 3.12.3. The bacteria were plated on BHI agar with 2% sucrose with 50 µg/ml kanamycin, since sucrose selects against undigested pNIC-CH vector.

3.9 Polymerase Chain Reaction

3.9.1 VWR Red Taq DNA Polymerase Master Mix

Materials:
Forward and reverse primers (see section 2.7)
VWR Red Taq DNA Polymerase 2X Master Mix

Methods:
The protocol "Suggested Protocol Using VWR Red Taq Master Mix" from the manufacturer, VWR, was followed for the mixing of reaction components in step 3.

1. A small part of a bacterial colony was extracted from a petri dish using a sterile toothpick and applied to the bottom of a sterile 0.2 ml PCR tube. The toothpick was then used to inoculate a glass tube containing 10 ml appropriate medium with antibiotics and cultured as detailed in section 3.1.

2. The PCR tubes were microwaved at 750W for 60 seconds in order to induce cell lysis and liberate the DNA template. The tubes were then put on ice.
3. After ensuring that all components were completely thawed, the reaction components were gently mixed on ice in 0.2 ml PCR tubes in the order and amount shown in Table 3.5.

Table 3.5. Setup for colony PCR using VWR Red Taq DNA Polymerase Master Mix.

Component	**Volume/reaction (μL)**	**Final concentration**
Taq 2X Master Mix	25	1x
Forward primer	1	0.1-1.0 uM
Reverse primer	1	0.1-1.0 uM
PCR-grade dH_2O	23	-

4. The PCR tubes were briefly centrifuged to remove any air bubbles and added to a preheated thermocycler. A thermocycling program was then run, as detailed in Table 3.6.

Table 3.6. Thermocycler program for colony PCR using VWR Red Taq DNA Polymerase Master Mix.

Step	**Cycles**	**Temperature (° C)**	**Cycle duration (min:sec)**
Initial denaturation	1	95	2:00
Denaturation	25-35	95	0:20
Annealing	25-35	50-55*	0:25
Elongation	25-35	72	0:30
Final elongation	1	72	5:00

*The annealing temperature varies by primer and was generally set to 3-5° C below the melting temperature (T_m) of the primer with lowest T_m.

3.9.2 Q5® High Fidelity 2X Master Mix

Materials:

Forward and reverse primers (See section 2.7)

Q5® High-Fidelity 2X Master Mix

Template DNA

Methods:

A protocol from New England BioLabs® Inc. was used as the basis for this procedure.

1. All reaction components were gently mixed on ice in 0.2 ml PCR tubes in the order and amount shown in Table 3.7.

Table 3.7. Setup for PCR using Q5® High Fidelity 2X Master Mix.

Component	**Volume/reaction (μL)**	**Final concentration**
Q5® High-Fidelity 2X Master Mix	25	1x
10 μM Forward primer	1	0.5 uM
10 μM Reverse primer	1	0.5 uM
Template DNA	variable	< 1000 ng
PCR-grade dH_2O	To 50	-

2. The PCR tubes were briefly centrifuged to remove air bubbles and transferred to a preheated thermocycler. The thermocycling parameters are shown in Table 3.8.

Table 3.8. Thermocycling program for PCR using Q5® High Fidelity 2X Master Mix.

Step	**Cycles**	**Temperature (° C)**	**Cycle duration (minutes:seconds)**
Initial denaturation	1	98	0:30
Denaturation	20-25	95	0:10
Annealing	20-25	50-55*	0:20
Elongation	20-25	72	0:20

Final elongation	1	72	2:00

*The annealing temperature varies by primer and was generally set to 3-5° C below the melting temperature (T_m) of the primer with lowest T_m.

3.10 Sequencing of DNA

Materials:

Plasmid with DNA insert

Primers (see section 2.7)

Methods:

1. The plasmid to be sequenced first had its concentration determined as detailed in section 3.4. 4-500 ng plasmid was then added to each of two Eppendorf tubes.
2. 2.5 µL of forward primer with a concentration of 10 pmol/µL relevant to the chosen plasmid was added to one of the Eppendorf tubes. The equivalent amount of reverse primer was added to the other tube.
3. After primer addition, sterile dH_2O was added to each tube to a total volume of 11 µL.
4. The samples were labeled and sent to GATC Biotech for sequencing. The results were received digitally, and CLC Main Workbench was used to look for any alterations in the DNA sequence.

3.11 Preparation of electrocompetent *Lactobacillus plantarum* WCFS1

Materials:

L. plantarum WCFS1

MRS medium

MRS medium with 1% glycine

MRSSM medium

30% PEG1450

Methods:

1. *L. plantarum* from a glycerol stock was added to a glass tube containing 10 ml MRS medium and incubated overnight at 37° C.
2. A serial dilution from 10^{-1} to 10^{-10} was made with the overnight culture in MRS medium with 1% glycine. The fresh cultures were then incubated overnight at 37° C.
3. 2 ml of culture with an Optical Density measured at 600 nm (OD_{600}) of 2.5 ± 0.5 was diluted 1:20 in 40 ml MRS with 1% glycine. The culture was then incubated at 37° C until it reached an OD_{600} of 0.7 ± 0.07 and placed on ice for 10 minutes.
4. The culture was centrifuged at 4500 RPM for 10 minutes at 4° C. The supernatant was discarded and the pellet was resuspended in 5 ml cold 30% PEG1450 in a cold corex tube.
5. An additional 20 ml cold 30% PEG1450 was added to the tube and the culture was mixed gently before being placed on ice for 10 minutes.
6. The cells were centrifuged as in step 4. The supernatant was discarded and the pellet was resuspended in 400 µL 30% PEG1450. This was aliquoted in 40 µL portions into sterile Eppendorf tubes. The tubes that were not to be used for transformation immediately were flash frozen using liquid N_2.
7. The frozen cells were stored at -80° C until required for transformation.

3.12 Transformation of bacteria

3.12.1 Rapid transformation of chemically competent *Escherichia coli* GeneHogs® or TOP10

When there is no potential for re-ligated vector present in the DNA, a rapid transformation method of chemically competent *E. coli* can be used. In this thesis, the rapid transformation method was used for the lyophilized plasmid DNA received from GenScript.

Materials:

Lyophilized plasmid DNA (GenScript)

Agar plates with appropriate antibiotics

Methods:

The plasmid DNA was dissolved and transformation was carried out according to the protocol from Invitrogen.

1. The vial containing lyophilized plasmid DNA was centrifuged at 6000 x g for 1 minute at 4° C.
2. 20 µL sterile dH_2O was added and the vial was vortexed for 1 minute to dissolve the DNA.
3. 30 µL *E. coli* GeneHogs® or TOP10 was transferred to a corex tube on ice. 1 µL plasmid DNA was added and gently mixed in by tapping the tube. The mix was incubated for 20 minutes on ice.
4. The corex tube was incubated without movement in a water bath for 30 seconds at 42° C.
5. The tube was returned to ice and incubated for 2 minutes before 250 µL S.O.C. medium at room temperature was gently added.
6. Under sterile conditions, 50 and 100 µL transformation mixture was spread on plates with BHI agar and 200 µg/ml ampicillin and incubated overnight at 37° C.
7. The next day, working sterile, single colonies were plucked from the agar plates and overnight cultures and glycerol stocks were made in accordance with section 3.2.
8. The remaining overnight culture was used for plasmid isolation as detailed in section 3.5.

3.12.2 Transformation of electrocompetent *Lactobacillus plantarum*

Materials:

Bio-Rad GenePulser® II

Bio-Rad Pulse Controller Plus

Electroporation cuvettes

Electrocompetent *L. plantarum* WCFS1

Ligation mixture or plasmid solution

MRS agar plates with 10 µg/ml erythromycin

MRSSM medium

Methods:

1. Eppendorf tubes containing 40 µL electrocompetent cells were thawed on ice and 20 µL ice cold ligation mixture or 5 µL plasmid solution was gently mixed in.
2. The mixture was transferred to an ice cold electroporation cuvette, taking care not to introduce any air bubbles.
3. The cuvette was transferred to the Bio-Rad GenePulser® II, pre-set to 25 uF capacitance, 1.5 kV voltage and 400 Ω resistance, and an electric pulse was applied to the cells.
4. 950 µL pre-heated MRSSM medium was transferred to the cuvette and gently mixed in. The cell suspension was then transferred to a sterile Eppendorf tube and incubated for 2 hours at 37° C.
5. After incubation, 50 or 100 µL cell suspension was spread on MRS agar plates and incubated for 2-3 days at 37° C.

3.12.3 Transformation of chemically competent *Escherichia coli* TOP10 or GeneHogs®

Materials:

Agar plates with appropriate antibiotics
Chemically competent *E. coli* TOP10 or GeneHogs®
Plasmid DNA or ligation mixture
S.O.C medium

Methods:

1. S.O.C medium was warmed to room temperature and agar plates were warmed to 37° C.
2. One Eppendorf tube containing *E. coli* TOP10 was thawed on ice for each transformation. 30 µL bacteria was transferred to a cold corex tube.
3. 1-5 µL plasmid DNA or 21 µL ligation mixture was added to the tube and gently mixed in by tapping. The mix was incubated for 30 minutes on ice.
4. The bacteria were heat-shocked by holding the corex tube in a water bath for 30 seconds at 42° C without shaking.
5. The tube was returned to ice and incubated for 2 minutes before 250 µL S.O.C. medium at room temperature was gently added and mixed in

6. The tubes were capped tightly and incubated at 37° C for 1 hour with 225 rpm shaking.
7. Under sterile conditions, 50 and 100 µL transformation mixture was spread on pre-warmed plates with BHI agar and appropriate antibiotics and incubated overnight at 37° C. For *E. coli* TOP10 harboring pNIC-CH vector, BHI + 2 % sucrose was used instead of BHI.

3.12.4 Transformation of chemically competent *Escherichia coli* BL21

Materials:

Agar plates with appropriate antibiotics

Chemically competent *E. coli* BL21

Plasmid DNA

S.O.C medium

Methods:

1. S.O.C medium was warmed to room temperature and agar plates were warmed to 37° C.
2. One Eppendorf tube containing *E. coli* TOP10 was thawed on ice for each transformation. 25 µL bacteria was transferred to a cold corex tube.
3. 1 µL plasmid DNA was added to the tube and gently mixed in by tapping. The mix was incubated for 5 minutes on ice.
4. The bacteria were heat-shocked by holding the corex tube in a water bath for 30 seconds at 42° C without shaking.
5. The tube was returned to ice and incubated for 2 minutes before 75 µL S.O.C. medium at room temperature was gently added and mixed in.
6. The tubes were capped tightly and incubated at 37° C for 30 minutes to 1 hour with 225 rpm shaking.
7. Under sterile conditions, 50 and 100 µL transformation mixture was spread on plates with BHI agar and appropriate antibiotics and incubated overnight at 37° C.

3.13 Protein production in *Escherichia coli* BL21

3.13.1 Cultivation of *Escherichia coli* BL21

Materials:

Antifoam 204

E. coli BL21 with plasmid

Harbinger phosphate buffer

IPTG

Kanamycin

TB medium

Methods:

1. Overnight cultures with *E. coli* BL21 containing selected plasmids were made in accordance with section 3.1.
2. 500 ml TB was added to 1 L bottles with hose and air diffuser-equipped blue caps. The bottles were autoclaved at 115° C for 15 minutes.
3. After cooling, 50 ml sterile filtered phosphate buffer, 150 µL Antifoam 204 and kanamycin to a final concentration of 50 µg/ml was added to each bottle.
4. 3 ml *E. coli* BL21 culture was added to each bottle.
5. The bottles were attached to the LEX Bioreactor. The oxygen flow was turned on and adjusted and the cultures were incubated overnight at 23° C with aeration.
6. The following day, 100 µL IPTG was added to each bottle to induce protein production. The cultures were incubated overnight at 23° C with aeration and immediately harvested in accordance with section 3.13.2

3.13.2 Harvesting and sonication of *Escherichia coli* BL21

Materials:

Buffer A (5 mM imidazole, 50 mM Tris pH 8.0, 500 mM NaCl, sterile filtered)

E. coli BL21 culture

TB medium

PMSF

Methods:

1. The *E. coli* BL21 culture made in section 3.13.1 was transferred to a 500 ml centrifugation tube.
2. The tube was centrifuged at 5000 x g for 15 minutes at 4° C. The supernatant was saved and used in the next step.
3. The pellet was resuspended in 50 ml TB medium and transferred to a 50 ml falcon tube.
4. The resuspended pellet was centrifuged at 5000 x g for 15 minutes at 4° C and the supernatant was discarded. The pellet was stored at – 80° C or sonicated immediately.
5. Working on ice, the pellet was resuspended in 30 ml ice cold Buffer A. The tube was placed on ice in a small container and sonicated with the Vibra-Cell VCX 500 at 30 % amplitude for 3 minutes with 5 second on/off cycles.
6. 2 µL cold PMSF was added per 1 ml sample and mixed. The sample was transferred to an ultracentrifugation tube and centrifuged at 20 000 x g for 15 minutes at 4° C.
7. was run on both supernatant and pellet after centrifugation to check for indications of inclusion bodies. The pellet was then discarded and the supernatant used for further analysis.

3.14 Purification of protein

3.14.1 Immobilized metal ion affinity chromatography

Materials:

Buffer A (5 mM imidazole, 50 mM Tris pH 8.0, 500 mM NaCl, sterile filtered)

Buffer B (250 mM imidazole, 50 mM Tris pH 8.0, 250 mM NaCl, sterile filtered)

Chromatography column

20% ethanol

Protino® Ni-NTA Agarose

Methods:

1. 2 ml Protino® Ni-NTA Agarose was added to the chromatography column. The BioLogic LP system was assembled and the column connected.
2. The system was pre-run with buffer A by running at 1.5 ml/min for 10 minutes. The system was then auto-zeroed.
3. The protein-containing *E. coli* BL21 supernatant, made in section 3.13.2, was added to the system and run at the same flow rate. The proteins which did not bind and immediately eluted caused a peak on the elution diagram. The system was then flushed with buffer A until the graph had returned to the zero value.
4. Buffer B was added to the system until the read-out showed a new peak, indicating elution of the bound protein. The eluted protein suspended in buffer B was collected in a 15 ml tube.
5. After elution was complete, the system was flushed through with 20% ethanol and disconnected. A buffer exchange was then performed as detailed in section 3.14.2

3.14.2 Buffer exchange of purified protein

After purifying protein with IMAC, the solubilized proteins are suspended in a buffer containing imidazole and NaCl at high molarities. In order to remove these components, the solution is pushed through a filter by centrifugation. The filter has pores with a cut-off value for molecules of a certain size, measured in Da, so a filter can be selected with pores smaller than the purified protein. The desired buffer is then added and centrifugation is repeated until the salts are removed.

Materials:
Amicon® Ultra 15 ml Centrifugal Filters Ultracel® (3000 or 10 000 Da MWCO)
20 mM tris pH 8.0

Methods:

1. The purified sample from section 3.14.1 was added to a centrifugal filter with a molecular weight membrane cutoff (MWCO) smaller than the predicated size of the protein of interest.
2. The sample was centrifuged at 4° C in a swing-out rotor at 4500 x g until approximately 1 ml remained in the upper part of the tube.

3. The flow-through was discarded and 10-15 ml 20mM cold Tris pH 8.0 was added to the upper part of the tube and mixed with the protein sample.
4. Step 2 and 3 were repeated 4 times, to a total of 5 buffer exchanges.
5. After the final centrifugation, the concentrated protein sample was pipetted into a sterile Eppendorf tube and stored at 4° C. If the buffer exchange caused precipitation, section 3.14.3 was followed to dissolve the protein in a different buffer.
6. To determine purity, the sample was run on SDS-PAGE in accordance with section 3.18. Concentration was determined by section 3.15 or section 3.16.

3.14.3 Dialysis of precipitated protein

Some of the proteins expressed using *E. coli* BL21 as expression host may precipitate when exchanging buffers from Buffer B (See section 3.14.2) to 20 mM Tris pH 8.0. In order to reverse this, the precipitated protein was first dissolved in 8 M urea. The buffer was then gradually changed to 20 mM glycine with pH 9.2 by diffusion through a dialysis membrane, using the concentration gradient across the membrane to exchange the buffers.

Materials:
8 M urea
20 mM glycine pH 9.2
SnakeSkin® Dialysis Tubing (MWCO 10 000)
Spectra/Por® Membrane (MWCO 3500)
Spectra/Por® Closures

Methods:

1. The sample containing precipitated protein from section 3.14.2 was centrifuged at 20 000 x g for 20 minutes at 4° C in order to collect all the precipitate. The supernatant was aspirated and saved for running SDS-PAGE later.
2. The pellet was dissolved by adding 8 M urea until no precipitate was visible.
3. The sample was centrifuged at 20 000 x g for 20 minutes at 4° C.
4. The supernatant was transferred to a pre-moistened SnakeSkin® Dialysis Tubing or Spectra/Por® Membrane, depending on the size of the protein. The membrane tube was then sealed.

5. The membrane was placed in 2 L 20 mM glycine pH 9.2 and left overnight at 4° C with magnet stirring at 100 rpm.
6. The following day, step 5 was repeated with 2L new 20 mM glycine pH 9.2.
7. After the final dialysis, the sample was extracted from the membrane tube and transferred to a 15 ml nunc tube. The sample was stored at 4° C.
8. The proteins in supernatant from step 1 and step 7 were run on SDS-PAGE as detailed in section 3.18 in order to determine where the target protein is located.

3.15 Measurement of protein concentration using Bradford assay

Materials:

Samples

Disposable cuvettes, 1,5 ml semi-micro

Protein Assay Dye Reagent Concentrate

Eppendorf BioPhotometer

Methods:

1. Samples to be measured were mixed with dH_2O in Eppendorf tubes to a total volume of 600 µL at an appropriate dilution. A blank sample containing 600 µL dH_2O was also made.
2. 200 µL Protein Assay Dye Reagent Concentrate was added to each tube and briefly vortexed to mix. The tubes were then incubated for 5 minutes at room temperature.
3. The blank sample was used to zero the Eppendorf BioPhotometer. The samples were then measured and the readout was multiplied by the dilution factor to calculate the concentration of protein in the sample.

3.16 Measurement of protein concentration using Qubit® assay

Materials:

Qubit® assay tubes

Qubit® fluorometer

Qubit® Protein Assay Kit (see section 2.9)

Methods:

The assay was carried out in accordance with the protocol in "QuBit Protein Assay Kits" from the manufacturer, life technologies.

1. Qubit® Working Solution was prepared by mixing Qubit® Protein Reagent and Qubit® Protein Buffer in a 1:200 ratio in an Eppendorf tube.
2. 190 µL Qubit® Working Solution was mixed with 10 µL of Qubit® Protein Standard #1, #2 or #3 in 3 Qubit® assay tubes.
3. 1 µL protein-containing sample was mixed with 199 µL Qubit® Working Solution in a Qubit® assay tube.
4. Standards and samples were vortexed and briefly centrifuged before incubating 15 minutes at room temperature.
5. After incubation, the Qubit® fluorometer was calibrated using Standard #1, #2 and #3 in that order. Samples were then immediately analysed and the protein concentration calculated by the Qubit® fluorometer by inputting the amount of sample used.
6. If the results returned were out of range (concentration too low), new samples were prepared from step 3 with up to 20 µL sample, to a total volume of 200 µL when mixed with Qubit® Working Solution.

3.17 Production and analysis of gene products from *Lactobacillus plantarum*

Gene products from *L. plantarum* were produced by making cultures and adding the inducer peptide SppIP, resulting in genetic expression of the gene of interest. In order to analyse production of the target protein, the cells were disrupted with glass beads, liberating the cytoplasmic content. Presence of the target protein in the resulting cell-free protein extract was verified by using Western blot.

3.17.1 Cultivation and harvesting of *Lactobacillus plantarum*

Materials:

Cuvettes

Inducer peptide SppIP (0.1 mg/ml)

MRS medium with 10 µg/ml erythromycin

PBS (See section 2.11)
Ultrospec 10 Cell density meter

Methods:

1. 10 ml MRS media with 10 µg/ml erythromycin was inoculated with *L. plantarum* from a glycerol stock and incubated overnight at 37° C.
2. The overnight culture was diluted in 50 ml pre-heated MRS medium with 10 µg/ml erythromycin to an OD_{600} of 0.15 ± 0.01.
3. The culture was incubated at 37° C until it reached an OD_{600} of 0.3 ± 0.03.
4. Expression of the gene of interest was induced by adding SppIP to a final concentration of 25 ng/ml. The inducer was gently mixed into the culture and the culture was incubated for 3 or 4 hours at 37° C.
5. After the incubation time was complete, the culture was put on ice to stop growth and OD_{600} was measured. If a certain number of bacteria were needed, the volume of culture was calculated using the equation $4 * 10^8 * OD_{600}$ (See Appendix, Fig. A.1). Otherwise, the entire volume was used further.
6. The culture was then centrifuged at 5000 g for 10 minutes at 4° C.
7. The supernatant was discarded and the pellet resuspended in 5 ml ice cold PBS.
8. Step 6 was repeated.
9. The supernatant was discarded and the pellet resuspended in 1 ml ice cold PBS in an Eppendorf tube. It was then stored at 4° C overnight, at -20° C long-term or used for further analysis immediately.

3.17.2 UV-inactivation of *Lactobacillus plantarum*

Materials:
Falcon® Tissue Culture Plates, 6-well

Methods:

1. The sample to be UV-inactivated was cultivated and harvested as detailed in section 3.17.1.
2. The sample was transferred in a maximum volume of 1 ml ice cold PBS to a sterile 6-well plate on ice.

3. The plate was placed on ice inside a GelDoc Imager, which was turned on for 45 minutes.
4. The UV-inactivated sample was transferred to a sterile Eppendorf tube and stored overnight at 4° C or used immediately.
5. In order to verify UV-inactivation of the bacteria, they were plated on MRS agar with 10 µg/ml erythromycin and incubated 1-2 days at 37° C.

3.17.3 Disruption of *Lactobacillus plantarum* with glass beads

Materials:

FastPrep® Tubes and Blue Caps

Glass beads, acid-washed (<106 um)

Methods:

1. 1.5 g acid-washed glass beads were added to FastPrep® tubes with blue caps and chilled on ice. 1 ml of *L. plantarum* suspended in PBS (from section 3.17.1) was added to the tubes on ice.
2. The tubes were placed in the FastPrep® FP120 Cell Disruptor and the machine was run at 6.5 m/s for 45 seconds.
3. The tubes were centrifuged at 11 000 x g for 5 minutes at 4° C. The supernatant was transferred to clean Eppendorf tubes and the pellet discarded.
4. Step 3 was repeated in order to remove any remaining glass beads.
5. The remaining protein extract was analysed with SDS-PAGE directly or stored at -20° C.

3.18 Polyacrylamide Gel Electrophoresis

Materials:

MagicMark™ XP Western Standard

Mini-PROTEAN® TGX Stain-Free™ Precast Gels

NuPAGE® LDS Sample Buffer (4x)

NuPAGE® Sample Reducing Agent (10x)

TGS buffer (See section 2.11)

Methods:

1. 250 µL LDS Sample Buffer, 100 µL Sample Reducing Agent and 150 µL dH_2O was mixed to make a 2x stock buffer solution.
2. If frozen, the protein sample was thawed on ice. 10 µL sample was mixed with 10 µL stock buffer solution in an Eppendorf tube.
3. The sample was boiled in a water bath at 100° C for 10 minutes in order to denature the proteins. The tube was then centrifuged briefly to collect the sample at the bottom.
4. The inner gel electrophoresis chamber was assembled and both inner and outer chambers were filled with 1x TGS buffer up to indicated levels.
5. The sample and protein standard were then applied to the gel, which was run at 280V for 18 min.
6. The gel was extracted from the assembly and developed in a GelDoc Imager on a Stain Free Plate for imaging. The gel was then transferred to a plastic tray filled with dH_2O for analysis with Western blot.

3.19 Western blot

3.19.1 Blotting with iBlot™

Materials:

Pre-run protein gel with samples

iBlot Gel Transfer Device

iBlot Gel Transfer Stack, mini (See section 2.9)

TBS (See section 2.11)

Methods:

1. The iBlot™ Anode Stack (bottom) was placed on the Gel Transfer Device, in its plastic tray, and the gel was aligned on top. The gel was trimmed with a scalpel to remove any excess outside of the Anode Stack.

2. An iBlot™ Filter Paper, soaked in dH_2O, was aligned on top of the gel and any air bubbles were removed by gently rolling on top of the Filter Paper with a blotting roller.
3. The iBlot™ Cathode Stack was removed from its plastic tray and placed on top of the filter paper. Air bubbles were removed by using a blotting roller.
4. An iBlot™ Disposable Sponge was placed in the lid of the Gel Transfer Device, aligning the brass metal contact on the sponge and the lid.
5. The lid was closed and the iBlot Gel Transfer Device was run at 23 V for 7 minutes.
6. After the run was completed, the membrane was transferred using tweezers to a tray with TBS for further use.

3.19.2 SNAP i.d.® 2.0 protein quantification

SNAP i.d.® is a method of hybridizing antibodies to a membrane in a Western blot. While traditional Western blotting relies on diffusion for components to permeate the membrane, SNAP i.d.® 2.0 is based on using a vacuum to actively pull reagents through the membrane. This reduces the amount of time needed to complete the procedure.

Materials:

SNAP i.d.® 2.0 system (see section 2.9)
TTBS (See section 2.11)
TTBS with 0.5% BSA
TTBS with 1.0% BSA

Methods:

1. The membrane layer of the blot holder was wetted with dH_2O. The nitrocellulose membrane, blotted in section 3.19.1, was then applied to the blot holder, with the protein side facing down.
2. A filter paper was wetted with dH_2O and applied onto the membrane. Air bubbles were removed by gently rolling with the Blot Roller.
3. The blot holder was closed and placed inside the SNAP i.d.® Mini Frame, protein side down. The frame was closed and locked.

4. 30 ml of blocking buffer was added and the vacuum was turned on. The system knob was turned to apply the vacuum, which was immediately turned off when the frame was empty.
5. 3 ml of TTBS with 0.5% BSA, containing primary antibody (diluted 1:5000) was added, taking care to cover the membrane evenly, and incubated for 10 minutes.
6. The vacuum was applied and the blot was washed 3 times with 10 ml TTBS. The vacuum was then shut off.
7. 3 ml of TTBS with 0.5% BSA, containing secondary antibody (diluted 1:10 000) was added, taking care to cover the membrane evenly, and incubated for 10 minutes.
8. The washing step was repeated.
9. The blot holder was removed from the frame and the membrane was incubated with a detection substrate appropriate to the secondary antibody before detection by X-ray film or with an Azure c400, as detailed in section 3.19.3 and section 3.19.4.

3.19.3 Chemiluminescent detection of proteins

Materials:

CL-Xposure™ film

Developer solution

Fixing solution

SuperSignal® West Pico Chemiluminescent Substrate

Luminol/Enhancer Solution

Stable Peroxide Buffer

Methods:

1. The substrate solution was made by mixing 10 ml of Stable Peroxide Buffer with 10 ml of Luminol/Enhancer Solution immediately before use.
2. The substrate solution was poured into a plastic tray and the membrane, prepared in section 3.19.2, was submerged in the solution. The membrane was incubated with shaking for 5 minutes at room temperature.
3. After 5 minutes, the membrane was transferred with the protein side up to a lightproof film cassette and carefully covered with plastic foil before the cassette was closed.

4. Working in the dark, CL-Xposure™ film was cut to the size of the membrane using scissors. Developer, fixative solution and H_2O were poured into separate plastic trays.
5. The film was placed on top of the membrane in the cassette and incubated for 2-15 minutes, depending on the strength of the signal.
6. The exposed film was first incubated in developer solution until the protein bands were clearly visible.
7. The developed film was incubated in fixing solution for approximately 2 minutes.
8. The finished film was then put in the tray with water to remove traces of fixing solution before being air dried.

3.19.4 Development of Western Blot using Azure c400

The Azure biosystems Azure c400 is a digital imaging system using a cooled CCD camera to achieve capture of chemiluminescent signals without the use of film and developer. In addition, its sensitivity compared to film allows for a wider dynamic range in the protein bands, making quantitation of protein amount easier than with the traditional method.

Materials:

Azure c400

SuperSignal® West Pico Chemiluminescent Substrate

Luminol/Enhancer Solution

Stable Peroxide Buffer

Methods:

1. The Azure c400 was turned on at least 30 minutes before use to allow the CCD to cool.
2. The nitrocellulose membrane was prepared as detailed in section 3.19.1.
3. The substrate solution was made by mixing 10 ml of Stable Peroxide Buffer with 10 ml of Luminol/Enhancer Solution immediately before use.
4. The substrate solution and membrane were added to a plastic tray and incubated with shaking for 5 minutes at room temperature.
5. After incubation, the membrane was placed protein side up on the sample tray using tweezers, taking care to leave the entire membrane covered with substrate.

6. The membrane was imaged using the chemiluminscent program in the cSeries Capture Software for between 2 and 10 minutes and between low and high sensitivity, depending on the strength of the signal.

3.20 Cultivation of Caco-2 cells

3.20.1 Preparation of Caco-2 cells

Materials:

Caco-2 cells

cRPMI-1640

250 ml Falcon® Tissue Culture Flask

Methods:

1. Two tubes containing Caco-2 cells were removed from storage at -196° C and thawed on ice.
2. The contents of each tube were added into 9 ml of ice cold RPMI-1640 in a 15 ml nunc tube. The tubes were centrifuged at 350 x g for 5 minutes at room temperature.
3. The supernatant was discarded and each pellet resuspended in 10 ml cRPMI-1640 preheated to 37° C.
4. The tubes were centrifuged at 350 x g for 5 minutes. The supernatant was discarded and each pellet resuspended in 2 ml RPMI-1640 at 37° C.
5. Both resuspended pellets were transferred to a 250 ml Falcon® Tissue Culture Flask and 25 ml cRPMI-1640 at 37° C was added to the flask.
6. The flask was maintained in a humidified incubator at 37° C with 5% CO2 until the cells had reached approximately 80% confluence before they were used further.

3.20.2 Partial digestion of Caco-2 cells

Materials:

cRPMI-1640

Sterile Dulbecco's PBS

250 ml Falcon® Tissue Culture Flask containing Caco-2 cells
Trypsin EDTA
0.4% Trypan Blue Solution
Countess chamber slides

Methods:

1. cRPMI-1640 and sterile PBS was preheated to 37° C in a water bath
2. The medium in the flask containing Caco-2 cells was aspirated.
3. The cell layer was carefully washed with 20 ml PBS to remove dead cells, proteins and cations which inhibit the trypsin activity.
4. The PBS was aspirated.
5. 5 ml trypsin-EDTA was added to the flask, ensuring it covered the entire cell layer. The cells were then incubated at 37° C for 5-10 minutes.
6. When all cells had dislodged from the flask as visually confirmed in a microscope, 10 ml cRPMI-1640 was added to stop the trypsin digestion of the cells.
7. The cells were transferred to a 50 ml nunc tube and fully resuspended by gently pipetting up and down.
8. The cells were centrifuged at 350 x g for 10 minutes. The supernatant was discarded and the pellet resuspended in 1 ml cRPMI-1640.
9. 10 µL cell suspension was mixed with 10 µL 0.4% Trypan Blue Solution and the number of cells was calculated using a Countess® II Automated Cell Counter.
10. Approximately 10^6 cells were added to a new flask. 20 ml cRPMI-1640 was added and the subculture was maintained in a humidified incubator at 37° C with 5% CO_2.

3.21 Stimulation of Caco-2 cells

Materials:
cRPMI-1640
IL-1β

Methods:

1. Cultured Caco-2 cells were partially digested with trypsin-EDTA, as detailed in section 3.20.2.

2. After digestion with trypsin, the cells were added to a 24-well plate at a concentration of $3*10^5$ cells per well in 500 µL preheated cRPMI and incubated in a humidified incubator for 2 days at 37° C with 5% CO_2, in order for the cells to attach to the bottoms of the wells.
3. After incubation, the medium was aspirated and 500 µL new medium containing one of the following was added:
    a. $1*10^7$ UV-inactivated whole *L. plantarum,* made in accordance with section 3.17.2. The amount of bacteria was calculated using OD_{600}-values and the equation $4 * 10^8 * OD_{600}$ (see Appendix, Fig. A.1)
    b. Cell-free protein extract from $1*10^7$ disrupted *L. plantarum*, made in accordance with section 3.17.3. The amount of bacteria was calculated using OD_{600}-values and the equation $4 * 10^8 * OD_{600}$ (see Appendix, Fig. A.1)
    c. Purified protein from *E. coli* BL21 at 3 µg/ml.
4. After addition of medium containing bacterial components, the cells were stimulated with recombinant human IL-1β at 15 ng/ml and incubated in a humidified incubator at 37° C with 5% CO2 for 24 hours.
5. 100 µL media was aspirated and centrifuged after 6 and 24 hours. The supernatant was stored at -20° C until further analysis.

3.22 Enzyme-Linked Immunosorbent Assay

Materials:

ABTS liquid substrate

Avidin-HRP

H_2O_2

IL-8 ELISA Development Kit (See section 2.9)

PBS (See section 2.11)

Block buffer (PBS with 1% (w/v) BSA)

Diluent (PBS with 0.1% (w/v) BSA and 0.05% (v/v) Tween-20)

Wash buffer (PBS with 0.05% (v/v) Tween-20)

Methods:

The procedure was carried out in accordance with the recommended protocol from PeproTech, the supplier of the IL-8 ELISA Development Kit.

1. Capture antibody was diluted with PBS to a concentration of 0.5 μg/ml and 100 μL was added to each well on an ELISA plate.
2. The plate was sealed with Parafilm and incubated overnight at room temperature.
3. The capture antibody solution was aspirated and the plate was washed 4 times with 300 μL wash buffer per well before blotting off the remaining liquid on a paper towel.
4. 300 μL block buffer was added to each well and the plate was incubated for 1 hour at room temperature.
5. The plate was washed as in step 3. The standard was diluted in diluent at a ratio of 1:2 from 1000 pg/ml to 7.8 pg/ml and 100 μL per well was immediately added to the plate.
6. Supernatant from stimulation of Caco-2 cells was diluted in diluent at a 1:10 ratio. 100 μL was added to the wells in triplicates and incubated for 2 hours at room temperature.
7. The plate was washed as in step 3. Detection antibody was diluted in diluent to a concentration of 0.5 μg/ml and 100 μL was added to each well. The plate was incubated for 2 hours at room temperature.
8. The plate was washed as in step 3. 5.5 μL avidin-HRP was diluted in diluent at a ratio of 1:2000 to a total volume of 11 ml and 100 μL was added to each well. This was incubated for 30 minutes at room temperature.
9. The plate was washed as in step 3. 10 μL 3% H_2O_2 was added to 12.5 ml ABTS liquid substrate. 100 μL substrate was immediately added to each well and incubated at room temperature. Color development was monitored with a Tecan Sunrise™ microplate reader (405 nm, wavelength correction set at 650 nm) at 2, 5, 10 and 15 minutes after addition of ABTS.
10. Results where the zero standard concentration was ≤ 0.2 and the highest standard concentration was ≤ 1.5 were used for further analysis.

3.23 Transepithelial electrical resistance assay with Caco-2 cells

Materials:

cRPMI-1640 (See section 2.10)

EVOM^2 Epithelial Voltohmmeter

Falcon® 0.4 micron Cell Culture Inserts PET

Falcon® Tissue Culture Plates, Multiwell, 24 wells

Recombinant human TNF-α (TNF-α)

Methods:

1. Cultured Caco-2 cells were partially digested as detailed in section 3.20.2.
2. Sterile Falcon® 0.4 micron Cell Culture Inserts were added to a sterile Falcon® Tissue Culture Plate with 24 wells.
3. The cells were added to the Cell Culture Inserts at a concentration of 10^6 cells/cm^2, in 250 µL preheated cRPMI-1640. 750 µL medium was added to the wells in the Tissue Culture Plate.
4. The cells were incubated in a humidified incubator at 37° C with 5% CO2 for 21 days. The medium in the wells and inserts was changed every two days. After this period, transepithelial electrical resistance (TEER) was measured in accordance with section 3.23.1. Wells with a value ≥ 500 Ω*cm^2 were used for the assay.
5. The medium was aspirated from the filters and wells, taking care not to disturb the Caco-2 monolayer.
6. 750 µL preheated cRPMI or preheated cRPMI containing 10 ng/ml TNF-α was added to each well in the Tissue Culture Plate.
7. 10^7 UV-inactivated *L. plantarum* bacteria or cell-free protein extract from an equivalent amount, prepared as detailed in section 3.17.2 and section 3.17.3, were mixed with pre-heated cRPMI to a total volume of 250 µL and added to the filter inserts.
8. Purified protein was added to separate filters in the same way, to a final concentration of 3 µg/ml.
9. The TEER value of the filters were measured at 2, 4, 6, 12, 24, 36 and 48 hours as detailed in section 3.23.1. The cells were incubated at 37° C with 5% CO2 between measurements.

3.23.1 Measuring transepithelial electrical resistance

Materials:

cRPMI-1640 (See section 2.10)

Ethanol
EVOM^2 Epithelial Voltohmmeter

Methods:

1. The voltohmmeter probe was sterilized with 70% ethanol for 15 minutes and washed twice with 750 µL pre-heated cRPMI-1640 before measurements.
2. 750 µL pre-heated cRPMI-1640 was added to the probe well and the probe was zeroed. Using sterile tweezers, a Cell Culture Insert was carefully moved from the 24 well plate to the probe well and the probe was inserted.
3. After allowing 5-10 seconds for the value to stabilize, the TEER value was noted down. The Cell Culture Filter was moved back to the 24-well plate for continued incubation.
4. The probe was washed twice with cRPMI-1640 between measurements of different samples.
5. After completion of the measurements, the probe was washed with 70% ethanol and dH_2O, then stored dry until the next measurement.

3.24 Large scale preparation of lyophilized *Lactobacillus plantarum* lysate

L. plantarum harbouring pSIP401_MAM was needed in larger amounts for use as a protein source in a feeding trial with mice. 3- and 15-liter bioreactors from Applikon Biotechnology were used for this purpose. The bioreactors used in this thesis allow for measurement and control of a range of parameters including temperature, pH, O_2 concentration and stirring. After harvesting, the cells were lysed with a French press, where the cells are sent through a narrow valve under high pressure. This causes shear stress and rapid decompression of the cells, leading to lysis. The lysate was then lyophilized to ensure stability and ease of transport.

3.24.1 Bioreactor fermentation of *Lactobacillus plantarum*

Materials:

20 g/L D-(+)-glucose in dH_2O, autoclaved for 15 minutes at 115° C
Erythromycin
Glass Autoclavable Lab Scale Bioreactor, 3 L or 15 L, jacketed

MRS medium
5 M NaOH
0.1 µg/ml SppIP

Methods:

1. The bioreactor was autoclaved dry and the pH-meter to be used was calibrated using Technical Buffer Solution pH 4.01 and pH 7.00 and autoclaved.
2. 2 or 12 L sterile MRS medium was added to the bioreactor of corresponding size. The D-(+)-glucose was added, doubling the glucose concentration in the medium. Erythromycin was added to a final concentration of 10 µg/ml.
3. The pH meter and an external temperature probe were attached to the bioreactor. The heat jacket was then filled with water circulating at 37° C and the stirring rod was coupled on and started. The pH value of the medium was equilibriated and kept at 6.5 using 5 M NaOH.
4. An overnight culture with *L. plantarum* containing pSIP401_MAM or pEV was made in MRS medium containing 10 µg/ml erythromycin. For 2 L fermentations, the volume of the overnight culture was 20 ml. For 12 L fermentations, it was 120 ml.
5. Once the medium was at 37° C, the overnight culture was added and incubated for one hour or until the culture had reached an OD_{600} of 0.3 ± 0.03.
6. SppIP was added to the bioreactor to a final concentration of 25 ng/ml in order to induce expression of MAM. SppIP was also added to cultures with pEV to avoid confounding factors. The culture was then incubated for 12 or 16 hours.
7. At the end of the incubation time, the bioreactor was shut down and the culture was aseptically aspirated into clean centrifugation bottles on ice to stop growth. It was then immediately harvested as detailed in section 3.24.2.

3.24.2 Harvesting of *Lactobacillus plantarum* from bioreactor fermentations

Materials:
PBS (See section 2.11)

Methods:

1. 1 ml culture from section 3.24.1 was sampled for OD_{600} measurement. The rest of the culture was centrifuged in 1L centrifuge bottles at 5000 g for 10 minutes at 4° C.
2. The supernatant was used as zero-sample and diluent for measuring OD_{600} of the culture. After measuring, the supernatant was discarded.
3. The pellet from each bottle was resuspended in ice cold PBS to a total volume of 50 ml in Falcon® tubes.
4. The cell suspension was centrifuged at 5000 g for 10 minutes at 4° C and the supernatant was discarded.
5. Step 3 and 4 was repeated for a second PBS wash.
6. The pellet was stored at -80° C or French pressed immediately as detailed in section 3.24.3.

3.24.3 French pressing of *Lactobacillus plantarum*

Materials:

Carver Laboratory Press, Model C

40 ml French pressure cell

Methods:

1. The 40 ml French pressure cell was assembled, cleaned with 70% ethanol and chilled on ice before use.
2. The pellet from section 3.24.2 was resuspended in approximately 40 ml ice cold dH_2O and aseptically transferred to the pressure cell.
3. The bacterial suspension was pressed 3 times at between 6000 and 7000 PSI in order to lyse the cells.
4. The cell lysate was stored in a 50 ml Falcon tube at – 20° C or lyophilized immediately.

3.24.4 Lyophilization of *Lactobacillus plantarum* lysate

Materials:

Heto Drywinner Freeze Drier

Round-bottom flask

Methods:

1. The Heto Drywinner freeze drier was turned on and pre-chilled for 30 minutes.
2. The cell lysate prepared in section 3.24.3 was aseptically transferred to a round-bottom flask on ice.
3. The lysate was chilled to -60° C and the surface area maximized by spinning the round-bottom flask for 30 minutes in a water bath filled with denatured alcohol at -60° C.
4. The flask was transferred to the Heto Drywinner freeze drier and the valve was slowly opened to allow moisture to escape from the flask. The freeze drier was then run overnight.
5. The next day, the valve was slowly closed and the freeze drier turned off. The flask was removed and the dried cell lysate was transferred to an 800 ml plastic container. The lyophilized cell lysate was stored at room temperature, without light.
6. For verification of protein expression, 3 mg freeze dried bacteria were mixed with 10 µL sterile dH_2O until homogenous. The mixture was diluted 1:10 in sterile dH_2O and SDS-PAGE and Western blot was run as detailed in section 3.18 and 3.19.

4. RESULTS

The progression of work performed in this thesis is illustrated as a flow chart in Fig. 4.1.

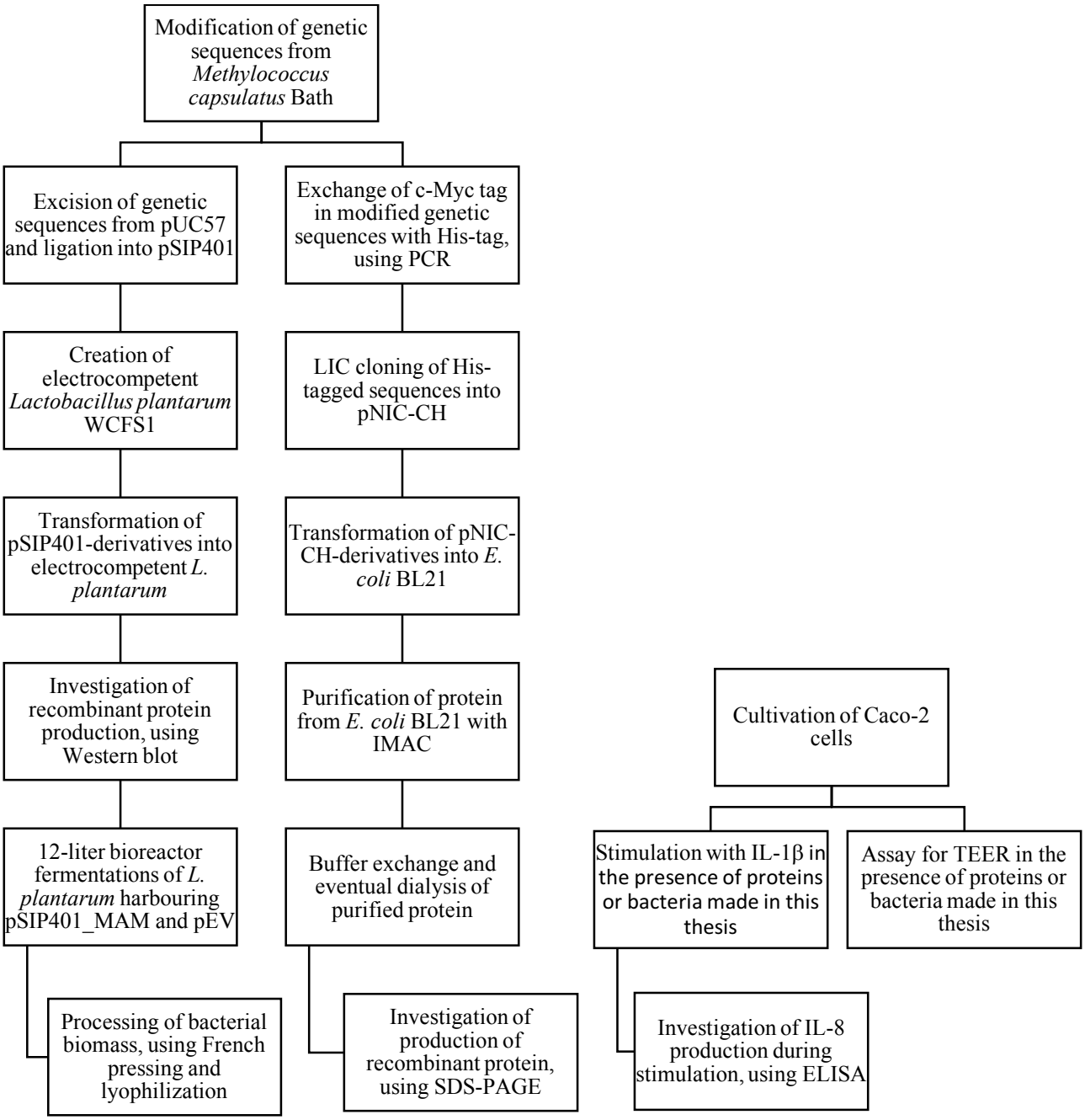

Figure 4.1. Flow chart of the progression of work performed in this thesis.

As Fig. 4.1 shows, the first step was obtaining modified genetic sequences (*mam, tir, mif* and *sim*) from *M. capsulatus* Bath, after which it was divided into three main parts.

First, the genes were excised from the pUC-57 vectors they were ordered in. They were then cloned into a pSIP401 backbone, creating the pSIP401-derived plasmids pSIP401_MAM, pSIP401_TIR2, pSIP401_MIF and pSIP401_SIMPL. These plasmids were amplified in *E. coli* GeneHogs. *L. plantarum* WCFS1 was made electrocompetent and the plasmids were cloned into this species. The production of recombinant protein in *L. plantarum* WCFS1 harbouring any of these plasmids was investigated by disrupting the cells and using Western blot. The results from all these steps are covered in sections 4.1 to 4.4. In addition, production of *L. plantarum* WCFS1 harbouring pSIP401_MAM was scaled up to 12-liter fermentations by using a bioreactor. These results are covered in section 4.5.

The second part of the work started with the exchange of the c-Myc tag in the modified genetic sequences with His-tags for protein purification. These sequences were cloned into a pNIC-CH plasmid backbone using LIC, creating the plasmids pNIC-CH_MAM, pNIC-CH_TIR2, pNIC-CH_MIF and pNIC-CH_SIMPL. The plasmids were amplified in *E. coli* GeneHogs, transformed into *E. coli* BL21 and purified using immobilized metal ion affinity chromatography (IMAC). After buffer exchange, the presence of purified protein was investigated with an SDS-PAGE analysis. These results are covered in section 4.2 and 4.6.

Finally, Caco-2 cells were cultured in order to perform two *in vitro* assays. In the first assay, Caco-2 cells were incubated in the presence of the pro-inflammatory cytokine IL-1β, together with either cell-free protein extracts from *L. plantarum* WCFS1 or purified protein from *E. coli* BL21. An ELISA was then performed to investigate whether the bacterial stimuli could influence the production of IL-8. In the second assay, Caco-2 cells were grown on permeable filters until they formed a differentiated monolayer. Then, they were incubated with bacterial stimuli apically and the pro-inflammatory cytokine TNF-α basolaterally. The permeability of the cell layer was measured to investigate whether it was influenced by the bacterial stimuli. These results are covered in section 4.7 and 4.8.

4.1 Construction of pSIP401-derived plasmids

In order to examine whether the proteins Mam, Tir, Mif and Sim had any effect in biological systems, they first had to be produced. To achieve this goal, the genes *mam, tir, mif* and *sim* were inserted into pSIP401, a plasmid from the pSIP inducible gene expression system. The new plasmids were then cloned into *L. plantarum* WCFS1 for inducible protein production. As *M. capsulatus* Bath was delivered as a lyophilized, disrupted extract in the diet in previous animal trials (Kleiveland et al. 2013; Romarheim et al. 2011), the plasmid system was adapted for intracellular overexpression of the genes.

The recombinant genes were designed in the pDraw32 software. First, the c-Myc tag sequence (GAA CAA AAG TTA ATT AGT GAA GAA GAT TTA, translated to EQKLISEEDL) was added 5' of the stop codon of each gene for a C-terminal placement in the translated protein. This sequence motif, originally derived from the human c-myc-protein, is an epitope for the widely available 9E10 monoclonal antibody (Hilpert et al. 2001). It was therefore used for verification of protein expression with Western blot. Restriction sites were then added to the genetic sequence to enable ligation into the vector with restriction enzymes. The sequence *Nde*I (CATATG) was added to the 5' end and *Hin*dIII (AAGCTT) was added to the 3' end, as these sites were upstream and downstream of the insertion site in the vector.

Once the genetic sequences were modified, they were sent to the company GenScript which optimized them for expression in *L. plantarum*, synthesized and inserted them into a pUC57 vector, which is commonly used for cloning in *E. coli*. GenScript's optimization process involves modifying the codon usage and GC content of the gene, as each organism has different preferences for these factors. Species-specific abundance of tRNA means rare codons can lead to expression problems (McNulty et al. 2003). *M. capsulatus* has an average genomic GC-content of 63.6 % (Ward et al. 2004), while *L. plantarum* has 44.5% (Kleerebezem et al. 2003). Correcting for these factors means expression of genes from one species can be increased in another. This also extends to expression of eukaryote genes in prokaryotes, e.g. human genes in *E. coli* (Burgess-Brown et al. 2008).

After the plasmids pUC57_MAM, pUC57_TIR2, pUC57_MIF and pUC57_SIMPL were received, they were transformed into and amplified in *E. coli* GeneHogs (See section 3.12.1). *E. coli* GeneHogs harbouring the plasmid pLp1261_Ag85B-ESAT6 was provided by Lise

Øverland (Øverland 2013) and used to obtain the pSIP401 vector backbone. The isolated recombinant gene inserts and pSIP401 backbone were obtained by restriction digestion with the restriction enzymes NdeI and HindIII (Section 3.5). After purifying the desired fragments from an agarose gel, the genes were ligated into pSIP401 (section 3.8.1), creating the new plasmids pSIP401_MAM, pSIP401_TIR2, pSIP401_MIF and pSIP401_SIMPL. See Fig. 4.2 for a graphical representation of the process. These were then transformed into *E. coli* GeneHogs (Section 3.12.3). After cultivating the bacteria and isolating the plasmids, they were sent to GATC Biotech for DNA sequencing, to verify that the transformations had been successful, and that no changes had occurred in the DNA sequences. *L. plantarum* WCFS1 was made electrocompentent and the pSIP401 plasmids were transformed into the bacteria (Sections 3.11 and 3.12.2).

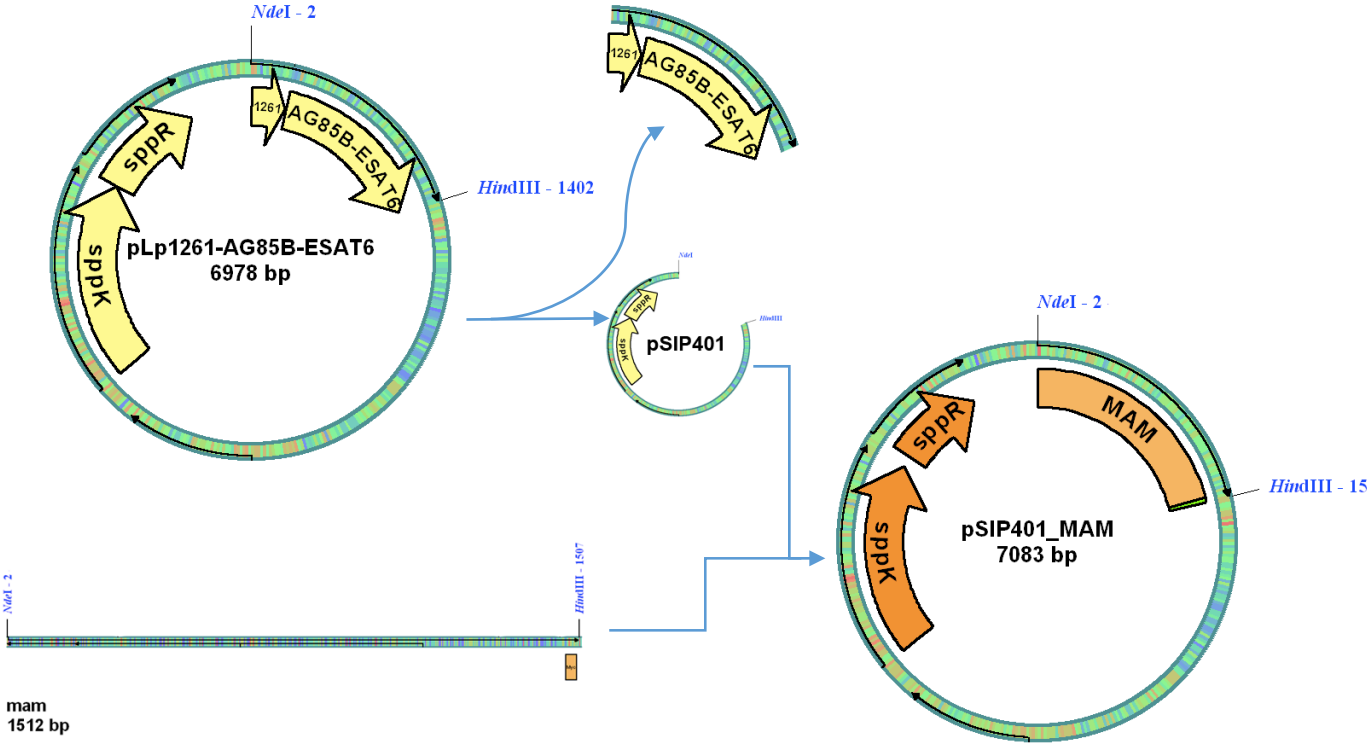

Figure 4.2 Graphical representation of construction of pSIP401_MAM from pLp1261_Ag85B-ESAT6 and recombinant *mam*. The figure shows pLp_1261-Ag85B-ESAT6 and *mam* to the left, the pSIP401 backbone after excision of 1261-Ag85B-ESAT6, then the completed pSIP401_MAM construct. The relevant restriction sites *Nde*I and *Hin*dIII are also indicated. Sequences are not to scale.

4.2 Primer design and insertion of His- and Myc-tags

The recombinant genes used in this thesis were equipped with a c-Myc-tag sequence at the 3' end of each gene, for verification of expression with Western blot. In order to produce purified protein from *E. coli* BL21, this tag had to be replaced with a His-tag for binding to an IMAC column. The His-tag has a high affinity to immobilized Ni^{2+} ions in the column and binds strongly to it. For this purpose, forward and reverse primers had to be designed for each gene. In addition, pUC57_SIMPL was ordered from GenScript without the 3' c-Myc tag sequence. In-Fusion-compatible primers were designed to clone this tag into the gene for verification of expression.

When designing primers, guidelines were taken from the In-Fusion® HD Cloning Kit User Manual by Clontech Laboratories Inc (Clontech 2014). Following the guidelines (except the addition of a 15 bp overhang, which is only used when performing In-Fusion cloning), individual primers (section 2.7) were designed for insertion of a hexa-His-tag upstream of the c-Myc-tag, effectively replacing this tag in the genetic sequence. A PCR was then run using Q5 DNA polymerase, chosen to minimize the chance of transcriptional errors, on pSIP401-constructs isolated from *E. coli*. The individual primers for each gene (e.g. Mam_F, Mam_R) allowed PCR fragments with a 3' His-tag to be created, see Fig. 4.3 for a graphical representation.

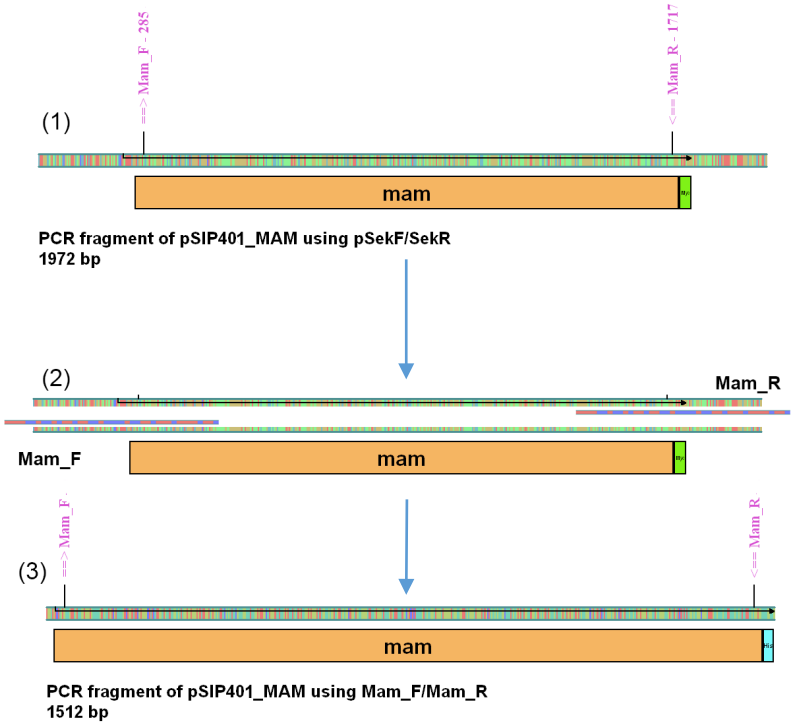

Figure 4.3. Graphical representation of exchange of tags in the genetic sequence *mam*. (1), PCR fragment of *mam* amplified from pSIP401_MAM with pSekF and SekR. c-Myc-tag is indicated as a green box at the 3' end of the gene; (2) Simplified view of Q5 PCR reaction with primers; (3), PCR fragment with the c-Myc-tag having been replaced with a His-tag, indicated as a blue box at the 3' end of the gene. The starts of primer annealing sites are indicated with pink text. Primers are not to scale.

For insertion of c-Myc into *sim*, primers were designed with the same guidelines referred to above. In addition, they were designed to be In-Fusion compatible, which involves adding a 15 bp overhang to the genetic sequence at both ends for the In-Fusion cloning reaction. First, a two-step PCR was performed, using Q5 DNA Polymerase in order to minimize the chance of transcriptional errors (See section 3.9). The first reaction used the primers Simpl_F and Simpl_R1, adding a 15 bp overlap to the 5' end of the gene and half the c-Myc sequence to the 3' end. The second reaction used the same forward primer, Simpl_F and a new reverse primer, Simpl_R2. Simpl_R2 allowed for the addition of the rest of the c-Myc sequence, a stop codon and a 15 bp overlap at the 3' end. See Fig. 4.4 for a graphical overview. The SIMPL-Myc-fragment was then ligated into a pre-digested pSIP401 vector via In-Fusion (See section 3.8.2).

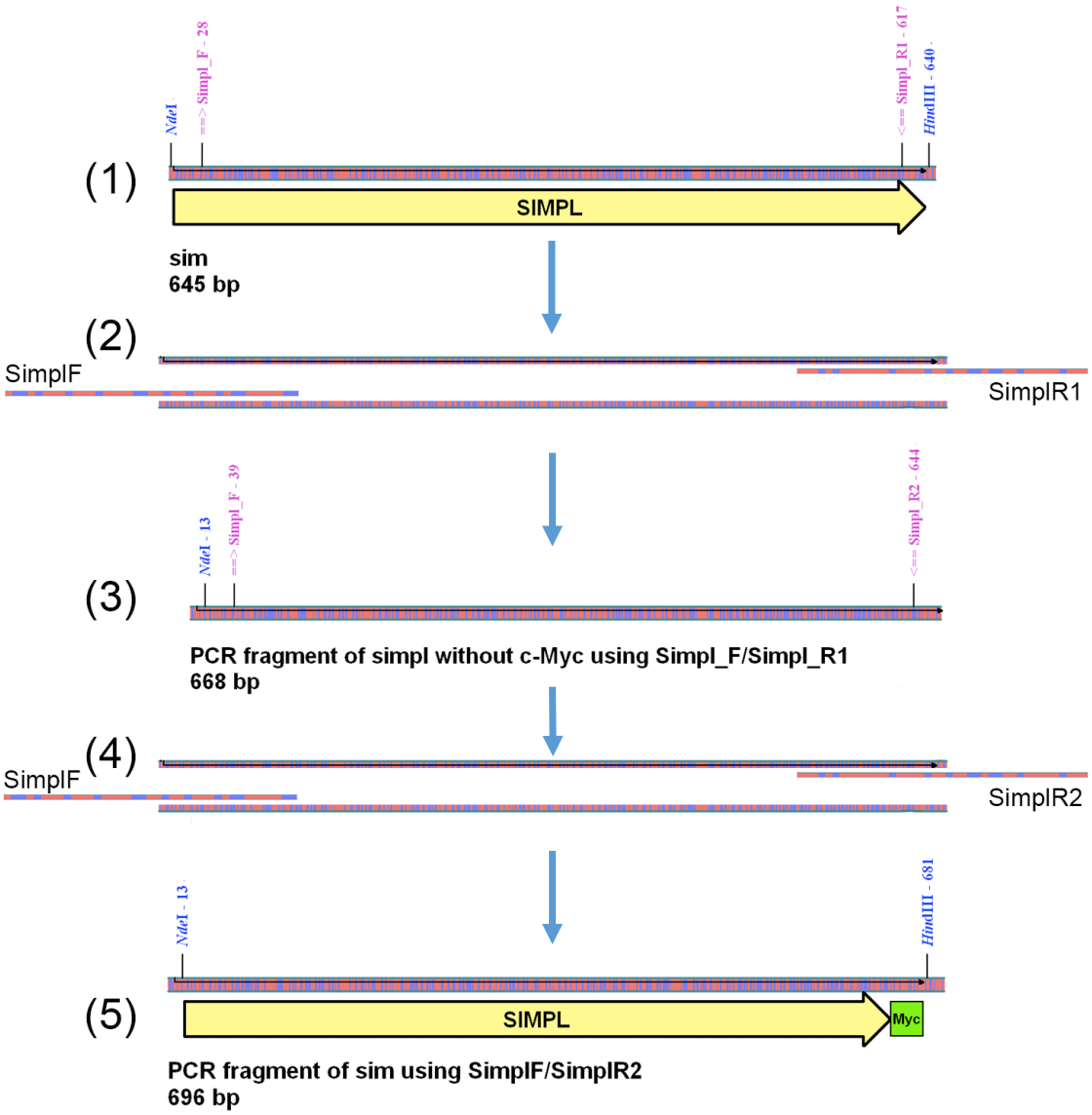

Figure 4.4. Schematic representation of insertion of c-Myc-tag into the *sim* gene. (1), *sim* gene without tags; (2) simplified view of Q5 PCR reaction 1 with primers; (3), PCR fragment with 5' 15 bp overlap and partial c-Myc-tag; (4) simplified view of Q5 PCR reaction 2 with primers; (5) finished PCR fragment with complete c-Myc-tag. The restriction sites *Nde*I and *Hin*dIII are indicated with blue text. The start of primer annealing sites are indicated with pink text. Primers are not to scale.

The final PCR-amplified gene sequence contained a 5' 15 bp overlap as well as a 3' c-Myc tag and 15 bp overlap. In-Fusion was then performed to ligate the insert into a linearized pSIP401-vector, as detailed in section 3.8.2. The finished pSIP401_SIMPL plasmid was sent for DNA sequencing by GATC Biotech, amplified in *E. coli* GeneHogs, isolated and transformed into *L. plantarum* WCFS1.

4.3 Growth characteristics of *L. plantarum* harbouring different plasmids

When introducing and expressing exogenous proteins in bacteria, the bacteria are put under higher metabolic stress than normal. This is due to a range of factors, e.g. codon usage, secretion stress or function of the expressed protein (Fakruddin et al. 2013; Mathiesen et al. 2008; McNulty et al. 2003). Previous studies on production of proteins destined for membrane anchoring or secretion have shown reduced growth rates compared to pEV (Øverland 2013; Solberg 2015; Tjåland 2011). Those proteins are more metabolically expensive for the bacteria, as they have to be transported to the surface. However, intracellular production of the *M. capsulatus* Bath proteins could also potentially affect the growth rate. Therefore, growth curves were made with *L. plantarum* harbouring the different pSIP401-constructs.

L plantarum harbouring pSIP401-constructs (pSIP401_MAM, etc) were cultured until they had an optical density measured at 600 nm (OD_{600})–value of 0.3 ± 0.03, then induced with 25 ng/ml SppIP and harvested every hour for 4 hours (see section 3.17.1). A strain harbouring pEV was used as NC. All strains, except the one harbouring pSIP401_SIMPL, were also harvested at 6 and 8 hours. The results are shown in Fig. 4.5.

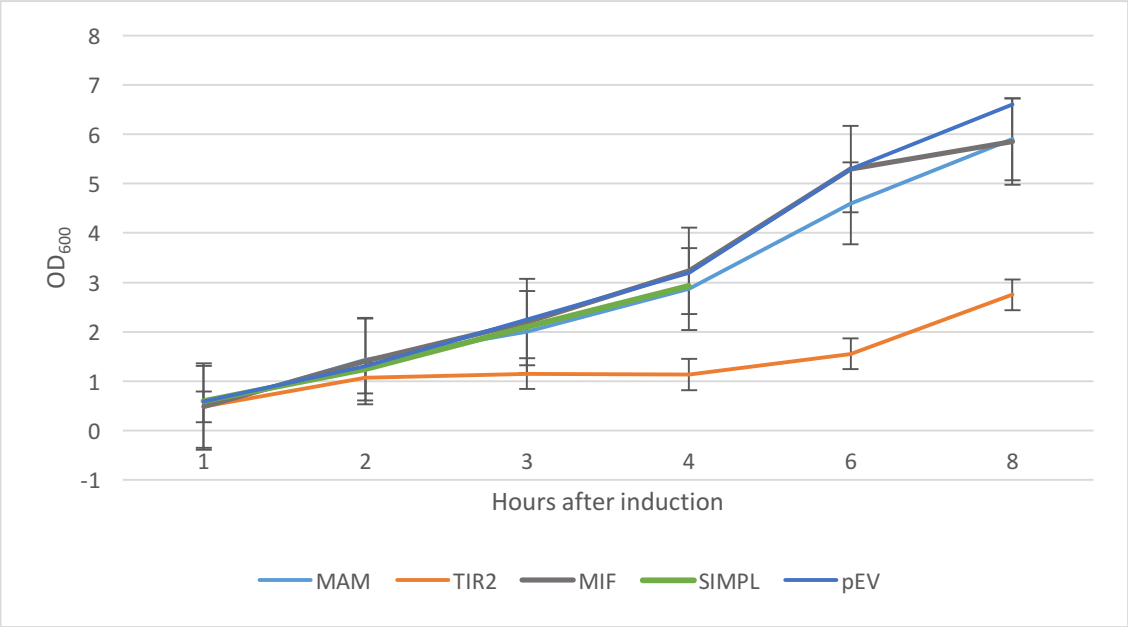

Figure 4.5. Growth curves for *L. plantarum* harbouring different plasmids. The curves show the average OD_{600}-value of three separate harvests at given times after induction with SppIP. The error bars represent one standard error.

As the figure shows, the cultures harbouring pSIP401_MAM, pSIP401_MIF and pSIP401_SIMPL grew in close parallel to pEV. Cultures harbouring pSIP401_TIR2 demonstrated significantly slower growth rate than the other cultures after 3 hours.

4.4 Analysis of protein production with Western blot

In order to determine whether the recombinant proteins had been produced, a Western blot analysis was run. Western blot is a method used to identify proteins in a sample with high sensitivity and accuracy, using the principle of antibody hybridization. First, *L. plantarum* harbouring pSIP401-derived plasmids were cultured and harvested, then disrupted by using glass beads (See section 3.17.1 and 3.17.3, respectively). The resulting cell-free protein extracts were used for Western blot analysis (Section 3.19), with volume adjustments according to the OD_{600} measurements at the time of harvest in order to include approximately equal amounts of cells in each sample. Fig. 4.6 below shows a Western blot of cell-free protein extracts. The predicted size of each protein, including the Myc-tag, was calculated from the DNA sequence with a protein calculator in pDraw32. These are shown in Table 4.1.

Table 4.1. Recombinant proteins from *M. capsulatus* with predicted sizes, including Myc-tag.

Protein	Mam	Tir	Mif	Sim
Size (kDa)	55,4	36,4	13,5	24,2

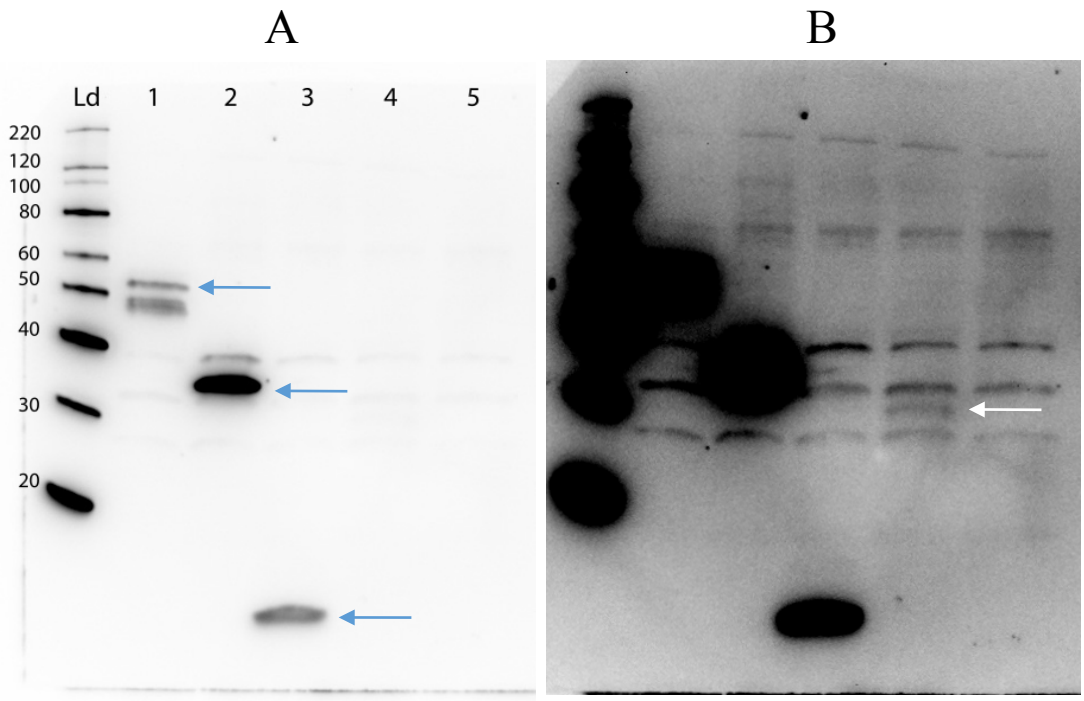

Figure 4.6. Western blot analysis of Mam, Tir, Mif and Sim in cell-free protein extracts. Blot A and B are the same Western blot at 1 minute (A) and 5 minute (B) exposure times and show proteins from induced *L. plantarum* harbouring different pSIP401-constructs. (Ld) MagicMark XP protein ladder with sizes of protein bands indicated to the left, in kDa; (1) pSIP401_MAM; (2) pSIP401_TIR2; (3) pSIP401_MIF; (4) pSIP401_SIMPL; (5) Negative control.

Fig. 4.6A shows bands, indicated with arrows, at approximately the expected sizes for Mam, Tir and Mif. The band intensity indicates that Tir was produced in larger amounts than the other proteins, while Mam and Mif were produced in relatively similar amounts. Mam also seems to have been digested at some point, producing at least two bands. As seen in Fig. 4.6B, a band was visible in the lane with pSIP401_SIMPL when increasing the exposure time. This band was only visible at a similar intensity as unspecific background proteins, but was not found in any other samples. However, it appears to be larger in size than the predicted size of Sim. A band at approximately 40 kDa also appears as an unspecific protein in all samples, but more strongly in the bacteria producing Tir.

4.5 Bioreactor fermentation of *L. plantarum* WCFS1

One of the proteins examined in this thesis, Mam, was selected to be used in a diet intervention experiment using a murine model of diet-induced obesity. Thus, it had to be

produced in large quantities. An estimated 180-200 g of lyophilized bacterial biomass was needed for *L. plantarum* harbouring pSIP401_MAM as well as an equivalent amount harbouring pEV, for use as NC. A 15-liter bioreactor, holding up to 12 liters of medium, was chosen as the vessel for the fermentations.

When performing smaller cultivations and harvesting of *L. plantarum* (See section 3.17.1), the only controlled parameters were temperature and concentration of the IP. In addition, the bacteria were generally harvested 4 hours after induction. In order to maximize the biomass extracted from each larger fermentation, longer times were used and additional parameters were controlled. Nguyen, T. L. A. et al. (2015) investigated the effects of conditions such as pheromone dose, induction timing, pH and glucose concentration on the production of β-galactosidase in *L. plantarum*, using a pSIP403-construct as the inducible gene expression system. They found optimal expression of that protein with a culture pH = 6.5 and a doubling of glucose in the medium to 40 g/l. There was also a clear dose-response curve for SppIP concentration up to 40 ng/ml.

For the fermentations in this thesis, the pH and glucose parameters were chosen according to (Nguyen, T. T. et al. 2015) and 20 ng/ml SppIP was used. A pilot fermentation was first performed as detailed in section 3.24.1, with 2 liters of medium. Samples were drawn every 2 hours to make a growth curve, shown in fig. 4.7. 12-liter fermentations were then performed for either 12 or 16 hours. The fermented broth was harvested as detailed in section 3.24.2 and OD_{600}-values were recorded. Average OD_{600}-values for 12-liter fermentations are shown in Table 4.2.

After fermenting, the cells were disrupted via French press and lyophilized (See section 3.24.3 and 3.24.4, respectively) for storage. To confirm production of protein, a Western blot analysis was performed on lyophilized material from each fermentation with *L. plantarum* harbouring pSIP401_MAM, as explained in section 3.24.4. All fermentations were shown to be successfully induced (data not shown).

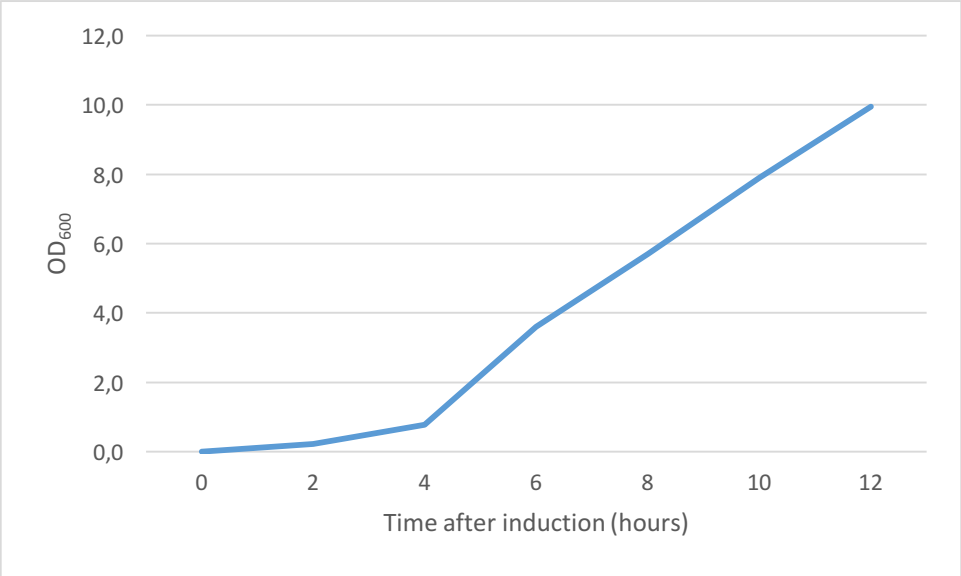

Figure 4.7. Growth curve of pSIP401_MAM harvested from a 2-liter bioreactor fermentation. The graph shows OD_{600}-values from samples harvested at set time points.

Table 4.2. OD_{600}-values at harvesting of pSIP401_MAM and pEV. Values shown are for 12-liter fermentations and represent the average of three fermentations, except for late-induced pSIP401_MAM which was one repetition.

	pSIP401_MAM (12 hours, early-induced)	pSIP401_MAM (12 hours, late-induced)	pSIP401_MAM (16 hours)	pEV (16 hours)
OD_{600}	10,2	13,0	14,8	16,1

Fig. 4.7 shows that the culture started out with exponential growth up until the 4 or 6 hour mark, after which the increase in biomass became more linear. Fig 4.7 and Table 4.2 show that the OD_{600} value was similar for fermentations with pSIP401_MAM at the 12-hour mark regardless of whether the volume is 2 or 12 liters. At 16 hours, the OD_{600} was slightly lower for cultures producing Mam than for control cultures with pEV, with an average of 14,8 for the former and 16,1 for the latter. For the 12-liter fermentations, SppIP was added to the medium 1 hour after inoculation (early-induced) with bacteria instead of at the standard OD_{600}–value of 0.3 ± 0.03. A 12-hour fermentation where induction took place at the standard OD_{600}–value (late-induced, 2 hours 30 minutes after inoculation) was also performed to see if this led to a difference in production of protein. Compared to the early-induced fermentations, this led to a higher OD_{600}-value at 12 hours (13,0 compared to an average of 10,2). A Western blot with equivalent amounts of bacteria from one early-induced and the late-induced culture was performed. The results are shown in Fig. 4.8.

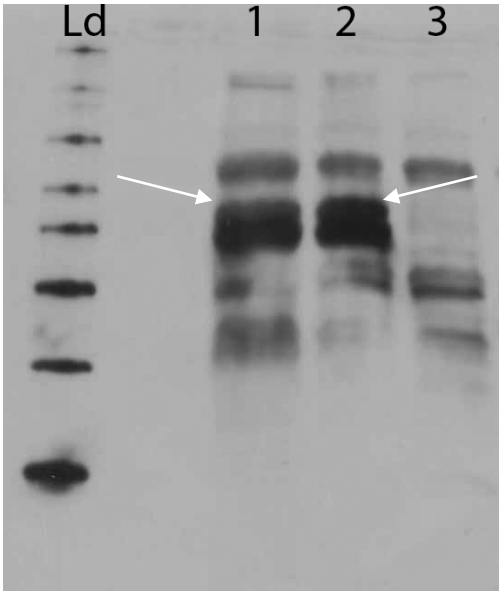

Figure 4.8. Western blot analysis of Mam in lyophilized *L. plantarum*. The blot shows proteins from induced *L. plantarum* harbouring pSIP401_MAM induced at two different times. Protein bands containing Mam are indicated with arrows. (Ld), MagicMark XP protein ladder; (1), Early-induced pSIP401_MAM; (2), Late-induced pSIP401_MAM; (3) Negative control, early-induced pEV.

As the figure shows, the intensity of the bands is relatively similar for the early- and late-induced cultures. There is also a significant amount of cleaved protein in each sample, as well as significant amounts of unspecific protein.

4.6 Production and purification of protein from *Escherichia coli* BL21

While production of the recombinant proteins from *M. capsulatus* Bath was achieved in *L. plantarum* WCFS1, this system also included all other proteins produced by *L. plantarum*. In order to examine potential effects of the proteins without this background interference, the genes were further modified to include a hexa-His-tag instead of the c-Myc-tag. This allows for purification of the protein by using IMAC, which is one of the most well-documented ways of producing purified protein (Structural Genomics Consortium 2008).

After obtaining PCR fragments with His-tagged genes (See section 4.2), the fragments were digested with T4 DNA polymerase and cloned with LIC (See section 3.8.3) into a pre-digested, linearized pNIC-CH vector. This vector, constructed by Gileadi (2006), includes sites for LIC cloning and a fragment which includes the SacB gene, allowing negative

selection on 5 % sucrose. The cloning resulted in the plasmids pNIC-CH_MAM, pNIC-CH_TIR2, pNIC-CH_MIF and pNIC-CH_SIMPL. The mixture was then transformed into *E. coli* TOP10 (See section 3.12.3). which were plated on BHI agar with 2% sucrose and 50 µg/ml kanamycin. Colonies which grew on this agar did not contain uncut vector and were chosen for further culturing. After amplification of the plasmids, they were isolated and transformed into *E. coli* BL21 (Sections 3.3 and 3.12.4, respectively). The plasmids were also sent for sequencing by GATC Biotech. *E. coli* BL21 harbouring the pNIC-CH-derivatives were then incubated, harvested and disrupted (Sections 3.13.1 and 3.13.2). After centrifugation, both the supernatant and the pellet were analysed SDS-PAGE to verify that the proteins were found in the supernatant. See Fig. 4.9 for the results. The supernatant was then used for protein purification as outlined in section 3.14. Fig. 4.10 shows a modified sample graph, from the purification of Mif and Tir. After purification, the elution buffer was then exchanged with 20 mM Tris pH 8.0 for storage of the proteins. This caused Mam to precipitate, so it was re-dissolved in 8 M urea before being dialysed against 20 mM glycine pH 9.2 (Sections 3.14.2 and 3.14.3). The presence of purified proteins was then investigated with SDS-PAGE, see Fig. 4.11.

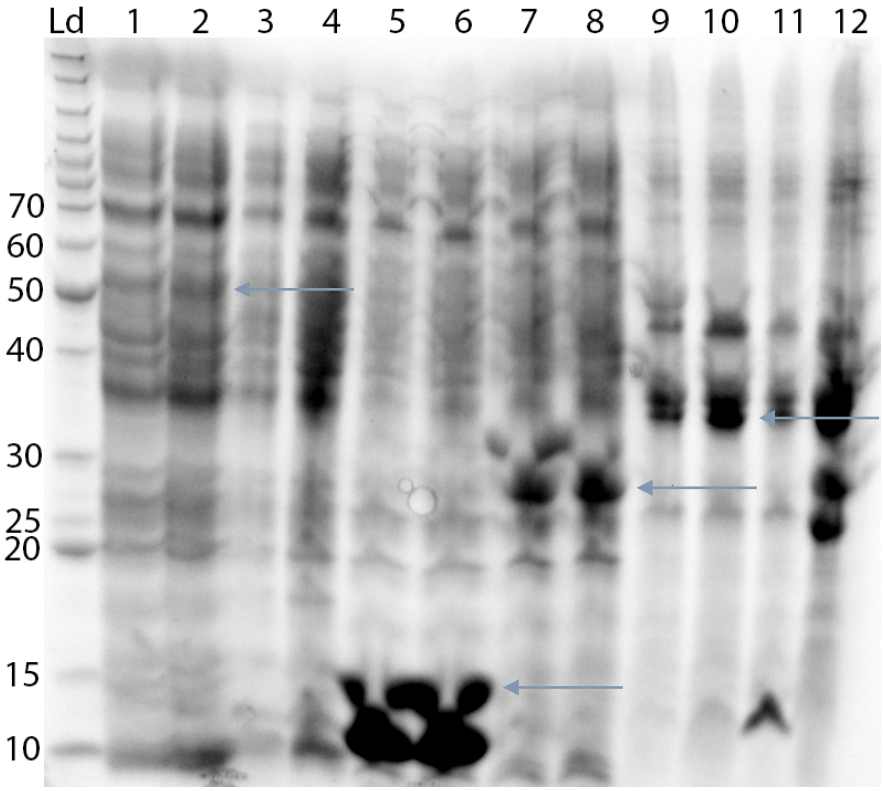

Figure 4.9. SDS-PAGE analysis of supernatant and pellet from lysed *E. coli* BL21. The gel shows proteins from induced *E. coli* BL21 harbouring different pNIC-CH-constructs. (Ld) Benchmark™ Protein Ladder with sizes of protein bands indicated to the left, in kDa; Samples 1-8 are supernatant, samples 9-12 are pellet. (1, 2, 9)

pNIC-CH_MAM; (3, 4, 10) pNIC-CH_TIR2; (5, 6, 11) pNIC-CH_MIF; (7, 8, 12) pNIC-CH_SIMPL. Possible target proteins are indicated with arrows.

As Fig. 4.9 shows, there is possibly a weak band for Mam in samples 1 and 2 and 9. There does not seem to be a strong band for Tir in samples 3 or 4, but there is one in sample 10. Mif and Sim both have strong bands in the samples from the supernatant and the pellet.

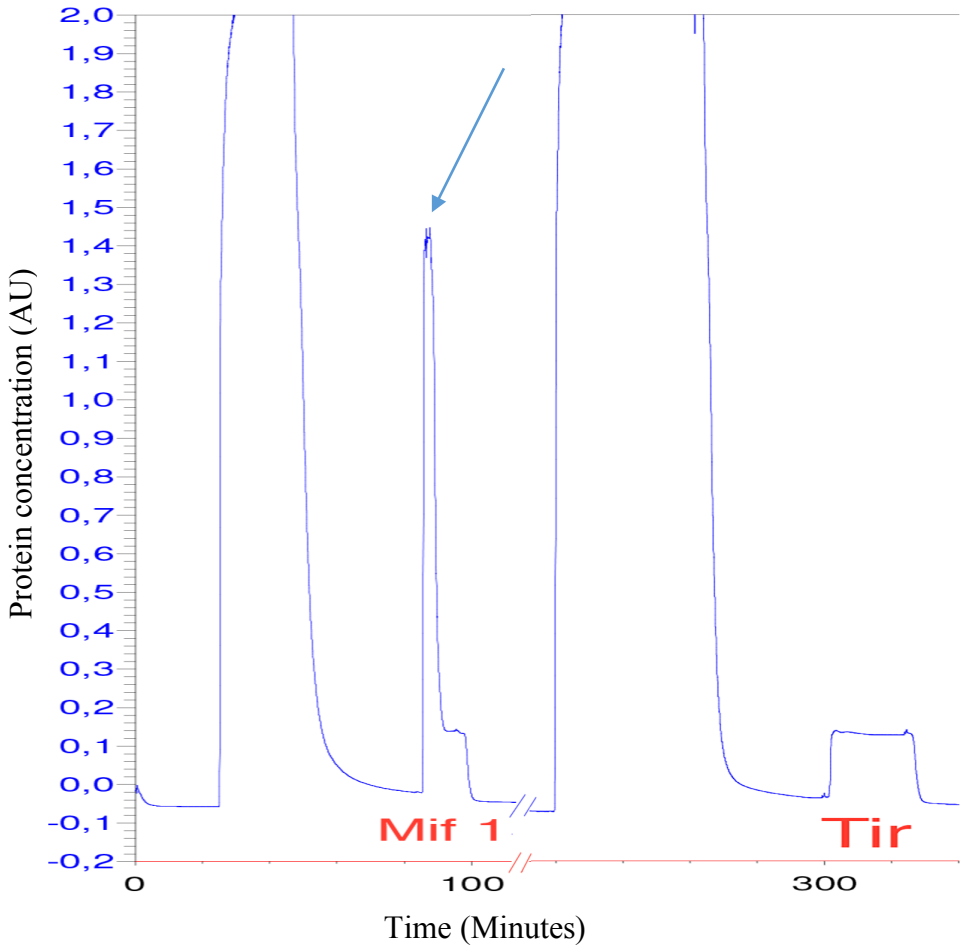

Figure 4.10. Elution diagram from LP Data View 1.03 for purification of Mif and Tir. The X axis shows minutes after start of run, with a break between the two samples. The Y axis shows amount of protein measured via UV light at 280 nm, to a cutoff value of 2,0, in absorbance units (AU). Peak showing elution of bound proteins is indicated with an arrow.

In Fig. 4.10, the first peak for each sample (with top above 2.0 AU) shows flow-through of proteins which do not bind to the column material. The second peak shows elution of bound protein. As seen for Mif, a significant amount of protein was eluted from the column when switching to Buffer B during IMAC. After the protein was eluted, the graph dropped to the baseline for buffer B, which is approximately 0,15 AU. The graphs for Mam, Mif and Sim all

showed similar peaks. As seen in the graph for Tir, however, this peak was absent, indicating little or no bound protein.

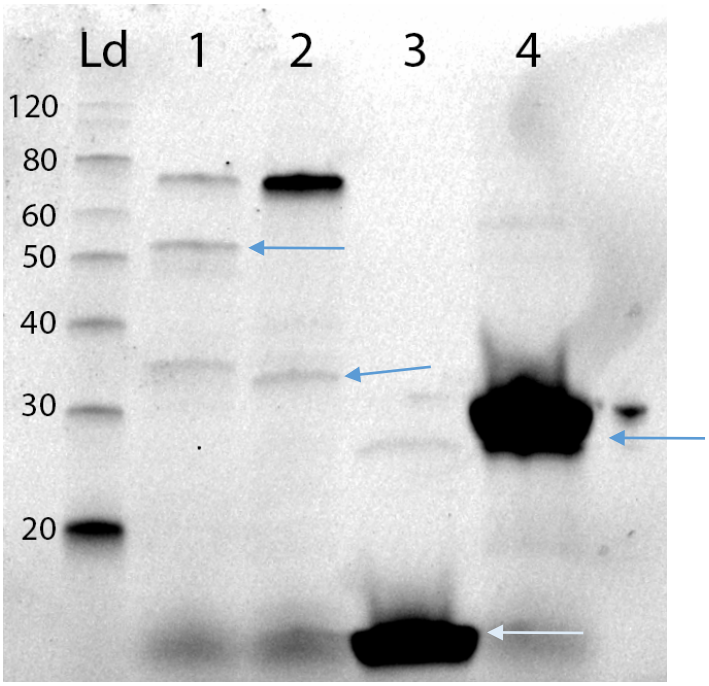

Figure 4.11. SDS-PAGE analysis of purified proteins: Mam in 20 mM glycine pH 9.2, Tir, Mif and Sim in 20 mM Tris pH 8.0 after IMAC and buffer exchange. The stained gel shows proteins from induced *E. coli* BL21 harbouring different pNIC-CH-constructs. (Ld) MagicMark XP protein ladder with sizes of protein bands indicated to the left, in kDa; (1) pNIC-CH_MAM; (2) pNIC-CH_TIR2; (3) pNIC-CH_MIF; (4) pNIC-CH_SIMPL.

Fig. 4.11 shows protein bands at around the expected sizes for each protein, indicated with arrows. The different samples were not accurately adjusted for concentration, as the purpose was a simple verification. This led to a significant difference in band strength, with Mif and Sim being present in very large amounts compared to Mam. Cleavage products of Mam may be present. Interestingly, there seemed to also be a potential band for Tir. This sample was therefore intended for further analyses with Caco-2 cells. (See sections 4.7 and 4.8).

4.7 IL-1β stimulation and ELISA for production of IL-8

After obtaining protein-producing *L. plantarum* WCFS1 and purified protein from *E. coli* BL21, the next step was to investigate whether there were any direct effects on eukaryotic cells. This was done via two assays involving Caco-2 cells. The first assay was an ELISA for

IL-8 production after stimulation of the cells with IL-1β. This assay was also used by Quevrain et al. (2016a) when investigating anti-inflammatory effects of MAM from *F. prausnitzii*. In that study, the presence of MAM in supernatant from *F. prausnitzii* exerted inhibitory effects on IL-1β-induced secretion of IL-8 from Caco-2 cells.

As Caco-2 cells are functionally similar to human small intestinal enterocytes, they produce cytokines in response to extracellular stimuli. IL-1β is a cytokine which is secreted into the interstitial fluid and blood during inflammation, and higher levels of IL-1β is correlated with increased levels of intestinal inflammation (Al-Sadi & Ma 2007). Incubating Caco-2 cells in the presence of IL-1β will cause the release of chemokines like IL-8. The main function of IL-8 is to recruit and activate neutrophils to a site of inflammation, as well as attracting NK cells, basophils and T cells. It is found in higher amounts at such sites in patients with inflammatory diseases such as reactive arthritis and psoriasis (Akdis et al. 2011). Lactobacilli such as *L. plantarum* and *L. rhamnosus* GG have also been shown to reduce the amount of IL-8 produced by Caco-2 cells stimulated by TNF-α or enterotoxigenic *E. coli*, which induces production of IL-1β (Ren et al. 2013; Roselli et al. 2006). Whole *L. plantarum* bacteria were therefore included in the stimulation, to investigate whether they might affect production of IL-8. The bacteria were UV-inactivated to ensure they did not cause altered parameters in the assay (e.g. reducing pH in the medium through production of lactic acid).

Caco-2 cells were cultivated until passage 25 and added to separate wells in a 24-well plate at a concentration of 10^5 cells/cm^2. The cells were allowed to settle overnight before being stimulated with IL-1β in the presence of either UV-inactivated *L. plantarum* harbouring pSIP401-derived constructs, a cell-free protein extract of the same or purified protein from *E. coli* BL21, as detailed in section 3.21. The supernatants from 6 and 24 hours were then analysed with ELISA, as detailed in section 3.22. The 6- and 24-hour stimulations had similar results, therefore only the data from the 6-hour stimulation are included. The standard curve was used to calculate the amount of IL-8 in each sample with the equation $y = -0{,}0671x + 0{,}3479$ (see Appendix, Fig. A2). The results are shown in Fig 4.12 below.

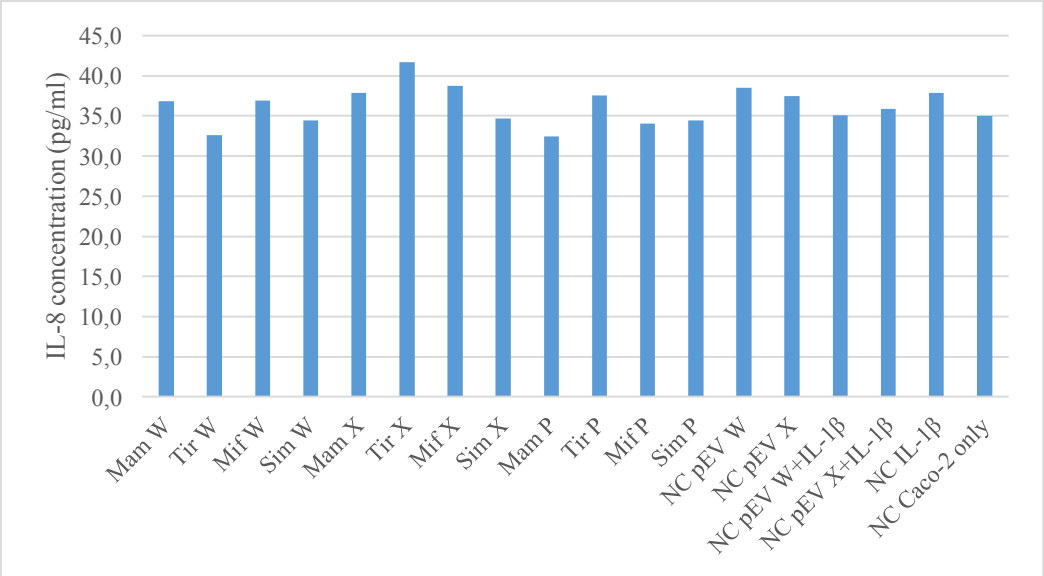

Figure 4.12. Analysis of IL-8 production by Caco-2 cells. The columns show the amount of IL-8 secreted by Caco-2 cells in the presence of bacterial stimuli after 6 hours of stimulation with IL-1β. The stimuli are indicated with the name of the produced protein and W (whole, inactivated cells), X (cell-free protein extract) or P (purified protein). Negative controls are indicated with NC and only contain IL-1β if specifically stated. Error bars have been omitted as there were no statistically significant differences between samples.

As Fig. 4.12 shows, there were no apparent trends or differences in IL-8 production between the samples, or between the samples and negative controls.

4.8 Assay for effects on transepithelial electrical resistance

The second of the assays involving eukaryotic cells in this thesis investigated transepithelial electrical resistance (TEER). TEER is the measure of permeability across an epithelial cell layer grown on a membrane. When grown to confluence in a monolayer, Caco-2 cells will spontaneously differentiate into a polarized single-cell layer with apical and basolateral sides reminiscent of human intestinal enterocytes. As such, they are susceptible to changes in tight junction permeability in the same way. TEER assays are simple and reproducible and are therefore often used to investigate whether various compounds may have an effect on intestinal permeability (Lea 2015a).

Intestinal epithelial tight junction permeability is regulated by many factors. One of them is the proinflammatory cytokine TNF-α which causes an increase in tight junction permeability

via NF-κB pathways (Ma et al. 2004). This cytokine was added basolaterally in the TEER assay to investigate whether cell-free protein extract or purified proteins could diminish a TNF-α-induced reduction in TEER. First, Caco-2 cells were cultured until at passage 20, as detailed in section 3.20. The cells were then added and grown to a differentiated monolayer on permeable filters, before a TEER assay was performed (see sections 3.23 and 3.23.1). Cell-free protein extracts or purified protein was added apically and 10 ng/ml TNF-α was added basolaterally. TEER was then measured every two hours for 12 hours, then every 12 hours until 48 hours after start. Measurements in Ω were multiplied with the area of the filter inserts (0,33 cm^2) to obtain an area-independent value (Ω*cm^2). The results are shown in Fig. 4.13 and Fig. 4.14 below.

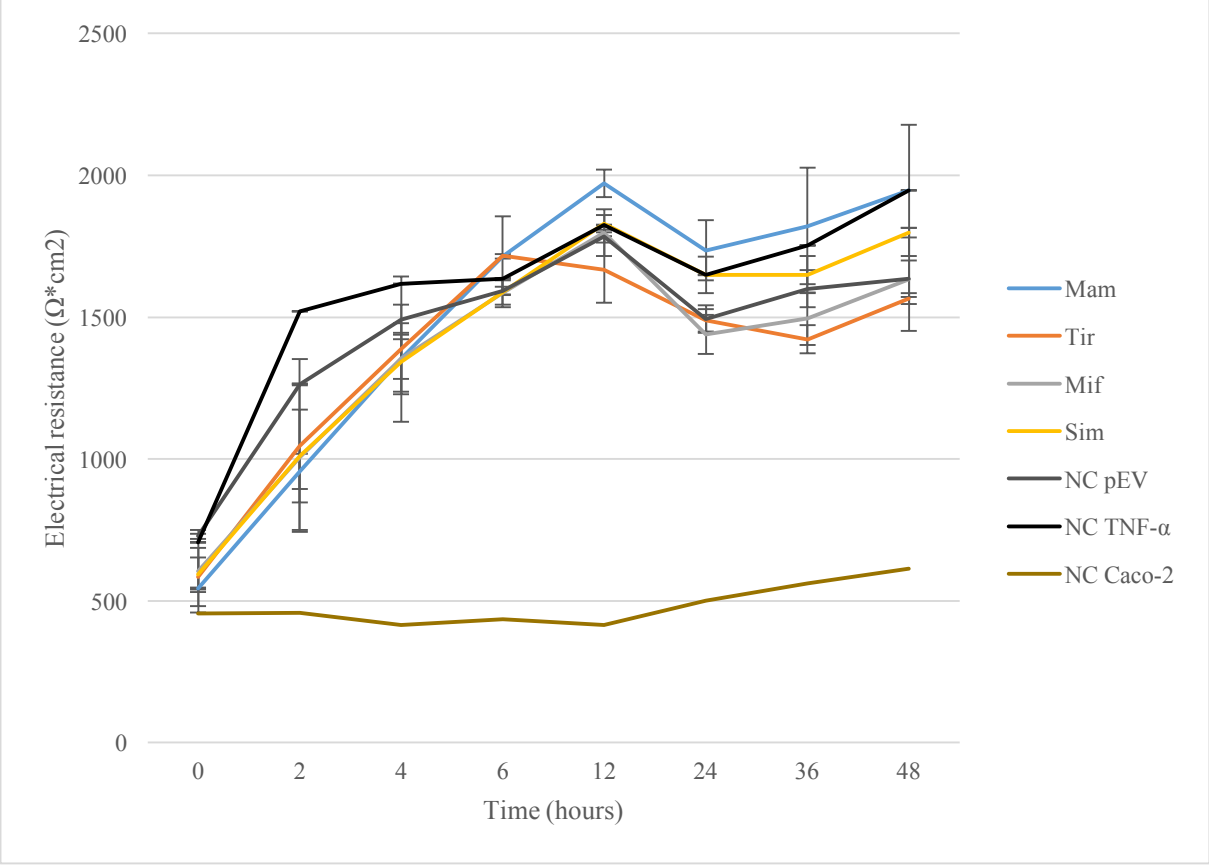

Figure 4.13. **Analysis of TEER-values of Caco-2 cells with cell-free protein extract.** The graph shows TEER-values in Ω*cm^2 measured at set times after start. The cells were incubated with bacterial stimuli apically and TNF-α basolaterally. Each series is indicated by the recombinant protein the sample contained. NC pEV, Caco-2 cells, pEV and TNF-α; NC-TNF-α, Caco-2 cells and TNF-α only; NC Caco-2, Caco-2 cells only. Error bars show one standard deviation. Samples and NC were in duplicates, NC TNF-α and NC Caco-2 were in singles.

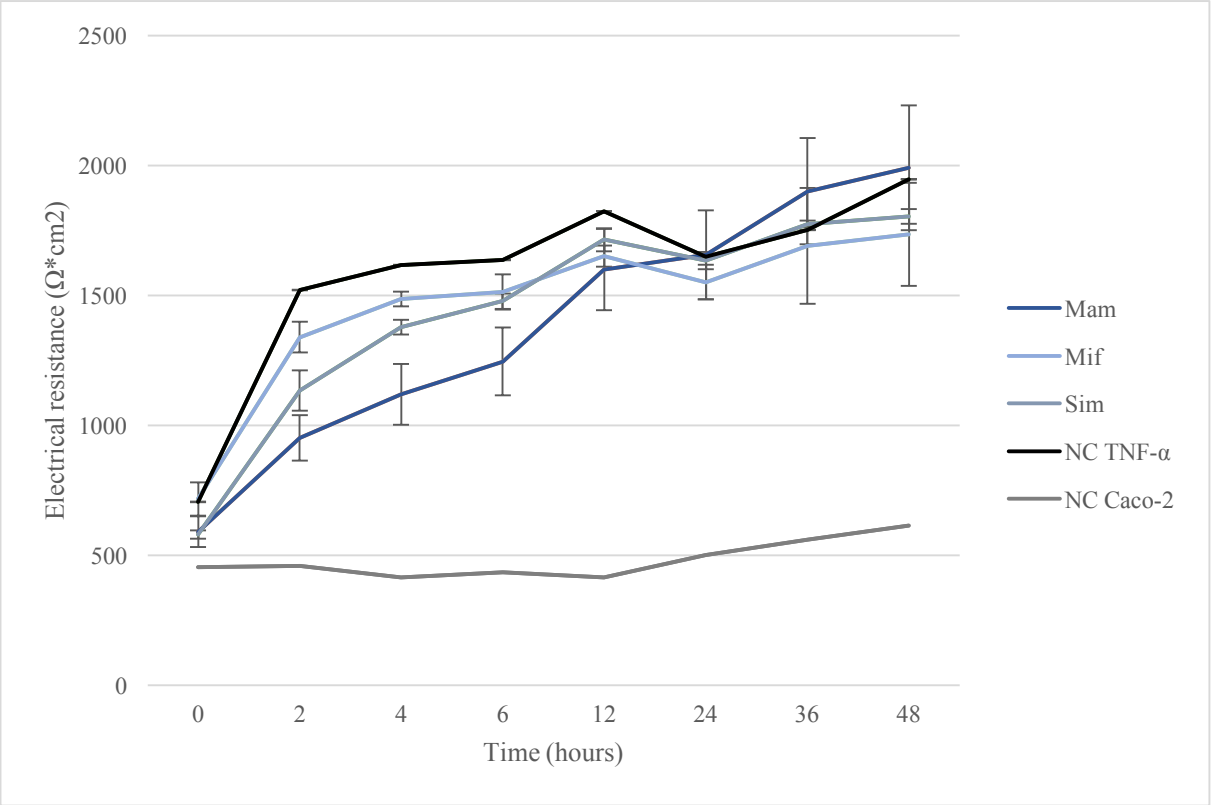

Figure 4.14 Analysis of TEER-values of Caco-2 cells with purified protein. The graph shows TEER-values in Ω*cm^2 measured at set times after start. The cells were incubated with bacterial stimuli apically and TNF-α basolaterally. Each series is indicated by the recombinant protein the sample contained. NC-TNF-α, Caco-2 cells and TNF-α only; NC Caco-2, Caco-2 cells only. Error bars show one standard deviation. Samples were in duplicates, NC TNF-α and NC Caco-2 were in singles.

As Fig. 4.13 shows, all samples with cell-free protein extract from *L. plantarum* WCFS1 paralleled each other relatively closely, except for the negative control with Caco-2 cells only. A visual inspection of this well in a light microscope showed holes in the cell monolayer, invalidating the values from this control. The NC containing only TNF-α, coloured black in the graphs, had TEER values around the same range of the samples, as did the NC containing pEV. The only data point with significant difference from the others was Mam at 6 hours, which had a higher value. As seen in Fig. 4.14, the samples containing purified protein from *E. coli* BL21 were more different from each other, with the sample containing Mam at a lower TEER value than the others from 2 to 6 hours. Purified Tir was not included in the assay due to issues with the sample. There were no statistically significant differences between the group with extracts and the group with purified protein. However, all samples followed a similar pattern of increasing TEER from start until the 12-hour mark, after which the value dropped at 24 hours before continuing to increase until 48 hours.

5. DISCUSSION

Lysate from *M. capsulatus* Bath has previously been shown to have anti-inflammatory effects on soy-induced enteritis in salmonids and DSS-induced colitis in mice (Kleiveland et al. 2013; Romarheim et al. 2011) as well as a potent reduction of both diet-induced obesity and insulin resistance in mice (Tor Lea, 12.08-2016, personal communication). Four genes from this strain were selected for further studies due to their potential immunomodulatory effects via genomic *in silico* analyses (Indrelid 2015, manuscript under preparation). Below, the results from these studies are discussed.

5.1 Construction of pSIP401- and pNIC-CH-derived plasmids

The genetic sequences *mam, tir, mif* and *sim* from *M. capsulatus* Bath were modified *in silico* to add restriction sites for insertion into the pSIP401 vector, for inducible expression in *L. plantarum.* A 3' c-Myc-tag was inserted for verification with Western blot. The proteins had not been folded *in silico*, so their conformations and any unintended interactions between the tag and the proteins were unknown. c-Myc-tag placement generally can be either N- or C-terminal without harmful effects, so the tag was placed C-terminally (Terpe 2003).

All plasmid construction, cloning and transformations performed were successful, with one exception. In this thesis, DNA inserts from the pSIP401- and pNIC-CH-derivatives were sent to GATC Biotech for sequencing to verify that the sequences had not been altered during transformation or due to mutations. Any such change can lead to drastic changes downstream. Substitution of one nucleotide for another can change the amino acid in the protein product, potentially altering the protein's conformation. Insertion or deletion of nucleotides can alter the reading frame of the entire sequence, leading to a completely different protein, or no protein at all. No changes had occurred to any sequences except for *mif* from pNIC-CH_MIF: A nucleotide substitution had occurred in this sequence, exchanging nucleotide 454 from G to T. This nucleotide was the first in the codon GTT, which instead became TTT, causing the amino acid coded for to change from valine to phenylalanine. Although both valine and phenylalanine are amino acids with hydrophobic side chains, phenylalanine contains an aromatic ring and is physically larger. This might have resulted in an alteration in the protein's conformation, potentially changing the folded structure of the final protein. The

implications of this were not investigated, and the protein was included in further analyses with Caco-2 cells.

5.2 Growth effects of protein production in *Lactobacillus plantarum*

In previous studies with the pSIP expression system, high intracellular production of protein has been achieved (Sørvig et al. 2003). By optimizing parameters for the species and protein, it has been demonstrated that the induced protein can constitute up to 70 % of the total intracellular protein in *L. plantarum* (Nguyen, T. T. et al. 2015). The introduction of foreign plasmids to bacteria may lead to reduced growth rates due to the increased use of resources necessitated by the overproduction of the target protein (Fakruddin et al. 2013). Growth curves were made to investigate whether these findings also held true for recombinant proteins from *M. capsulatus* Bath.

L. plantarum harbouring all pSIP401-derived strains in this thesis as well as pEV grew at equal rates when not induced (data not included). After induction, strains producing Mam, Mif and Sim paralleled the negative control with pEV, as seen in Fig 4.5. Strains harbouring Tir, however, had a greatly reduced growth rate, with roughly one third of the biomass of the other strains after 4 hours. Potential reasons for this are discussed in section 5.3.

5.3 Western blot analysis of protein production in *Lactobacillus plantarum*

Western blot analyses were performed to confirm the presence of recombinant c-Myc-tagged protein produced by *L. plantarum*. As seen in Fig. 4.6, there was successful production of the four proteins, but in varying amounts. Tir had the most intense band, indicating high production of this protein. Mam and Mif seemed to be produced at approximately similar, but somewhat lower levels. Initially, it seemed like Sim was not produced. By increasing the exposure time of the blots, a band not found in any other samples was observed. However, this protein appeared to be larger than the predicted size of Sim, which is 24.2 kDa including the c-Myc-tag. The observed band appeared to be approximately 30 kDa. The reason for the apparent increase in size could be post-translational modification. All proteins had been analyzed *in silico* with Signal-BLAST (Frank & Sippl 2008) for presence of signal sequences,

which cause proteins to be modified and transported to various regions intra- or extracellularly after translation. Sim was predicted to contain a signal sequence, suggesting that the protein might have been secreted or possibly anchored to the cell membrane. Thus, analyses of supernatant from *L. plantarum* harbouring pSIP401_SIMPL as well as pellet from disrupted bacteria should be performed. If it is not secreted or anchored, the low levels of Sim could be due to a variety of other factors, e.g. degradation by proteases, low mRNA stability, low protein folding efficiency and turnover or negative effects of the protein on the host cell (Sørvig et al. 2005). Since the 30 kDa band only showed up in the samples containing Sim, it is unlikely to be another native protein produced by *L. plantarum*. Because of the size difference and the low levels of expressed protein, these results should be further investigated.

Mam was unique compared with the other proteins in that it consistently seemed to be cleaved by *L. plantarum*, resulting in one band around the predicted size of 55.4 kDa and several bands around 45-50 kDa. These results were seen in every single harvest of Mam in this thesis, including the 12-liter fermentations discussed later. Unlike Sim, Mam did not contain any known signal sequences, meaning this is probably not the reason for the cleavage. Since the bands are similar in size and the c-Myc tag was placed on the C-terminal end of the protein, this indicates that the cleaving has taken place near the N-terminal end. The Mam peptides could be analyzed, e.g. with NMR, to clarify where the protein has been cleaved.

Tir was produced in large amounts by the bacteria (to the extent that this protein was also clearly visible on stained SDS-PAGE gels, unlike the other proteins (data not included)). A blastp search against the complete genome of *L. plantarum* WCFS1 revealed no proteins with significant similarity to Tir. As Tir has no homologs natively expressed by *L. plantarum* WCFS1, the reason for the large amounts produced, as well as potential biological effects of the protein on *L. plantarum,* are thus unknown.

It has previously been reported that production of recombinant proteins destined for secretion or cell wall anchoring leads to reduced growth in *L. plantarum* due to metabolic stress (Fredriksen et al. 2010; Øverland 2013; Solberg 2015; Tjåland 2011). However, Tir contained no known signal sequences and should not lead to any extra stress on the bacteria for that reason.

Although the reasons for the large production of Tir are unknown, the observed reduction in growth could be connected to the amounts produced, independent of any biological functions of Tir. Fekonja et al. (2012) have shown that overexpressed TIR domains can form aggregates beyond dimers in the cytosol. Tir may similarly have formed large aggregates, causing stress on the bacteria. It could also be that the bacteria used most of their energy, tRNA or cytosolic amino acids for creating the recombinant protein, resulting in metabolic stress. Interestingly, an unspecific band at approximately 40 kDa, found on Western blots of all samples, seemed to be more intense in the samples containing Tir. This could represent a native protein which is upregulated in response to Tir and could yield insights into effects of Tir on *L. plantarum*.

5.4 Production of purified protein from *Escherichia coli* BL21

In addition to obtaining cell-free protein extracts from *L. plantarum*, purified protein from *E. coli* BL21 was desired. This was both in order to investigate whether there would be any difference between cell-free protein extracts and purified proteins in cell assays, as well as for potential future research on the proteins.

After transforming the genetic sequences with 3' His-tag into pNIC-CH and amplifying in *E. coli* GeneHogs, the plasmids were further transformed into *E. coli* BL21. This strain is deficient in the two proteases OmpT and Lon. Therefore, a higher yield of recombinant protein can be expected compared to many other *E. coli* strains. After harvesting and disrupting the cells, the proteins were purified with IMAC.

As seen in Fig. 4.10, Mam, Mif and Sim all had peaks on the elution diagram. No peak was detectable for Tir on the elution diagram, which was partially expected: As seen in Fig 4.9, a band at the predicted size of Tir existed in the pellet, but was not visible in the supernatant. The absence of Tir might be due to the formation of inclusion bodies, which can happen when recombinant proteins are rapidly produced in *E. coli*. Inclusion bodies are large, spherical particles separated from the cytoplasm, and they end up in the pellet after disruption and high-speed centrifugation (Singh & Panda 2005). If production of purified Tir is repeated in the future, this should be taken into consideration. Cloning *tir* into a secretion vector and harvesting the supernatant might lead to more favourable results. Nevertheless, as shown in

Fig. 4.11, a band was visible at approximately the expected size of Tir. The sample was therefore used for the cellular assays performed later.

As seen in Fig. 4.11, the protein samples are not entirely pure and all samples contain other bands. The most prominent is found at approximately 70 kDa and is highly expressed in the sample containing Tir. This band is commonly found after purification of protein from *E. coli* BL21 (Geir Mathiesen, 10.02.2016, personal communication). Further purification of the protein solutions could be performed in order to remove these contaminating proteins, which could affect the results in future assays.

After purification, the presence of the proteins was observed by using SDS-PAGE and looking for bands at the expected size. This only verifies that a protein which bound strongly to the IMAC column is present, and that it is of approximately the same size as the expected protein. An additional verification step should be performed, e.g. a Western blot using anti-hexa-His-antibodies, to ensure that the bands represent the target proteins.

5.5 Bioreactor fermentations of *Lactobacillus plantarum*

When performing 12-liter fermentations of *L. plantarum* in a 15-liter bioreactor, an additional range of parameters described in section 4.5 were controlled. These parameters were chosen according to the optimizations performed by Nguyen, T. T. et al. (2015). The optimal parameters will differ depending on the protein to be produced. However, investigation of the optimal cultivation conditions for Mam were beyond the scope of this thesis due to time constraints. It is likely that optimal parameters for production of Mam would be different from those chosen, as reflected in the amount of biomass produced in this thesis (OD_{600}-values of 14.8 after 16 hours) compared to that produced by Nguyen, T. T. et al. (2015) (OD_{600}-values of up to 18 after 12 hours). The protein produced in that paper was a β-galactosidase; a native enzyme produced by lactobacilli when using lactose as an energy source. Mam is a protein from a different species, with unknown metabolic effects of overproduction, which might explain the growth reduction.

The lower OD_{600}-values could also be a direct effect of the pH control. The batch fermentations performed by Nguyen, T. T. et al. (2015) took place in 400 ml medium. When

using 12 liters, large amounts of NaOH had to be added to maintain a pH value of 6.5. In order to avoid overfilling the reactor, 5 M NaOH had to be added dropwise into the medium. This still resulted in a volume increase of approximately 500 ml per fermentation. Although the medium was constantly stirred, addition of 5 M NaOH to the culture directly might have caused cell death. This might have negatively influenced the growth of the culture.

The only parameter which was investigated in this thesis was time of induction. The amount of time between inoculation and induction could influence the amount of protein produced. As seen in Fig. 4.8, the late-and early-induced culture seemed to contain relatively similar amounts of Mam. The late-induced culture did obtain a 30 % higher OD_{600}-value after 12 hours than early-induced cultures. This was most likely a result of the late-induced culture being given an additional 1.5 hours to grow.

5.6 IL-1β stimulation and ELISA for production of IL-8

The IL-8 assay was performed in order to determine whether the presence of the recombinant proteins could influence IL-1β-induced IL-8 production. IL-1β is involved in the pathogenesis of intestinal inflammation in animal models as well as IBD in humans (Al-Sadi & Ma 2007). When stimulated with IL-1β, Caco-2 cells produce the cytokine IL-8, which attracts and activates neutrophils and other immune cells (Akdis et al. 2011). Quevrain et al. (2016a) demonstrated a reduced IL-1β-induced production of IL-8 by Caco-2 cells when incubated with MAM from *F. prausnitzii*. This assay was thus selected, with Mam as the main protein of interest, to see if it would lead to similar results.

The results of the ELISA for production of IL-8, shown in Fig. 4.12, show that there was no significant difference between samples. More importantly, there was no difference between the control containing Caco-2 cells and IL-1β and the control containing unstimulated Caco-2 cells. This result shows that the addition of IL-1β had no effect on the production of IL-8 by the Caco-2 cells, contrary to what is expected (Lea 2015a). The results from the ELISA are therefore rendered invalid and must be repeated for any conclusions to be drawn.

The failed stimulation of the Caco-2 cells could be due to a variety of reasons. The specific IL-1β used in the stimulation could have lost its biological activity due to time in storage.

There might have been functional changes in Caco-2 due to the number of passages: Although the optimal passage number is generally believed to be 28-65 (Briske-Anderson et al. 1997), the possible downregulation of IL-1 receptors has not been investigated. Because of time constraints, no assay optimization took place. Only one concentration of IL-1β was used, which might have been too low to elicit a response. In future repetitions of the assay, dose-control should be included for both IL-1β and bacterial stimuli.

5.7 Assay for effects on transepithelial electrical resistance of Caco-2 cells

The TEER assay is a well-studied system for measuring changes in tight junction permeability induced by various stimuli. In this thesis, it was performed to determine whether any of the four proteins could influence TNF-α-induced changes in permeability. Previous studies have shown that the TNF-α induced increase in Caco-2 tight junction permeability requires activation of NF-κB (Ma et al. 2004). Of the proteins investigated in this thesis, Sim and Mif were the most promising candidates for effects in this assay. SIMPL is directly involved in TNF-α-mediated activation of NF-κB. If Mif binds to the MIF receptor CD74 on the cell surface, it might initiate a metabolic cascade leading to NF-κB activation (Starlets et al. 2006). Previous studies have not shown the expression of CD74 on the surface of Caco-2 cells, however, which would preclude the activation of CD74-induced pathways (Man et al. 2008).

As seen in Fig. 4.13 and 4.14, there were no significant differences between samples. In addition, the control containing Caco-2 cells and TNF-α without bacterial stimuli had the highest TEER values. This control was expected to have reduced TEER values. Due to the invalidated control with Caco-2 cells only, it is not possible to say whether this is due to a failed stimulation, or whether all samples with bacterial stimuli would lead to reduced TEER values compared to the control with TNF-α. Similarly to the IL-1β stimulation, the specific TNF-α used might have lost its biological activity. Additionally, like all *in vitro* assays, TEER assays require optimization. When working with *in vitro* cell systems, optimization of assay parameters, e.g. incubation time, concentration of stimuli or passage number of Caco-2 cells are decisive for a successful assay. Due to the time invested in creating pSIP401-

derivatives, purifying protein and producing *L. plantarum* harbouring pSIP401_MAM and pEV, assay optimization was outside the scope of this thesis.

L. plantarum has been shown to enhance the stability of tight junction complexes in humans (Karczewski et al. 2010). As such, it may counteract the increased permeability induced by TNF-α, an effect that has been proven for other probiotic species *in vitro* (Bischoff et al. 2014). In future repetitions, positive controls could therefore be included with Caco-2 cells and *L. plantarum*, with and without TNF-α. In addition, no control was included for purified protein from *E. coli*. These samples could contain LPS, which is a potent trigger of pro-inflammatory reactions (Cani et al. 2007). A control with LPS should therefore be included. The samples with purified protein also contained some unspecific contaminants, as seen in Fig. 4.11, which should be removed with additional purification steps.

5.8 Future perspectives and conclusions

There are many options for future research with basis in the studies performed in this thesis. In addition to optimization of the performed assays, the next planned analyses are assays for effects of the four proteins Mam, Tir, Mif and Sim on immune cells. *M. capsulatus* Bath has been shown to bind to and interact with human and murine DCs and macrophages, enhancing the expression of maturation markers and influencing the cytokine profile produced by these cells. Similar assays with *L. plantarum* harbouring the pSIP401-derivatives constructed in this thesis may elucidate whether this effect is due to any of the currently studied proteins.

Another possible explanation for the effects of *M. capsulatus* Bath, and hence another area for future studies, is via IL-22. IL-22 is a cytokine produced by ILCs, T_H17 and T_H22. Administration of exogenous IL-22 been shown to reduce body weight and total fat mass in murine models of diet-induced obesity (Wang et al. 2014). It also increases intestinal-stem-cell-mediated regeneration of epithelial cells (Lindemans et al. 2015). In the trial with *M. capsulatus* Bath, levels of IL-22 were significantly higher than in the controls (Tor Lea, 21.04.2016, personal communication), which might have contributed to the reductions in body weight observed there as well as the growth of colonic epithelium observed by Kleiveland et al. (2013).

Preliminary results from the murine trial of obesity with *L. plantarum* harbouring pSIP401_MAM produced in this study were negative. After a few days, the mice did not want to eat the feed containing Mam (Tor Lea, 12.08-2016, personal communication). The reasons for this are unknown. Although the specific amount of Mam in the feed was not determined, the protein was overexpressed. In addition, the *L. plantarum* lysate constituted 20 % of the feed by volume. The mice were thus exposed to far larger amounts of Mam than they would be in a feed with *M. capsulatus* Bath. The exposure to large amounts of Mam could cause adverse reactions in the animals. Additionally, Mam was here expressed in a Gram-positive species. The combined signal of Mam with peptidoglycan could lead to different effects than Mam with LPS from the Gram-negative *M. capsulatus* Bath.

Future studies on each protein may also be performed with consideration to their possible predicted functions:

Mam, a putative diguanylate phosphodiesterase, was investigated in this thesis because of its structural similarity to MAM from *F. prausnitzii*. Quevrain et al. (2016a) showed that this protein at least partially contributed to the anti-inflammatory effects of that commensal species. MAM is a 15 kDa GGDEF-like protein which lacks critical catalytic residues and has no known function related to c-di-GMP. As reviewed by Romling et al. (2013), GGDEF-EAL-proteins like Mam are involved in the metabolism of GMP into c-di-GMP, the reverse, or both. Intracellular receptors for c-di-GMP have been demonstrated in mammalian cells and binding leads to increased levels of IFN type I. Additionally, even if it retains no catalytic activity, the substrate-ligand interactions between Mam and cGMP may affect immunological responses.

The second protein, Tir, is predicted to be a SEFIR domain, which is involved in IL-17 signaling in human and mouse immune cells. Although the functions of non-pathogenic bacterial Tcps such as SEFIR are poorly understood, it is likely to interact with the host via interference with the IL-17RA pathway (Patterson & Werling 2013; Wu et al. 2012). As T_H17 cells produce IL-22 in addition to IL-17, Tir may play a potential role in the upregulation of IL-22 seen in studies on *M. capsulatus* Bath.

Human MIF is expressed by a wide range of cells, including immune cells such as macrophages and B cells, as well as epithelial cells (Calandra & Roger 2003). If Mif has a

similar biological activity as human MIF, it would be expected to bind CD74 in order to start a metabolic cascade, leading to NF-κB activation.

Sim is a homolog to the mammalian protein SIMPL, which is a signaling component used for TNF-α-dependent activation of NF-κB. Loss of SIMPL causes a reduction in TNF RI dependent release of NF-κB controlled cytokines in endothelial cells (Benson et al. 2010) The function of Sim and SIMPL-domains in bacteria is unexplored. It might be secreted and taken up by epithelial cells, causing interference with this pathway. An assay could be performed on Caco-2 cells stimulated with TNF-α in the presence of Sim to investigate whether Sim has an effect on the NF-κB-dependent cytokine profile.

In addition to further studying the presently produced proteins, they could be compared to the equivalent proteins produced by *M. capsulatus* Texas. This strain has different immunomodulatory effects than Bath, i.e. on cytokine profiles of DCs incubated with the bacteria (Christoffersen et al. 2015). This strain is also internalized by moDCs, but with different kinetics compared to Bath (Tor Lea, 12.08-2016, personal communication). A tblastn search on NCBI revealed that all four proteins examined in this thesis exist in *M. capsulatus* Texas as well as in Bath, with 82 – 99 % similarity. Investigation of the differences between these proteins may yield valuable information for future research.

A final important point to consider is that the mechanisms behind the anti-inflammatory effect *in vivo* of *M. capsulatus* Bath are still unknown. The effect could be due to direct interactions between one or more substances produced by the bacteria with the host's intestinal mucosa. In this thesis, four proteins were investigated for direct effects on Caco-2 cells, but only separately. The observed effects in salmonid and murine models could be due to synergistic effects from multiple substances. In addition, if the effect is direct, it could depend on additional signals from the host, e.g. from immune cells found in the lamina propria. The anti-inflammatory effects could also be due to indirect interactions, e.g. via modulation of the intestinal microbiota: Mice fed with standard chow, *M. capsulatus* Bath and *E. coli* Nissle (Tor Lea, 21.04.2016, personal communication) had different diversities of microbial taxa. If that is the cause, *in vitro* assays may lead to different conclusions than *in vivo* studies.

In conclusion, the studies performed in this thesis demonstrated the successful expression of proteins from *M. capsulatus* Bath in *L. plantarum*, with the possible exception of Sim. Purified protein was also successfully produced, with the possible exception of Tir. Both these lines of research have room for improvement with regards to cleavage of protein, amounts of protein expressed or protein isolation. The assays for TEER and production of IL-8 in Caco-2 cells did not succeed. Altogether, the results obtained in this thesis leave room for ample future research in many directions.

Appendix

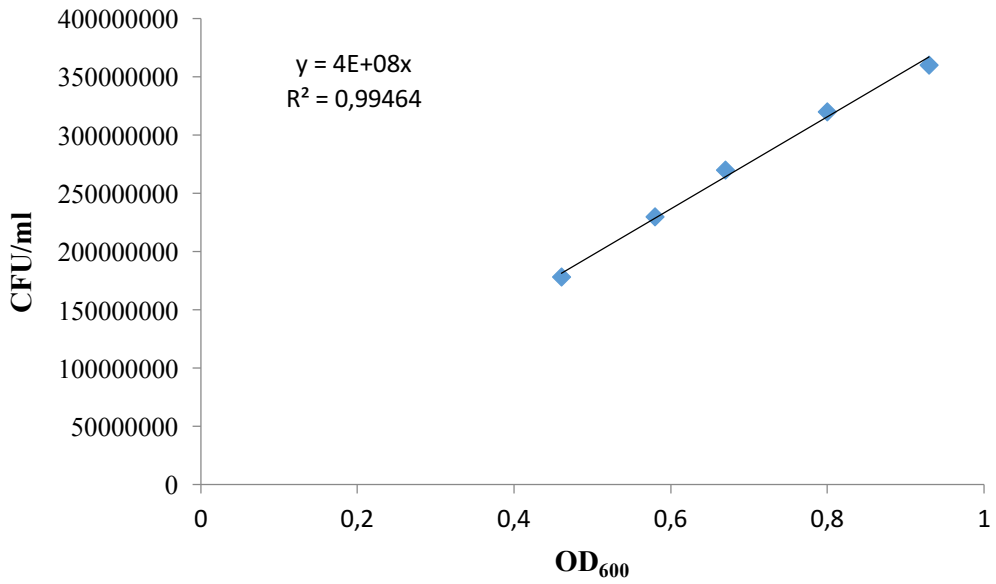

Figure A.1. Relationship between OD_{600}-values and CFU/ml for *L. plantarum* harbouring pEV. The graph was used to calculate approx. the same number of cells from different cultures when harvesting, based on the OD_{600}-value of each culture at the time of harvest. The graph was provided by Øverland (2013).

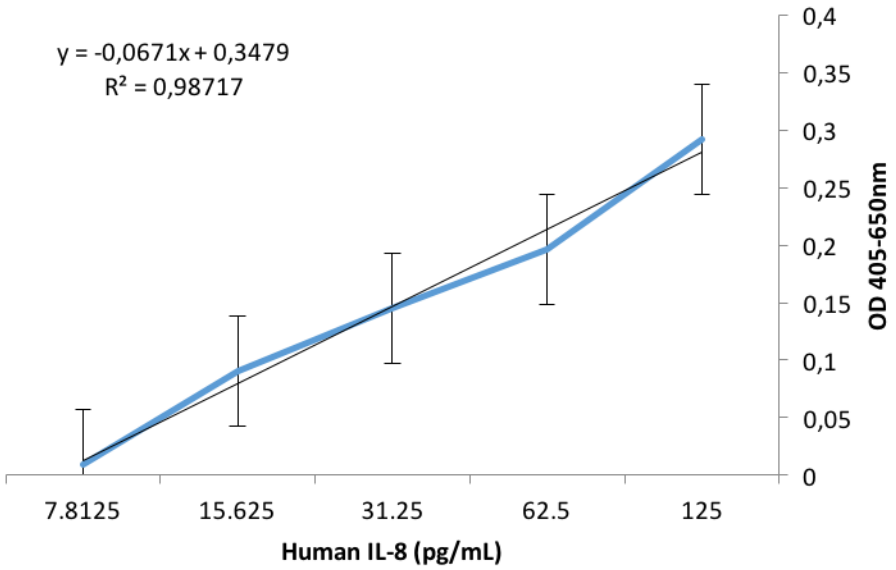

Figure A.2. Relationship between amount of human IL-8 and measured $OD_{405\text{-}650nm}$. The graph was used to calculate the amount of IL-8 produced (in pg/ml) by Caco-2 cells from the intensity of light emitted by ELISA.

References

Akdis, M., Burgler, S., Crameri, R., Eiwegger, T., Fujita, H., Gomez, E., Klunker, S., Meyer, N., O'Mahony, L., Palomares, O., et al. (2011). Interleukins, from 1 to 37, and interferon-gamma: receptors, functions, and roles in diseases. *J Allergy Clin Immunol*, 127 (3): 701-21 e1-70.

Al-Sadi, R. M. & Ma, T. Y. (2007). IL-1beta causes an increase in intestinal epithelial tight junction permeability. *J Immunol*, 178 (7): 4641-9.

Artis, D. & Spits, H. (2015). The biology of innate lymphoid cells. *Nature*, 517 (7534): 293-301.

Augustijn, K. D., Kleemann, R., Thompson, J., Kooistra, T., Crawford, C. E., Reece, S. E., Pain, A., Siebum, A. H., Janse, C. J. & Waters, A. P. (2007). Functional characterization of the Plasmodium falciparum and P. berghei homologues of macrophage migration inhibitory factor. *Infect Immun*, 75 (3): 1116-28.

Benson, E. A., Goebl, M. G., Yang, F. C., Kapur, R., McClintick, J., Sanghani, S., Clapp, D. W. & Harrington, M. A. (2010). Loss of SIMPL compromises TNF-alpha-dependent survival of hematopoietic progenitors. *Exp Hematol*, 38 (2): 71-81.

Bermudez-Humaran, L. G., Aubry, C., Motta, J. P., Deraison, C., Steidler, L., Vergnolle, N., Chatel, J. M. & Langella, P. (2013). Engineering lactococci and lactobacilli for human health. *Curr Opin Microbiol*, 16 (3): 278-83.

Bettelli, E., Carrier, Y., Gao, W., Korn, T., Strom, T. B., Oukka, M., Weiner, H. L. & Kuchroo, V. K. (2006). Reciprocal developmental pathways for the generation of pathogenic effector TH17 and regulatory T cells. *Nature*, 441 (7090): 235-8.

Bischoff, S. C., Barbara, G., Buurman, W., Ockhuizen, T., Schulzke, J.-D., Serino, M., Tilg, H., Watson, A. & Wells, J. M. (2014). Intestinal permeability – a new target for disease prevention and therapy. *BMC Gastroenterology*, 14: 189.

Briske-Anderson, M. J., Finley, J. W. & Newman, S. M. (1997). The influence of culture time and passage number on the morphological and physiological development of Caco-2 cells. *Proc Soc Exp Biol Med*, 214 (3): 248-57.

Brurberg, M. B., Haandrikman, A. J., Leenhouts, K. J., Venema, G. & Nes, I. F. (1994). Expression of a chitinase gene from Serratia marcescens in Lactococcus lactis and Lactobacillus plantarum. *Appl Microbiol Biotechnol*, 42 (1): 108-15.

Burger-Kentischer, A., Gobel, H., Kleemann, R., Zernecke, A., Bucala, R., Leng, L., Finkelmeier, D., Geiger, G., Schaefer, H. E., Schober, A., et al. (2006). Reduction of the aortic inflammatory response in spontaneous atherosclerosis by blockade of macrophage migration inhibitory factor (MIF). *Atherosclerosis*, 184 (1): 28-38.

Burgess-Brown, N. A., Sharma, S., Sobott, F., Loenarz, C., Oppermann, U. & Gileadi, O. (2008). Codon optimization can improve expression of human genes in Escherichia coli: A multi-gene study. *Protein Expr Purif*, 59 (1): 94-102.

Calandra, T., Bernhagen, J., Metz, C. N., Spiegel, L. A., Bacher, M., Donnelly, T., Cerami, A. & Bucala, R. (1995). MIF as a glucocorticoid-induced modulator of cytokine production. *Nature*, 377 (6544): 68-71.

Calandra, T. & Roger, T. (2003). Macrophage migration inhibitory factor: a regulator of innate immunity. *Nat Rev Immunol*, 3 (10): 791-800.

Cani, P. D., Amar, J., Iglesias, M. A., Poggi, M., Knauf, C., Bastelica, D., Neyrinck, A. M., Fava, F., Tuohy, K. M., Chabo, C., et al. (2007). Metabolic endotoxemia initiates obesity and insulin resistance. *Diabetes*, 56 (7): 1761-72.

Cella, M., Engering, A., Pinet, V., Pieters, J. & Lanzavecchia, A. (1997). Inflammatory stimuli induce accumulation of MHC class II complexes on dendritic cells. *Nature*, 388 (6644): 782-7.

Chapman, T. M., Plosker, G. L. & Figgitt, D. P. (2007). Spotlight on VSL#3 probiotic mixture in chronic inflammatory bowel diseases. *BioDrugs*, 21 (1): 61-3.

Christoffersen, T. E., Olsen Hult, L. T., Solberg, H., Bakke, A., Kuczkowska, K., Huseby, E., Jacobsen, M., Lea, T. & Kleiveland, C. R. (2015). Effects of the non-commensal Methylococcus capsulatus Bath on mammalian immune cells. *Mol Immunol*, 66 (2): 107-16.

Clontech. (2014). *In-Fusion® HD Cloning Kit User Manual* Clontech Laboratories Inc. Available at: http://www.clontech.com/xxclt_ibcGetAttachment.jsp?cItemId=17497 (accessed: 30.11.15).

Colby, J., Stirling, D. I. & Dalton, H. (1977). The soluble methane mono-oxygenase of Methylococcus capsulatus (Bath). Its ability to oxygenate n-alkanes, n-alkenes, ethers, and alicyclic, aromatic and heterocyclic compounds. *Biochem J*, 165 (2): 395-402.

de Ruyter, P. G., Kuipers, O. P. & de Vos, W. M. (1996). Controlled gene expression systems for Lactococcus lactis with the food-grade inducer nisin. *Appl Environ Microbiol*, 62 (10): 3662-7.

Doyle, S. L. & O'Neill, L. A. (2006). Toll-like receptors: from the discovery of NFkappaB to new insights into transcriptional regulations in innate immunity. *Biochem Pharmacol*, 72 (9): 1102-13.

Everard, A., Belzer, C., Geurts, L., Ouwerkerk, J. P., Druart, C., Bindels, L. B., Guiot, Y., Derrien, M., Muccioli, G. G., Delzenne, N. M., et al. (2013). Cross-talk between Akkermansia muciniphila and intestinal epithelium controls diet-induced obesity. *Proceedings of the National Academy of Sciences*, 110 (22): 9066-9071.

Fakruddin, M., Mohammad Mazumdar, R., Bin Mannan, K. S., Chowdhury, A. & Hossain, M. N. (2013). Critical Factors Affecting the Success of Cloning, Expression, and Mass Production of Enzymes by Recombinant E. coli. *ISRN Biotechnol*, 2013: 590587.

Fekonja, O., Bencina, M. & Jerala, R. (2012). Toll/interleukin-1 receptor domain dimers as the platform for activation and enhanced inhibition of Toll-like receptor signaling. *J Biol Chem*, 287 (37): 30993-1002.

Fogh, J., Wright, W. C. & Loveless, J. D. (1977). Absence of HeLa cell contamination in 169 cell lines derived from human tumors. *J Natl Cancer Inst*, 58 (2): 209-14.

Frank, K. & Sippl, M. J. (2008). High-performance signal peptide prediction based on sequence alignment techniques. *Bioinformatics*, 24 (19): 2172-6.

Fredriksen, L., Mathiesen, G., Sioud, M. & Eijsink, V. G. (2010). Cell wall anchoring of the 37-kilodalton oncofetal antigen by Lactobacillus plantarum for mucosal cancer vaccine delivery. *Appl Environ Microbiol*, 76 (21): 7359-62.

Gareau, M. G., Sherman, P. M. & Walker, W. A. (2010). Probiotics and the gut microbiota in intestinal health and disease. *Nat Rev Gastroenterol Hepatol*, 7 (9): 503-14.

Gileadi, O., Burgess-Brown, N. and Loppnau, P. (2006). Vectors for Ligation-independent Cloning (LIC). *Unpublished*.

Guven-Maiorov, E., Keskin, O., Gursoy, A., VanWaes, C., Chen, Z., Tsai, C. J. & Nussinov, R. (2015). The Architecture of the TIR Domain Signalosome in the Toll-like Receptor-4 Signaling Pathway. *Sci Rep*, 5: 13128.

Helander, H. F. & Fandriks, L. (2014). Surface area of the digestive tract - revisited. *Scand J Gastroenterol*, 49 (6): 681-9.

Hilpert, K., Hansen, G., Wessner, H., Kuttner, G., Welfle, K., Seifert, M. & Hohne, W. (2001). Anti-c-myc antibody 9E10: epitope key positions and variability characterized using peptide spot synthesis on cellulose. *Protein Eng*, 14 (10): 803-6.

Hooper, L. V., Littman, D. R. & Macpherson, A. J. (2012). Interactions between the microbiota and the immune system. *Science*, 336 (6086): 1268-73.
Hua, Z. & Hou, B. (2013). TLR signaling in B-cell development and activation. *Cell Mol Immunol*, 10 (2): 103-6.
Indrelid, S., Mathiesen, G., Jacobsen, M., Lea, T. & Kleiveland, C. R. (2014). Computational and Experimental Analysis of the Secretome of Methylococcus capsulatus (Bath). *PLoS ONE*, 9 (12): e114476.
Iwasaki, A. & Medzhitov, R. (2010). Regulation of Adaptive Immunity by the Innate Immune System. *Science*, 327 (5963): 291-295.
Karaolis, D. K., Means, T. K., Yang, D., Takahashi, M., Yoshimura, T., Muraille, E., Philpott, D., Schroeder, J. T., Hyodo, M., Hayakawa, Y., et al. (2007). Bacterial c-di-GMP is an immunostimulatory molecule. *J Immunol*, 178 (4): 2171-81.
Karczewski, J., Troost, F. J., Konings, I., Dekker, J., Kleerebezem, M., Brummer, R. J. & Wells, J. M. (2010). Regulation of human epithelial tight junction proteins by Lactobacillus plantarum in vivo and protective effects on the epithelial barrier. *Am J Physiol Gastrointest Liver Physiol*, 298 (6): G851-9.
Kemp, B. E. (2004). Bateman domains and adenosine derivatives form a binding contract. *J Clin Invest*, 113 (2): 182-4.
Kleerebezem, M., Beerthuyzen, M. M., Vaughan, E. E., de Vos, W. M. & Kuipers, O. P. (1997). Controlled gene expression systems for lactic acid bacteria: transferable nisin-inducible expression cassettes for Lactococcus, Leuconostoc, and Lactobacillus spp. *Appl Environ Microbiol*, 63 (11): 4581-4.
Kleerebezem, M., Boekhorst, J., van Kranenburg, R., Molenaar, D., Kuipers, O. P., Leer, R., Tarchini, R., Peters, S. A., Sandbrink, H. M., Fiers, M. W., et al. (2003). Complete genome sequence of Lactobacillus plantarum WCFS1. *Proc Natl Acad Sci U S A*, 100 (4): 1990-5.
Kleiveland, C. R., Hult, L. T., Kuczkowska, K., Jacobsen, M., Lea, T. & Pope, P. B. (2012). Draft genome sequence of the methane-oxidizing bacterium Methylococcus capsulatus (Texas). *J Bacteriol*, 194 (23): 6626.
Kleiveland, C. R., Hult, L. T., Spetalen, S., Kaldhusdal, M., Christofferesen, T. E., Bengtsson, O., Romarheim, O. H., Jacobsen, M. & Lea, T. (2013). The noncommensal bacterium Methylococcus capsulatus (Bath) ameliorates dextran sulfate (Sodium Salt)-Induced Ulcerative Colitis by influencing mechanisms essential for maintenance of the colonic barrier function. *Appl Environ Microbiol*, 79 (1): 48-56.
Krieg, A. M., Yi, A. K., Matson, S., Waldschmidt, T. J., Bishop, G. A., Teasdale, R., Koretzky, G. A. & Klinman, D. M. (1995). CpG motifs in bacterial DNA trigger direct B-cell activation. *Nature*, 374 (6522): 546-9.
Kuipers, O. P., de Ruyter, P. G., Kleerebezem, M. & de Vos, W. M. (1997). Controlled overproduction of proteins by lactic acid bacteria. *Trends Biotechnol*, 15 (4): 135-40.
Kuipers, O. P., de Ruyter, P. G. G. A., Kleerebezem, M. & de Vos, W. M. (1998). Quorum sensing-controlled gene expression in lactic acid bacteria. *Journal of Biotechnology*, 64 (1): 15-21.
Kwon, H. J., Breese, E. H., Vig-Varga, E., Luo, Y., Lee, Y., Goebl, M. G. & Harrington, M. A. (2004). Tumor necrosis factor alpha induction of NF-kappaB requires the novel coactivator SIMPL. *Mol Cell Biol*, 24 (21): 9317-26.
Lankelma, J. M., Nieuwdorp, M., de Vos, W. M. & Wiersinga, W. J. (2015). The gut microbiota in internal medicine: implications for health and disease. *Neth J Med*, 73 (2): 61-8.
Larson, D. F. & Horak, K. (2006). Macrophage migration inhibitory factor: controller of systemic inflammation. *Crit Care*, 10 (2): 138.

Latz, E., Verma, A., Visintin, A., Gong, M., Sirois, C. M., Klein, D. C., Monks, B. G., McKnight, C. J., Lamphier, M. S., Duprex, W. P., et al. (2007). Ligand-induced conformational changes allosterically activate Toll-like receptor 9. *Nat Immunol*, 8 (7): 772-9.

Le Chatelier, E., Nielsen, T., Qin, J., Prifti, E., Hildebrand, F., Falony, G., Almeida, M., Arumugam, M., Batto, J. M., Kennedy, S., et al. (2013). Richness of human gut microbiome correlates with metabolic markers. *Nature*, 500 (7464): 541-6.

Lea, T. (2015a). Caco-2 Cell Line. In Verhoeckx, K. (ed.) *The Impact of Food Bioactives on Health*, pp. 103-111: Springer International Publishing.

Lea, T. (2015b). Epithelial Cell Models; General Introduction. In Verhoeckx, K. (ed.) *The Impact of Food Bioactives on Health*, pp. 95-102: Springer International Publishing.

Lee, Y. K. & Mazmanian, S. K. (2010). Has the Microbiota Played a Critical Role in the Evolution of the Adaptive Immune System? *Science*, 330 (6012): 1768-1773.

Leech, M., Metz, C., Hall, P., Hutchinson, P., Gianis, K., Smith, M., Weedon, H., Holdsworth, S. R., Bucala, R. & Morand, E. F. (1999). Macrophage migration inhibitory factor in rheumatoid arthritis: evidence of proinflammatory function and regulation by glucocorticoids. *Arthritis Rheum*, 42 (8): 1601-8.

Lindemans, C. A., Calafiore, M., Mertelsmann, A. M., O'Connor, M. H., Dudakov, J. A., Jenq, R. R., Velardi, E., Young, L. F., Smith, O. M., Lawrence, G., et al. (2015). Interleukin-22 promotes intestinal-stem-cell-mediated epithelial regeneration. *Nature*, 528 (7583): 560-4.

Ma, T. Y., Iwamoto, G. K., Hoa, N. T., Akotia, V., Pedram, A., Boivin, M. A. & Said, H. M. (2004). TNF-alpha-induced increase in intestinal epithelial tight junction permeability requires NF-kappa B activation. *Am J Physiol Gastrointest Liver Physiol*, 286 (3): G367-76.

MACHEREY-NAGEL. (2014). *NucleoSpin® Gel and PCR Clean-up User Manual*. Rev. 03 ed.

MACHEREY-NAGEL. (2015). *Plasmid DNA Purification User Manual*. Rev. 09 ed.

Madsen, K., Cornish, A., Soper, P., McKaigney, C., Jijon, H., Yachimec, C., Doyle, J., Jewell, L. & De Simone, C. (2001). Probiotic bacteria enhance murine and human intestinal epithelial barrier function. *Gastroenterology*, 121 (3): 580-91.

Makarova, K., Slesarev, A., Wolf, Y., Sorokin, A., Mirkin, B., Koonin, E., Pavlov, A., Pavlova, N., Karamychev, V., Polouchine, N., et al. (2006). Comparative genomics of the lactic acid bacteria. *Proc Natl Acad Sci U S A*, 103 (42): 15611-6.

Man, A. L., Lodi, F., Bertelli, E., Regoli, M., Pin, C., Mulholland, F., Satoskar, A. R., Taussig, M. J. & Nicoletti, C. (2008). Macrophage migration inhibitory factor plays a role in the regulation of microfold (M) cell-mediated transport in the gut. *J Immunol*, 181 (8): 5673-80.

Manichanh, C., Borruel, N., Casellas, F. & Guarner, F. (2012). The gut microbiota in IBD. *Nat Rev Gastroenterol Hepatol*, 9 (10): 599-608.

Marchler-Bauer, A., Derbyshire, M. K., Gonzales, N. R., Lu, S., Chitsaz, F., Geer, L. Y., Geer, R. C., He, J., Gwadz, M., Hurwitz, D. I., et al. (2015). CDD: NCBI's conserved domain database. *Nucleic Acids Res*, 43 (Database issue): D222-6.

Mathiesen, G., Sveen, A., Piard, J. C., Axelsson, L. & Eijsink, V. G. (2008). Heterologous protein secretion by Lactobacillus plantarum using homologous signal peptides. *J Appl Microbiol*, 105 (1): 215-26.

McNulty, D. E., Claffee, B. A., Huddleston, M. J., Porter, M. L., Cavnar, K. M. & Kane, J. F. (2003). Mistranslational errors associated with the rare arginine codon CGG in Escherichia coli. *Protein Expr Purif*, 27 (2): 365-74.

Merk, M., Mitchell, R. A., Endres, S. & Bucala, R. (2012). D-dopachrome tautomerase (D-DT or MIF-2): doubling the MIF cytokine family. *Cytokine*, 59 (1): 10-7.
Mestas, J. & Hughes, C. C. (2004). Of mice and not men: differences between mouse and human immunology. *J Immunol*, 172 (5): 2731-8.
Miquel, S., Martin, R., Rossi, O., Bermudez-Humaran, L. G., Chatel, J. M., Sokol, H., Thomas, M., Wells, J. M. & Langella, P. (2013). Faecalibacterium prausnitzii and human intestinal health. *Curr Opin Microbiol*, 16 (3): 255-61.
Morand, E. F., Leech, M. & Bernhagen, J. (2006). MIF: a new cytokine link between rheumatoid arthritis and atherosclerosis. *Nat Rev Drug Discov*, 5 (5): 399-410.
Mowat, A. M. & Agace, W. W. (2014). Regional specialization within the intestinal immune system. *Nat Rev Immunol*, 14 (10): 667-685.
New England Biolabs. *Quick Ligation Protocol (M2200)*. Available at: https://www.neb.com/protocols/1/01/01/quick-ligation-protocol (accessed: 24.09.15).
Nguyen, T. L. A., Vieira-Silva, S., Liston, A. & Raes, J. (2015). How informative is the mouse for human gut microbiota research? *Disease Models & Mechanisms*, 8 (1): 1-16.
Nguyen, T. T., Nguyen, H. M., Geiger, B., Mathiesen, G., Eijsink, V. G., Peterbauer, C. K., Haltrich, D. & Nguyen, T. H. (2015). Heterologous expression of a recombinant lactobacillal beta-galactosidase in Lactobacillus plantarum: effect of different parameters on the sakacin P-based expression system. *Microb Cell Fact*, 14: 30.
O'Neill, L. A., Golenbock, D. & Bowie, A. G. (2013). The history of Toll-like receptors - redefining innate immunity. *Nat Rev Immunol*, 13 (6): 453-60.
Øverland, L. (2013). *Secretion and anchoring of proteins in Lactobacillus plantarum: Studies of a dendritic cell-targeted Mycobacterium tuberculosis antigen*. Norwegian University of Life Sciences, Ås: Norwegian University of Life Sciences, Ås, IKBM.
Patterson, N. J. & Werling, D. (2013). To con protection: TIR-domain containing proteins (Tcp) and innate immune evasion. *Vet Immunol Immunopathol*, 155 (3): 147-54.
Pavan, S., Hols, P., Delcour, J., Geoffroy, M. C., Grangette, C., Kleerebezem, M. & Mercenier, A. (2000). Adaptation of the nisin-controlled expression system in Lactobacillus plantarum: a tool to study in vivo biological effects. *Appl Environ Microbiol*, 66 (10): 4427-32.
Peterson, L. W. & Artis, D. (2014). Intestinal epithelial cells: regulators of barrier function and immune homeostasis. *Nat Rev Immunol*, 14 (3): 141-153.
Quevrain, E., Maubert, M. A., Michon, C., Chain, F., Marquant, R., Tailhades, J., Miquel, S., Carlier, L., Bermudez-Humaran, L. G., Pigneur, B., et al. (2016a). Identification of an anti-inflammatory protein from Faecalibacterium prausnitzii, a commensal bacterium deficient in Crohn's disease. *Gut*, 65 (3): 415-25.
Quevrain, E., Maubert, M. A., Sokol, H., Devreese, B. & Seksik, P. (2016b). The presence of the anti-inflammatory protein MAM, from Faecalibacterium prausnitzii, in the intestinal ecosystem. *Gut*, 65 (5): 882.
Ramanan, D., Bowcutt, R., Lee, S. C., Tang, M. S., Kurtz, Z. D., Ding, Y., Honda, K., Gause, W. C., Blaser, M. J., Bonneau, R. A., et al. (2016). Helminth infection promotes colonization resistance via type 2 immunity. *Science*, 352 (6285): 608-12.
Ren, D. Y., Li, C., Qin, Y. Q., Yin, R. L., Du, S. W., Ye, F., Liu, H. F., Wang, M. P., Sun, Y., Li, X., et al. (2013). Lactobacilli reduce chemokine IL-8 production in response to TNF-alpha and Salmonella challenge of Caco-2 cells. *Biomed Res Int*, 2013: 925219.
Roger, T., Froidevaux, C., Martin, C. & Calandra, T. (2003). Macrophage migration inhibitory factor (MIF) regulates host responses to endotoxin through modulation of Toll-like receptor 4 (TLR4). *J Endotoxin Res*, 9 (2): 119-23.

Romarheim, O. H., Overland, M., Mydland, L. T., Skrede, A. & Landsverk, T. (2011). Bacteria grown on natural gas prevent soybean meal-induced enteritis in Atlantic salmon. *J Nutr*, 141 (1): 124-30.
Romling, U., Galperin, M. Y. & Gomelsky, M. (2013). Cyclic di-GMP: the first 25 years of a universal bacterial second messenger. *Microbiol Mol Biol Rev*, 77 (1): 1-52.
Roselli, M., Finamore, A., Britti, M. S. & Mengheri, E. (2006). Probiotic bacteria Bifidobacterium animalis MB5 and Lactobacillus rhamnosus GG protect intestinal Caco-2 cells from the inflammation-associated response induced by enterotoxigenic Escherichia coli K88. *Br J Nutr*, 95 (6): 1177-84.
Rosengren, E., Aman, P., Thelin, S., Hansson, C., Ahlfors, S., Bjork, P., Jacobsson, L. & Rorsman, H. (1997). The macrophage migration inhibitory factor MIF is a phenylpyruvate tautomerase. *FEBS Lett*, 417 (1): 85-8.
Sambuy, Y., De Angelis, I., Ranaldi, G., Scarino, M. L., Stammati, A. & Zucco, F. (2005). The Caco-2 cell line as a model of the intestinal barrier: influence of cell and culture-related factors on Caco-2 cell functional characteristics. *Cell Biol Toxicol*, 21 (1): 1-26.
Sender, R., Fuchs, S. & Milo, R. (2016). Revised estimates for the number of human and bacteria cells in the body. *bioRxiv*.
Seshasayee, A. S., Fraser, G. M. & Luscombe, N. M. (2010). Comparative genomics of cyclic-di-GMP signalling in bacteria: post-translational regulation and catalytic activity. *Nucleic Acids Res*, 38 (18): 5970-81.
Siegal, F. P., Kadowaki, N., Shodell, M., Fitzgerald-Bocarsly, P. A., Shah, K., Ho, S., Antonenko, S. & Liu, Y. J. (1999). The nature of the principal type 1 interferon-producing cells in human blood. *Science*, 284 (5421): 1835-7.
Siezen, R. J., Francke, C., Renckens, B., Boekhorst, J., Wels, M., Kleerebezem, M. & van Hijum, S. A. (2012). Complete resequencing and reannotation of the Lactobacillus plantarum WCFS1 genome. *J Bacteriol*, 194 (1): 195-6.
Singh, S. M. & Panda, A. K. (2005). Solubilization and refolding of bacterial inclusion body proteins. *J Biosci Bioeng*, 99 (4): 303-10.
Sokol, H., Pigneur, B., Watterlot, L., Lakhdari, O., Bermudez-Humaran, L. G., Gratadoux, J. J., Blugeon, S., Bridonneau, C., Furet, J. P., Corthier, G., et al. (2008). Faecalibacterium prausnitzii is an anti-inflammatory commensal bacterium identified by gut microbiota analysis of Crohn disease patients. *Proc Natl Acad Sci U S A*, 105 (43): 16731-6.
Solberg, E. (2015). *Targeting of lactobacillus to M-cells to improve its potential as vaccine delivery vector*. Norwegian University of Life Sciences, Ås: Norwegian University of Life Sciences, Ås, IKBM.
Sørvig, E., Gronqvist, S., Naterstad, K., Mathiesen, G., Eijsink, V. G. & Axelsson, L. (2003). Construction of vectors for inducible gene expression in Lactobacillus sakei and L plantarum. *FEMS Microbiol Lett*, 229 (1): 119-26.
Sørvig, E., Mathiesen, G., Naterstad, K., Eijsink, V. G. & Axelsson, L. (2005). High-level, inducible gene expression in Lactobacillus sakei and Lactobacillus plantarum using versatile expression vectors. *Microbiology*, 151 (Pt 7): 2439-49.
Starlets, D., Gore, Y., Binsky, I., Haran, M., Harpaz, N., Shvidel, L., Becker-Herman, S., Berrebi, A. & Shachar, I. (2006). Cell-surface CD74 initiates a signaling cascade leading to cell proliferation and survival. *Blood*, 107 (12): 4807-16.
Structural Genomics Consortium, A. e. F. d. M. B., Berkeley Structural Genomics Center, China Structural Genomics Consortium, Integrated Center for Structure and Function Innovation, Israel Structural Proteomics Center, Joint Center for Structural Genomics, Midwest Center for Structural Genomics, New York Structural GenomiX Research

Center for Structural Genomics, Northeast Structural Genomics Consortium, Oxford Protein Production Facility, Protein Sample Production Facility, Max Delbrück Center for Molecular Medicine, RIKEN Structural Genomics/Proteomics Initiative & SPINE2-Complexes. (2008). Protein production and purification. *Nat Meth*, 5 (2): 135-146.

Terpe, K. (2003). Overview of tag protein fusions: from molecular and biochemical fundamentals to commercial systems. *Appl Microbiol Biotechnol*, 60 (5): 523-33.

Thompson, G. R. & Trexler, P. C. (1971). Gastrointestinal structure and function in germ-free or gnotobiotic animals. *Gut*, 12 (3): 230-5.

Tjåland, R. (2011). *Secretion and anchoring of Mycobacterium tuberculosis antigens in Lactobacillus plantarum*. Norwegian University of Life Sciences, Ås: Norwegian University of Life Sciences, Ås, IKBM.

Tremaroli, V. & Backhed, F. (2012). Functional interactions between the gut microbiota and host metabolism. *Nature*, 489 (7415): 242-9.

van den Nieuwboer, M., van Hemert, S., Claassen, E. & de Vos, W. M. (2016). Lactobacillus plantarum WCFS1 and its host interaction: a dozen years after the genome. *Microb Biotechnol*, 9 (4): 452-65.

van Nood, E., Vrieze, A., Nieuwdorp, M., Fuentes, S., Zoetendal, E. G., de Vos, W. M., Visser, C. E., Kuijper, E. J., Bartelsman, J. F., Tijssen, J. G., et al. (2013). Duodenal infusion of donor feces for recurrent Clostridium difficile. *N Engl J Med*, 368 (5): 407-15.

Vinuesa, C. G., Tangye, S. G., Moser, B. & Mackay, C. R. (2005). Follicular B helper T cells in antibody responses and autoimmunity. *Nat Rev Immunol*, 5 (11): 853-65.

Vrieze, A., Van Nood, E., Holleman, F., Salojarvi, J., Kootte, R. S., Bartelsman, J. F., Dallinga-Thie, G. M., Ackermans, M. T., Serlie, M. J., Oozeer, R., et al. (2012). Transfer of intestinal microbiota from lean donors increases insulin sensitivity in individuals with metabolic syndrome. *Gastroenterology*, 143 (4): 913-6 e7.

Wang, X., Ota, N., Manzanillo, P., Kates, L., Zavala-Solorio, J., Eidenschenk, C., Zhang, J., Lesch, J., Lee, W. P., Ross, J., et al. (2014). Interleukin-22 alleviates metabolic disorders and restores mucosal immunity in diabetes. *Nature*, 514 (7521): 237-41.

Ward, N., Larsen, O., Sakwa, J., Bruseth, L., Khouri, H., Durkin, A. S., Dimitrov, G., Jiang, L., Scanlan, D., Kang, K. H., et al. (2004). Genomic insights into methanotrophy: the complete genome sequence of Methylococcus capsulatus (Bath). *PLoS Biol*, 2 (10): e303.

Whittenbury, R., Phillips, K. C. & Wilkinson, J. F. (1970). Enrichment, isolation and some properties of methane-utilizing bacteria. *J Gen Microbiol*, 61 (2): 205-18.

Wu, B., Gong, J., Liu, L., Li, T., Wei, T. & Bai, Z. (2012). Evolution of prokaryotic homologues of the eukaryotic SEFIR protein domain. *Gene*, 492 (1): 160-6.

Yang, P., Wang, J. & Qi, Q. (2015). Prophage recombinases-mediated genome engineering in Lactobacillus plantarum. *Microb Cell Fact*, 14: 154.

Zhang, Y., Li, J., Yu, F., Tong, Y., Zhang, Y., Xiang, Z. & Yu, Z. (2014). Identification and functional characterization of SIMPL in Crassostrea gigas reveals its ancient origin and involvement in the regulation of Rel/NF-kappaB transcription activity. *Fish Shellfish Immunol*, 40 (1): 239-44.

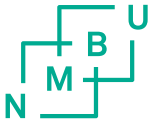

Norges miljø- og biovitenskapelig universitet
Noregs miljø- og biovitskapelege universitet
Norwegian University of Life Sciences

Postboks 5003
NO-1432 Ås
Norway